QUADRUPOLE-PAIRING FORCE AND (p,t) REACTIONS

HIROSHI TOKI

(Doctor Thesis)

Department of Physics, Osaka University

Abstract

It is shown that the quadrupole-pairing force (P_2-P_2) is as important as the quadrupole force (Q-Q) to describe 2^+ states in the medium and heavy nuclei. 2^+ states are described by adding the P_2-P_2 force in the framework of the random-phase approximation. The physical quantities such as excitation energies, (p,t) reaction-cross sections and B(E2) values are systematically studied. The change of angular distribution patterns of (p,t) reactions for first 2^+ states is well accounted for in terms of the two-step process-calculations.

Quadrupole-Pairing Force and (p,t) Reactions

CHAPTER 1 Introduction

In 1950 Mayer and Jensen introduced the idea of the independent-particle model into the microscopic description of nuclear many-body system with the consideration of the spin-orbit force[1]. This so called shell model has been very successful in explaining a mass of properties of nuclei (magic number), spins and parities of nuclei in the ground states etc..

On the other hand, in 1952 A. Bohr introduced the liquid-drop model, by which a nucleus is a liquid drop and vibrates around the equibrium shape and rotates entirely like a rigid rotor.[2] The liquid-drop model has explained the over all trend of nuclear masses, the collective natures of nuclei, which are the excited states of vibrational nuclei and rotational nuclei etc.. These two models explained many aspects of nuclear phenomena.

However, many experimental facts such as even-odd mass difference, the moment of inertia of deformed nuclei etc. can not be explained by these models. These situations were well accounted for by introducing the BCS-theory[3] to the description of nuclei, which explained the superfluid and superconductivity phenomena of liquid helium by Bardeen, Cooper and Schriefer.[4]

In mind the above successes, the method to treat the collective motion of many-body system from the standpoint of particle excitations was investigated by many authors in terms of the random-phase approximation.[5] This method is the extension of the shell model for the nuclear system, in which the pairing correlation is dominant. The random-phase approximation has an advantage that the same equation describes single-particle excitations and collective excitations. This method is the most useful tool to investigate

the structures of medium and heavy nuclei. In fact, so far 2^+ states in the medium and heavy nuclei, especially for first 2^+ states, have been studied in terms of the random-phase approximation with using a simple interaction composed of the monopole-pairing force and a quadrupole force.[6] The enhancement of the B(E2) value between first 2^+ state and ground state is accounted for qualitatively by the simple model.

The nuclear many body problem, for convenience, is treated by using a suitable independent-particle solution as the zeroth-order approximation at first and by using an effective Hamiltonian as the residual part which is solved in terms of the random-phase approximation. Strictly speaking, the independent-particle solution must be obtained by the Hartree-Fock-Bogoliubov procedure.[7]

Since A. Bohr's prediction of pairing mode, many experiments of (p,t) reactions were carried out, because (p,t) reaction is the useful tool to study the pairing correlation in nucleus.[8] In these experiments the (p,t) reactions on the Nd isotopes, which were in the region around N=82, was done by Yagi et al..[9] There found new facts in these experiments, which were that the excited 2^+ states about 3.5MeV of all even-even nuclei were strongly excited. By the conventional model, using the monopole pairing force and the quadrupole force in terms of the random phase approximation, which has been believed to describe 2^+ states of even-even spherical nuclei, the facts are not explained at all.

Thus we introduce the quadrupole pairing force $(P_2\text{-}P_2)$, which is recognized as the force to make two particles combine strongly to the total angular momentum 2^+.[10] As can be seen in figure 1, this type of force surely exists in the two-body interaction. But it has been neglected, because we have restricted our interest in the quantities which have particle-hole nature, that is the gamma transition and the inelastic scattering etc.. In the normal state, the quadrupole-pairing force and

quadrupole force do not interfere with each other in the framework of the random-phase approximation, but in super because the particle number is not conserve these forces do.

In Chapter 2 we shall discuss how important the quadrupole-pairing force is to describe the 2^+ state and to explain the experimental results. The importance of the quadrupole-pairing force is pointed out in Chapter 2, then the form of the Hamiltonian change. Thus in Chapter 4 the model, containing the quadrupole-pairing force is applied to the first 2^+ states of the medium and heavy nuclei, which are the nuclei, the neutron number is between 50 and 82, and the possibility of the phase transition around N=70 is pointed out. In Chapter 5 the incident-energy dependence of (p,t) reaction is discussed, especially for the reaction $^{208}Pb(p,t)^{206}Pb$. In Chapter 6 the reaction mechanism of (p,t) reaction is discussed. The change of the angular distribution pattern leading to the first 2^+ state is not accounted for in terms of the distorted-wave Born-approximation. Thus the second order term of the Born series is taken into account and the calculation is done by using a macroscopic form factor for inelastic scattering.

References

1) M. G. Mayer and J. H. D. Jensen, Elementary Theory of Nuclear Shell Structure (John Wiley & Sons, Inc.)

2) A. Bohr, Dan. Mat. Fys. Medd. 26 (1952) 149

3) A. Bohr, B. R. Mottelson and D. Pines, Phys. Rev. 110 (1958) 936

4) J. Bardeen, L. N. Cooper and J. R. Schrieffer, Phys. Rev. 106 (1957) 162, and Phys. Rev. 108 (1957) 1175

5) T. Marumori, Prog. Theor. Phys. 24 (1960) 331;
R. Arvieu and M. Veneroni, Compt. rend. 250 (1960) 992;
M. Baranger, Phys. Rev. 120 (1960) 957

6) L. S. Kisslinger and R. A. Sorrensen, Rev. Mod. Phys. 35 (1963) 853

7) D. J. Thouless, Nucl. Phys. 21 (1960) 225;
N. N. Bogoliubov, Usp. Fiz. Nauk. 67 (1959) 549

8) A. Bohr, Proc. Intern. Symp. on Nuclear Structure (Dubna, 1968) 179

9) K. Yagi, Y. Aoki, J. Kawa and K. Sato, Phys. Lett. 29B (1969) 647;
Y. Ishizaki, Proc. Phys. Soc. Japan 26 (1971) 147

10) H. Toki and M. Sano, Osaka University, Laboratory of Nuclear Studies, OULNS 73-6 (1973), and to be published

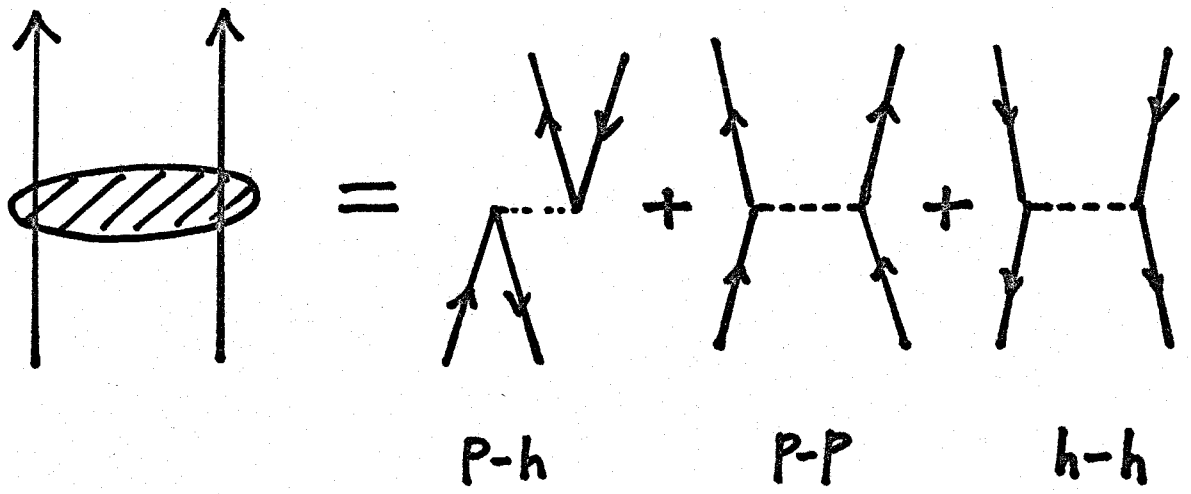

Fig. 1. Schematic representation of the two body interaction. Lines running upwards represent particles while running downwards represent holes.

CHAPTER 2 Importance of the Quadrupole-Pairing Force in (p,t) Excitations of 2^+ Vibrational States

1. Introduction

Two-neutron transfer reactions have proved to be especially sensitive in probing pair correlations in complex nuclei. The groups in INS and Osaka University have been currently studying (p,t) reactions on Nd isotopes[1] and the rare-earth nuclei[2] with about 50-MeV protons. In these experiments, they have found a new experimental evidence that there is an unexpectedly strong L = 2 transition to a state at about 3.5 - 4.0MeV. These 2^+ states were interpreted by them as being the quadrupole-pairing states . (Hereafter we also call it the quadrupole-pairing state.) For the Ba[3] and Nd isotopes with neutron number less than N = 82, the first 2^+ state also has a structure similar to the quadrupole pairing states. For most even nuclei except for nuclei near the closed shell, two-neutron transfer with L = 0 populates the ground states[4]. However, these excited 2^+ states have almost the same transition strengths as the ground states yield.

So far 2^+ states in heavy spherical nuclei, especially the first 2^+ states, have been well described in the random-phase approximation by using a simple interaction composed of a monopole-pairing force and a quadrupole force[5]. The observation of such a uniformly strong L = 2 transition can not be explained in terms of the conventional model, that is, the monopole pairing plus quadrupole force model. Previously, Udagawa et al.[6] have tried to explain a strong L = 2 transition to the first 2^+ state of ^{140}Nd taking into account the quadrupole-pairing

interaction on the basis of the pairing-vibrational mode proposed by A. Bohr[7]. However, it has been experimentally found that the simple zeroth order picture of the monopole-pairing vibrational-mode predicted by A. Bohr breaks down for N = 84 -88 nuclei[1,8].

The purpose of the present work is to show that the quadrupole-pairing interaction acting on particles in the nucleus can give rise to as large a (p,t) cross section for an excited 2^+ state as the monopole-pairing interaction does for the ground state. The calculation is especially focussed on the (p,t) reactions on spherical nuclei. The 2^+ states are described by adding the quadrupole-pairing force to the quadrupole force in the framework of the random-phase approximation. The quadrupole-type density-vibrational mode couples to the quadrupole pairing-type vibrational mode. In the conventional theory which has described 2^+ vibrational states, the latter effect has been neglected. It should be noted that the importance of this latter effect has been revealed in the experiment of two-neutron transfer reactions. Our method is a reasonable extension of the theory for the description of vibrational motion of nucleus in a superconducting phase.

A similar experiment on the Nd isotopes has also been reported by Ball et al.[8] with the (p,t) reaction at 31MeV. They did not observe any strong L = 2 excited states in these nuclei. Their results may be explained by the decreased intensity for the transition to the quadrupole-pairing states. The calculated cross sections for the quadrupole-pairing states certainly have a strong dependence on the incident proton energy, but those show a broad resonance-like peak with a maximum value around 30MeV lower than expected.

In sect.2, the 2^+ states are described by the quadrupole-pairing force in addition to the monopole pairing plus quadrupole forces in the random-

phase approximation. In sect. 3 the calculation method of the (p,t) reaction cross section in the distorted-wave Born approximation is briefly summarized and in sect. 4 sum rules for 2^+ states are discussed. Comparison with experiments are made for Ba and Nd isotopes in sect. 5 and qualitative discussions are presented in sect. 6.

2. Description of 2^+ Vibrational States

We consider a system of nucleons interacting with each other by the monopole-pairing, quadrupole-pairing[9], and quadrupole forces. The Hamiltonian may be written as

$$H = \sum (\varepsilon_j - \lambda) c^+_{jm} c_{jm} - \frac{1}{4} G_0 \hat{P}^+_{00} \hat{P}_{00} - \frac{1}{2} G_2 \sum_\mu \hat{P}^+_{2\mu} \hat{P}_{2\mu} - \frac{1}{2} V_2 \sum_\mu \hat{Q}^+_{2\mu} \hat{Q}_{2\mu}, \quad (1)$$

where

$$\hat{P}^+_{J\mu} = \sum \langle j_1 \| (i\kappa r)^J Y_J \| j_2 \rangle [c^+_{j_1} \otimes c^+_{j_2}]^{(J)}_\mu \times \begin{cases} \sqrt{4\pi}, & J=0 \\ 1, & J=2, \end{cases}$$

$$\hat{Q}^+_{J\mu} = \sum \langle j_1 \| (i\kappa r)^J Y_J \| j_2 \rangle [c^+_{j_1} \otimes c_{j_2}]^{(J)}_\mu .$$

The expressions $[c^+_{j_1} \otimes c^+_{j_2}]^{(J)}_\mu$ and $[c^+_{j_1} \otimes c_{j_2}]^{(J)}_\mu$ represent two-particle and particle-hole pair operators coupled to angular momentum J and its z-component μ, respectively. The parameter $\kappa = (m\omega_0/\hbar)^{1/2}$ describes the oscillator strength and λ is Fermi energy which will be determined later.

In spherical nuclei with partially filled shells, the most important effect of the two-body force is to produce monopole-pairing correlations. The simplest way to introduce these correlations in the wave function is to perform the Bogoliubov-Valatin transformation[10]:

$$C^{+}_{jm} = U_j \alpha^{+}_{jm} + V_j (-)^{j-m} \alpha_{j-m} \quad , \tag{2}$$

where α^{+}_{jm} and α_{jm} are the creation and annihilation operators of a quasiparticle, U_j and V_j are the unoccupied and occupied amplitudes of j orbit respectively, and are given by $U_j = [\frac{1}{2}(1+(\varepsilon_j-\lambda)/E_j)]^{\frac{1}{2}}$ and $V_j = (1-U_j^2)^{\frac{1}{2}}$. Further $E_j = [(\varepsilon_j-\lambda)^2+\Delta^2]^{\frac{1}{2}}$ is a quasiparticle energy, and λ and Δ are the two parameters fixed through the BCS equations[11].

The last two interaction terms in eq.(1) could be treated in the random phase approximation[5]. This procedure makes it possible to diagonalize these terms between all two-quasiparticle states and yields collective states which necessarily contain a large number of quasiparticles. Let us define some creation and annihilation operators for pairs of quasiparticles coupled to angular momentum 2,

$$A^{+}(j_1 j_2; 2\mu) = \sum_{m_1 m_2} (j_1 m_1, j_2 m_2 | 2\mu) \alpha^{+}_{j_1 m_1} \alpha^{+}_{j_2 m_2} \quad , \tag{3a}$$

$$A(j_1 j_2; 2\mu) = \sum_{m_1 m_2} (j_1 m_1, j_2 m_2 | 2\mu) \alpha_{j_2 m_2} \alpha_{j_1 m_1} \quad . \tag{3b}$$

In the random-phase approximation, a creation operator of 2^+ state is defined by a linear combination of the A's assumed as boson operators,

$$Q^{+}_{2\mu} = \frac{1}{2} \sum_{jj'} [\psi_{jj'} A^{+}(jj'; 2\mu) - \phi_{jj'} (-)^{2-\mu} A(jj'; 2-\mu)] . \tag{4}$$

The amplitudes ψ, ϕ and the excitation energy $\hbar\omega$ are determined by the following set of equations derived from the equation of motion $[H, Q^{+}] = \hbar\omega Q^{+}$:

$$\hbar\omega\psi_{jj'} = E_{jj'}\psi_{jj'} - \tfrac{1}{2}V_2\, q^{(0)}_{jj'}\sum q^{(0)}_{j_1j_1'}(\psi_{j_1j_1'} + \phi_{j_1j_1'})$$
$$-\tfrac{1}{2}G_2 P^{(0)}_{jj'}\sum P^{(0)}_{j_1j_1'}(\psi_{j_1j_1'} + \phi_{j_1j_1'}) - \tfrac{1}{2}G_2 P^{(1)}_{jj'}\sum P^{(1)}_{j_1j_1'}(\psi_{j_1j_1'} - \phi_{j_1j_1'}), \tag{5a}$$

$$-\hbar\omega\phi_{jj'} = E_{jj'}\phi_{jj'} - \tfrac{1}{2}V_2\, q^{(0)}_{jj'}\sum q^{(0)}_{j_1j_1'}(\psi_{j_1j_1'} + \phi_{j_1j_1'})$$
$$-\tfrac{1}{2}G_2 P^{(0)}_{jj'}\sum P^{(0)}_{j_1j_1'}(\psi_{j_1j_1'} + \phi_{j_1j_1'}) + \tfrac{1}{2}G_2 P^{(1)}_{jj'}\sum P^{(1)}_{j_1j_1'}(\psi_{j_1j_1'} - \phi_{j_1j_1'}). \tag{5b}$$

Here the abbreviations $E_{jj'} = E_j + E_{j'}$, $q^{(s)}_{jj'} = \langle j\|(i\kappa r)^2 Y_2\|j'\rangle(U_jV_{j'} + (-)^s U_{j'}V_j)$, and $p^{(s)}_{jj'} = \langle j\|(i\kappa r)^2 Y_2\|j'\rangle(U_jU_{j'} - (-)^s V_jV_{j'})$ were used. From these equations we obtain the coupled dispersion equation which determines values of $\hbar\omega$.

$$\begin{vmatrix} 1 - V_2 S_0 & -G_2 R_0 & -G_2 R_1 \\ -V_2 R_0 & 1 - G_2 S_1 & -G_2 R_2 \\ -V_2 R_1 & -G_2 R_2 & 1 - G_2 S_2 \end{vmatrix} = 0 , \tag{6}$$

where

$$S_0 = \sum \frac{q^{(0)2}_{jj'} E_{jj'}}{E^2_{jj'} - (\hbar\omega)^2} , \qquad R_0 = \sum \frac{q^{(0)}_{jj'} P^{(0)}_{jj'} E_{jj'}}{E^2_{jj'} - (\hbar\omega)^2} ,$$

$$S_1 = \sum \frac{P^{(0)2}_{jj'} E_{jj'}}{E^2_{jj'} - (\hbar\omega)^2} , \qquad R_1 = \sum \frac{q^{(0)}_{jj'} P^{(1)}_{jj'} \hbar\omega}{E^2_{jj'} - (\hbar\omega)^2} , \tag{7}$$

$$S_2 = \sum \frac{P^{(1)2}_{jj'} E_{jj'}}{E^2_{jj'} - (\hbar\omega)^2} , \qquad R_2 = \sum \frac{P^{(0)}_{jj'} P^{(1)}_{jj'} \hbar\omega}{E^2_{jj'} - (\hbar\omega)^2} .$$

From the normalization condition of 2^+ states, one can easily deduce the relation

$$\sum_{jj'} \left(\psi_{jj',n} \psi_{jj',n'} - \phi_{jj',n} \phi_{jj',n'} \right) = 2\delta_{nn'} \quad . \tag{8}$$

The suffix n indicates the solution corresponding to an eigenvalue $\hbar\omega_n$. From eq.(5) and the normalization condition (8), the amplitudes ψ and ϕ are completely determined and are given in the following forms,

$$\psi_{jj',n} = \frac{1}{\sqrt{Z}} \frac{1}{E_{jj'} - \hbar\omega_n} \left[q^{(0)}_{jj'} + \gamma_1 P^{(0)}_{jj'} + \gamma_2 P^{(1)}_{jj'} \right] \quad , \tag{9a}$$

$$\phi_{jj',n} = \frac{1}{\sqrt{Z}} \frac{1}{E_{jj'} + \hbar\omega} \left[q^{(0)}_{jj'} + \gamma_1 P^{(0)}_{jj'} - \gamma_2 P^{(1)}_{jj'} \right] \quad . \tag{9b}$$

Here $1/\sqrt{Z}$ is the normalization constant and the last two terms in ψ and ϕ give the components of quasiparticle pair amplitudes caused by the quadrupole-pairing correlation. The constants Z, γ_1 and γ_2 are given by

$$Z = S_0' + \gamma_1^2 S_1' + \gamma_2^2 S_2' + 2\gamma_1 R_0' + 2\gamma_2 R_1' + 2\gamma_1\gamma_2 R_2' \quad , \tag{10a}$$

$$\gamma_1 = (a_2 c_1 - a_1 c_2) / (b_1 c_2 - b_2 c_1) \quad , \tag{10b}$$

$$\gamma_2 = (a_1 b_2 - a_2 b_1) / (b_1 c_2 - b_2 c_1) \quad , \tag{10c}$$

where the prime means the differential by $\hbar\omega$, for instance $S_0' = dS_0/d(\hbar\omega)$, and a_1 etc. are defined by

$$\begin{aligned}
a_1 &= S_0 (1 - V_2 S_0) - G_2 R_0^2 - G_2 R_1^2 \quad , \\
b_1 &= R_0 (1 - V_2 S_0) - G_2 S_1 R_0 - G_2 R_1 R_2 \quad , \\
c_1 &= R_1 (1 - V_2 S_0) - G_2 R_0 R_2 - G_2 S_2 R_1 \quad , \\
a_2 &= - V_2 S_0 R_0 + (1 - G_2 S_1) R_0 - G_2 R_1 R_2 \quad , \\
b_2 &= - V_2 R_0^2 + (1 - G_2 S_1) S_1 - G_2 R_2^2 \quad , \\
c_2 &= - V_2 R_0 R_1 + (1 - G_2 S_1) R_2 - G_2 S_2 R_2 \quad .
\end{aligned} \tag{11}$$

3. Spectroscopic amplitude for two-nucleon transfer reaction

Several attempts[12-14] have been made to write simply the cross section for two-nucleon transfer reactions in the distorted-wave Born approximation. The differential cross section for the(t,p) reaction is given in the zero-range approximation by

$$\frac{d\sigma}{d\Omega} = \frac{2I_f+1}{2I_i+1}\frac{m_t^* m_p^*}{(2\pi\hbar^2)^2}\frac{k_p}{k_t} V_{eff}^2 \sum_{LM_L}\frac{1}{2L+1}\left|\int f_p^{(-)*}\left(k_p,\frac{A}{A+2}R\right) F_L(R) i^{-L} Y_{LM_L}^*(\Omega_R) f_t^{(+)}(k_t,R)\,dR\right|^2 \quad (12)$$

where I_i and I_f are the spins of target and residual nuclei, respectively, m_t^* and m_p^* are the reduced masses of the triton and proton, k_t and k_p are the relative momenta of the triton and of the proton, and V_{eff} is strength of the Gauss-type interaction which causes the transfer reactions. The functions $f_t^{(+)}$ and $f_p^{(-)}$ are the distorted wave functions describing the relative motion in the initial and final reaction channels. The vector R defines the position of the center of mass of the captured di-neutron. The form factor F_L is given by

$$F_L(R) = \sum_{N\tilde{n}} B_{\tilde{n}NL} R_{NL}\left(\frac{2A}{A+2}\nu, R\right). \quad (13)$$

The function R_{NL} is the radial part of the harmonic oscillator wave function for the center of mass coordinate of the two neutrons with principal quantum number N and angular momentum L, and the parameter ν describes the oscillator strength. The coefficient B_{nNL}, which contains all the information about nuclear structure, is

$$B_{\tilde{n}NL} = \Omega_{\tilde{n}} \sum_{j_1 j_2} i^{L+l_1+l_2} g_{j_1 j_2} A(I_i I_f; j_1 j_2 J) \delta_{LJ} \langle n_1 l_1, n_2 l_2; L | \tilde{n} 0, NL; L\rangle \times \langle (\tfrac{1}{2} l_1) j_1, (\tfrac{1}{2} l_2) j_2; J | (\tfrac{1}{2}\tfrac{1}{2}) 0, (l_1 l_2) L; J\rangle. \quad (14)$$

The factor $g_{j_1 j_2}$ is equal to unity, if the two neutrons are captured in the same single-particel orbit ($j_1 = j_2$) and otherwise $g_{j_1 j_2} = \sqrt{2}$. The symbols $\langle(\frac{1}{2}\ell_1)j_1,(\frac{1}{2}\ell_2)j_2;J|\ (\frac{1}{2}\ \frac{1}{2})0,(\ell_1\ell_2)L;J\rangle$ and $\langle n_1\ell_1,n_2\ell_2;L|\tilde{n}0,\tilde{N}L;L\rangle$ are the 9j-coefficient of the transformation from the j-j coupling to the L-S coupling representation and the Talmi coefficient, respectively. The overlapping integral $\Omega_{\tilde{n}}$ of the wave functions for the relative motion of the two transferred neutrons in the initial and final state is given by

$$\Omega_{\tilde{n}} = \left(\frac{3\pi\nu\delta^4}{D^2C^2}\right)^{\frac{3}{4}} 2^{(9-2\tilde{n})/4}\sqrt{\frac{(2\tilde{n}-1)!!}{(\tilde{n}-1)!}}\left(1-\frac{4DC+a^4}{8DC^2}\nu\right)^{\tilde{n}-1} \qquad (15)$$

with $C = \frac{\nu}{4} + \frac{a^2}{4} + \frac{3}{2}\delta^2$ and $D = a^2 + 2\delta^2 - \frac{a^4}{4C}$. The parameters δ and a are the size parameters of triton and the interaction range of the Gauss potential.

The spectroscopic amplitude $A(l_i,I_f;j_1j_2J)$ that appears in eq.(14) is defined as

$$A(I_i,I_f;j_1j_2J) = \langle I_fM_f|\Sigma_{\cdot}(I_iM_iJM|I_fM_f)\frac{1}{\sqrt{1+\delta_{j_1j_2}}}[c_{j_1}^{+}\otimes c_{j_2}^{+}]_M^{(J)}|I_iM_i\rangle \qquad (16)$$

The amplitude with respect to the ground-state transition is equal to

$$A(I_i=0,I_f=0;j_1j_2J=0) = \delta_{j_1j_2}\sqrt{\frac{2j_1+1}{2}}\ U_{j_1}V_{j_1}\ . \qquad (17)$$

Here we assumed that the target and residual nuclei have the same ground-state wave function. Strictly speaking, both systems consist of different nucleon number and these wave functions are non-orthonormal to each other. In order to simplify the calculations, we neglect this effect here. On the

same assumption, the (t,p) spectroscopic amplitude associated with the excitation of 2^+_n state becomes

$$A_n(I_i=0, I_f=2; j_1 j_2 J=2) = \frac{1}{\sqrt{1+\delta_{j_1 j_2}}} \left(U_{j_1} U_{j_2} \psi_{j_1 j_2, n} - V_{j_1} V_{j_2} \phi_{j_1 j_2, n}\right). \quad (18)$$

For the (p,t) reactions it becomes

$$A_n(I_i=0, I_f=2; j_1 j_2 J=2) = \frac{1}{\sqrt{1+\delta_{j_1 j_2}}} \left(U_{j_1} U_{j_2} \phi_{j_1 j_2, n} - V_{j_1} V_{j_2} \psi_{j_1 j_2, n}\right). \quad (19)$$

In the transfer reactions, the largest contribution comes from around the nuclear surface. The cross section will become large for a form factor which is peaked around the nuclear radius R_o and has a long exponential tail. In the numerical calculations, the form factors for the external region of nucleus are then constructed by matching the form factor given by eq.(13) smoothly into the Hankel function with the correct asymptotic behaviour[12].

4. Sum rule for 2^+ states

In order to gain an insight into the type of spectroscopic information, it may be useful to study the spectroscopic factor defined as

$$S_n(I_i=0, I_f=2; J=2) = \left| \sum_{j_1 \geq j_2} g_{j_1 j_2} \langle j_1 \| (ir)^2 Y_2 \| j_2 \rangle A_n(I_i=0, I_f=2; j_1 j_2 2) \right|^2. \quad (20)$$

The cross section is proportional to the spectroscopic factor in the following two approximations[14]: One of them is to set the frequency of the harmonic oscillator potential of the relative motion of the two transferred neutrons equal to the frequency of the harmonic oscillator potential of the

target nucleus. In this approximation only the term $\widetilde{N} = \widetilde{N}_{max}$ in eq.(14) survives. The other approximation is to treat the triton as a point and to replace the Talmi coefficient by its average taken over all possible two-particle configurations. In this approximation the coefficient B_{nNL} reduces to the amplitude of the spectroscopic factor given in eq.(20)

In the Tamm-Dancoff approximation which neglects the backward scattering amplitude $\phi_{jj',n'}$ sum of the spectroscopic factor for (t,p) reactions over various 2^+ states becomes

$$S(t,p) = \sum_n S_n(I_i=0, I_f=2; J=2) = \sum_{j_1 j_2} \langle j_1 \| (i\times r)^2 Y_2 \| j_2 \rangle^2 U_{j_1}^2 U_{j_2}^2, \quad (21)$$

and also for (p,t) reactions it becomes

$$S(p,t) = \sum_{j_1 j_2} \langle j_1 \| (i\times r)^2 Y_2 \| j_2 \rangle^2 V_{j_1}^2 V_{j_2}^2. \quad (22)$$

The right hand side of each of the above equations is equal to sum of the spectroscopic factor over all the two-quasiparticle states coupled to the angular momentum J = 2. This sum rule cannot be derived when ground-state correlations are included in the description of states connected by the reaction as is done in the random-phase approximation. In surveying the data on two-neutron transfer reactions , however, the sum rule is useful to give a criterion for deciding whether the transition is strong. That is to say, the criterion is whether the transition exhausts a fair fraction of a sum-rule value. In the next section, we will show that the transition strength associated with the quadrupole-pairing state has the majority in the sum-rule value.

5. Comparison with experiments

We shall now present results of the numerical calculations for (p,t) and (t,p) reactions leading to the ground states, the first excited 2^+ states and the quadrupole-pairing states. The calculations are made in two steps. The first is to estimate cross sections for the ground-state transitions and to fix the monopole-pairing interaction-strengths and single-particle energy levels from these estimations. The second is to fix the interaction strengths V_2 and G_2 from the experimental data of the excitation energies and two-neutron transfer reactions associated with the first and quadrupole-pairing 2^+ states.

5.1. GROUND-STATE TRANSITIONS

In the calculations, all the single-particle levels lying between Z = 28 and 82 closed shells for protons and between N = 50 and 126 closed shells for neutrons were taken. Two sets of single-particle energies are used for neutrons and are listed in table 1 together with the set used for protons. The two sets for neutrons differ only in the energy interval between $5f_{7/2}$ and $4d_{3/2}$ levels (3.7 MeV for case I and 2.5 MeV for case II), and relative intervals of the levels above and below the closed shell at N = 82 are kept the same in both the cases. The value 3.7 MeV for case I was taken from the difference between the separation energies for the $5f_{7/2}$ and $4d_{3/2}$ levels. The strengths of the monopole-pairing force were set equal to $G_o = 20.0A^{-1}$ MeV for neutrons in case I and 18.4MeV in case II and $G_o = 23.0A^{-1}$MeV for protons. These values reproduce fairly well the experimental values for the energy gap and make all nuclei to be in the superconducting phase, except for N = 82, At N = 82, the energy-gap parameter becomes very small and therefore one can say that the neutrons in ^{142}Nd and ^{138}Ba are approximately in the normal phase. Figure 1 shows the

calculated and experimentally observed cross sections for the (p,t) reactions leading to the ground states of Nd-isotopes. All cross sections are sums of the differential cross sections taken for 5° intervals in the range of 5° to 40° and are plotted as a function of neutron number N in residual nucleus. The calculated cross sections are normalized to the reaction ^{146}Nd(p,t)^{144}Nd. The optical potential parameter used in the calculations were taken directly from the work of Ball et al.[17], and are listed in table 2. The parameters included in eq.(15) were taken as follows: $\nu = 0.96A^{-\frac{1}{3}}$ fm^{-2}, $a^2 = 0.3$ and $\delta^2 = 0.06$ fm^{-2} [13]. It is found that a set of the single-particle spectrum denoted as case II can reproduce the experimental trends better than in case I. Further, the calculated excitation energies of the quadrupole-pairing vibrational states for case II are in good agreement with the experimental values as shown in table 3, and for case I become higher by about 1 MeV for case I. In fig.1, however, the disagreement is remarkable at N = 88. The experimental data indicate the necessity of taking into account the change in the nuclear deformations of the target nucleus and residual one[15]. The reduced cross section is due to the decrease in the transition matrix element when the difference between the deformations of the target and residual nuclei is taken into account. The deformation parameter $\delta = 0.07$ for ^{150}Nd gives better agreement with the experimental cross section than the result shown in fig.1. However, this is too small compared with the experimental value $\delta = 0.26$. One should take a shape coexisting model[16] for ^{148,150}Nd-isotopes to explain the experimental data consistently. The differential cross sections for the ground state transitions are given in fig.2 and are found to be in good agreement with the experimental ones. Similar results have also been obtained for Ba-isotopes.

5.2. Excited 2^+ State Transitions

The experimental and calculated (p,t) cross sections relative to the ground-state transition are listed in table 3 together with the results of (t,p) reactions[18]. The parameter sets of V_2 and G_2 are taken so as to reproduce the experimental excitation energy of the first 2^+ state. We can not fix these values from the excitation energy only, but can express the parameter V_2 as a function of G_2. The (p,t) cross sections relative to the ground-state transition for 2^+ states in ^{146}Nd are shown in fig.3 as a function of G_2. In the case of $G_2 = 0$, the calculated cross section for the quadrupole-pairing state is apparently smaller by a factor of about 6 than the experimental value. However, the cross section increases with the quadrupole-pairing interaction strength G_2 and reaches the experimental value at $G_2 = 0.0064$MeV. In the case of $G_2 = 0$, on the other hand, the calculated cross section for the first 2^+ state is considerably larger than the experimental one, but it decreases with the interaction strength G_2 and reaches a minimum value around $G_2 = 0.006$MeV. For G_2 values exceeding the minimum point, the cross section tends to gradually increase. In the range of excitation energies below 10MeV, we can find another 2^+ state which gives rise to a large (p,t) cross section with the increase of G_2. Hereafter we like to call it the third 2^+ state. This state lies higher in energy by about 1MeV than the quadrupole-pairing state as seen in table 3. All cross sections listed in table 3 are normalized to the ground-state cross section for each nucleus. The (p,t) cross section for the third 2^+ state in ^{144}Nd is larger than for the quadrupole-pairing state. However, it decreases more rapidly with the increasing neutron number, resulting in relatively larger cross section values for the quadrupole-pairing state at higher neutron number (^{146}Nd and ^{148}Nd). The neutron-number dependence of the calculated cross sections for the quadrupole-pairing states is in good agreement with the experimental results. For the ^{150}Nd(p,t) ^{148}Nd reaction,

however, the difference between the nuclear deformations of the target and residual nuclei should be taken into account as pointed out in the last subsection 5.1. Then the agreement with the experiment will be improved much more. It should be noted, however, that these states interpreted by Yagi et al.[1] as being the quadrupole-pairing states are not always of pure quadrupole-pairing vibrational nature, although the cross sections are comparable to or larger than the ground-state cross sections.

It is interesting to know about how large a collectivity these states have for the two-neutron transfer reactions. The calculated spectroscopic factors for the 2^+ states and the sum-rule values are displayed in table 4 together with the results of (t,p) reactions. The values of the spectroscopic factors are given for G_2 = 0.0, 0.006 and 0.007 MeV. It is seen that the quadrupole-pairing states have transition strengths of about 30 $\sim$ 50% of the sum rule value and the sum of the transition strengths for three 2^+ states reaches to about 80 $\sim$ 99% of the sum rule value.

Figure 4 displays the calculated and experimental (p,t) angular distributions for the 2^+ states. The angular distributions for the transitions to the first excited 2^+ states can not be fit with the distorted-wave Born-approximation calculations. It has been shown that the effect on the cross section due to multi-step process[19,20] is quite important to fit the experimental angular distributions. However, this effect was not considered here.

For nuclei with neutrons less than N = 82, contrary to the case with N > 82, the first excited 2^+ states have a collective character of the pairing-vibrational type and almost exhaust L = 2 transition strength. The calculations done with the $G_2 = 20.7A^{-5/3}$ MeV are shown in table 5. The agreement with the experimental values is quite good. However, when the calculations were done with G_2 = 0, the values are apparently smaller by a factor of about 5 than the experimental ones. This agreement was

obtained not only for the summed cross sections associated with the ground and first excited 2^+ state transitions, but also for the angular distributions as shown fig.5.

In an earlier paper, Udagawa et al.[6] analyzed the data of ^{142}Nd(p,t)^{140}Nd with the coupled-channel Born approximation (CCBA) and obtained a good agreement with the measured angular distributions. As far as the strong quadrupole-pairing type L = 2 transitions are concerned, however, the angular distributions from these states can be fit quite easily with calculations in the distorted-wave Born-approximation. Compared with these 2^+ state transitions, the transitions to the first 2^+ states of nuclei with N > 82 are much more inhibited and have angular distributions that are quite different as can be seen by comparing fig.4a with figs 4b and 5. The angular distributions for these weak transitions were shown by Yagi et al.[21] to be reasonably accounted for in terms of two step coupled-channel Born-approximation calculations. As may be seen from their results, the good agreement of the CCBA result with experiment is obtained by the destructive interference between the one-step process and two-step process related to the inelastic scattering ($0^+ - 2^+$), although the magnitude of the cross section for the direct process is larger by a factor of about 10 than for the two-step process. In the case for N < 82, the magnitude of the cross section for the direct transition to the first 2^+ state is furthermore enlarged by a factor of about 10 than in the case for N > 82. Therefore, in this case it seems to us that the effect of the two-step process is less important in comparison with the case for N > 82. This is a reason why in the case for N < 82 the first 2^+ state transitions are well accounted for by the one step distorted-wave Born-approximation.

5.3. ENERGY DEPENDENCE OF CROSS SECITONS

We should like to mention the incident energy dependence of the cross sections for the 2^+ states. An experiment of the (p,t) reactions on the Nd isotopes has also been studied by Ball et al.[8] with 31MeV protons. In nuclei for $N > 82$, they have not observed any strong $L = 2$ transitions. It makes us suspect that there may be a strong dependence of the cross sections for the 2^+ states on the incident proton energy. For the case of $^{148}Nd(p,t)^{146}Nd$, the cross sections for the ground state and the 2^+ state transitions are plotted in fig.6 as a function of the incident proton energy E_p. A remarkable feature is the appearance of a broad resonance-like peak with a maximum value around 30MeV in the cross section for the quadrupole-pairing state and the third 2^+ state. The calculated results are contrary to the experimental ones. According to the experimental evidences, a strong 2^+ state transition must be observed around higher energy than 30MeV. There remains a possibility to explain why this discrepancy between the calculation and the experiment appears. That is to say, there is an ambiguity on the energy dependence of the optical potential parameter for tritons. We took the optical potential with the energy dependence for protons employed by Perey[17], but we did not for tritons. The resonance-like behaviour is caused by enhancement of the overlapping integral in eq.(12) of the distorted waves and the form factor of transitions associated with the 2^+ states. The form factors are shown in fig.7. The amplitudes of the form factors for the quadrupole-pairing state and the third 2^+ state transitions have a large peak in the outer region of nucleus. The main contribution to the overlapping integral of the distorted waves and the form factor comes from the outer region than the nuclear radius. These are reasons why the cross

sections associated with the quadrupole-pairing state and the third 2^+ state become larger than the first 2^+ state transition with increasing quadrupole-pairing interaction strength and why the strong energy dependence appears in the cross sections for the quadrupole-pairing state and the third 2^+ state. For the case with $N < 82$, the form factor for the first 2^+ state transition has a strong resemblance to that for the quadrupole-pairing state and the third 2^+ state transitions in the Nd-isotopes with $N > 82$.

6. Qualitative discussions

In the preceding sections we have shown that the enhanced (p,t) cross sections for the $L = 2$ transition in nuclei near the major closed neutron shell at $N = 82$ can be understood naturally within the "quadrupole plus quadrupole-pairing vibrational model". The conventional calculations of the quadrupole-type particel-hole vibrations do not display the large two-neutron transfer cross sections. We feel that it is necessary to make clear a mechanism to generate the excited 2^+ states which can display the enhanced (p,t) cross section.

In fig. 8 is displayed a schematic representation of possible distributions of two-quasiparticle states coupled to 2^+ in ^{146}Nd. The 2^+ states shown in (a), (b), and (c) are composed of levels above the closed shell at $N = 82$, of levels above and below the closed shell, and of levels below the closed shell, respectively. The lengths of the vertical bars give values of $(V_{j_1 j_2})^2$, $V_{j_1} V_{j_2} U_{j_1} U_{j_2}$, and $V_{j_1} V_{j_2} (U_{j_1} V_{j_2} + U_{j_2} V_{j_1})$, which are factors in the spectroscopic amplitudes related to the occupation of two-quasiparticel levels. Main contributions to the spectroscopic amplitude in eq. (19) come from the second term $V_{j_1} V_{j_2} \psi_{j_1 j_2, n}$. The magnitude is

especially determined by values of the components γ_1 and γ_2 in $\psi_{j_1 j_2, n}$. These are components of two-particle and two-hole amplitudes generated by the quadrupole-pairing interaction. In general, values of γ_1 and γ_2 are small except for the ones in the quarupole-pairing state and the third 2^+ state. Furthermore, a characteristic feature of γ_1 and γ_2 for the quadrupole pairing state and the third 2^+ state is that these have opposite signs and are approximately of the same magnitude, and $(\gamma_2-\gamma_1)$ becomes larger than the coefficient of (UV+VU) term by a factor of about 5. Therefore, if we neglect the (UV+VU) term is the transition amplitude, the spectroscopic factor for the quadrupole-pairing state and the third 2^+ state transitions becomes approximately:

$$S_n(I_i=0,\ I_f=2;\ J=2)=\left|\frac{(\gamma_2-\gamma_1)}{\sqrt{2}}\sum_{j_1 j_2}\frac{g_{j_1 j_2}\langle j_1\|(i\kappa r)^2 Y_2\|j_2\rangle^2 V_{j_1}^2 V_{j_2}^2}{E_{j_1 j_2}-\hbar\omega_n}\right|^2. \tag{23}$$

As is seen in fig.8, in the range of (a) the contribution of two-quasiparticle states to eq.(23) is smaller than that in (b) and (c) ranges. If these contributions are neglected, then the transition to the quadrupole-pairing state becomes completely coherent and has a large transition amplitude compared with other 2^+ states. For the third 2^+ state, the contribution of two-quasiparticle states in (b) should be substructed from that in (c). It seems to us, therefore, that the cross section of the third 2^+ state is smaller than of the quadrupole-pairing state. For ^{146}Nd(p,t)^{144}Nd reaction, however, the cross section of the third 2^+ state becomes larger than that of the quadrupole-pairing state because $(\gamma_2-\gamma_1)^2_{2^+_3}$ is greater than $(\gamma_2-\gamma_1)^2_{2^+_{qp}}$.

For the first 2^+ states of nuclei for N > 82, the situation is more complicated since the three terms in $\psi_{j_1 j_2}$, and also the term $U_{j_1} U_{j_2} \phi_{j_1 j_2}$ in eq.(19) contribute equally to the spectroscopic factor. Contributions of all two-quasiparticle states in (a), (b) and (c) are in the random phase and therefore the first 2^+ state transition can not be collective.

Empirically, the large value of $(\gamma_2-\gamma_1)$ appears only in energy below the lowest two-quasiparticle states in (b) and (c). There is an energy gap between the lowest levels in (a) and (b). For nuclei with less neutrons than N = 82, however, this energy gap vanishes. For the first 2^+ state, then, the term $(\gamma_2-\gamma_1)V_{j_1} V_{j_2}$ in $\psi_{j_1 j_2}$ becomes larger than other terms and the transition strength becomes rather large. This situation for an enhancement of the transition amplitude has a strong resemblance to that for the quadrupole-pairing state and the third 2^+ state in nuclei for N > 82.

7. Conclusions

The following conclusion may be drawn from the results of our calculations on the (p,t) reaction cross sections: The strong L = 2 transitions in (p,t) reactions on Nd- and Ba-isotopes can be explained by the vibrational model described by a simple interaction composed of a quadrupole force and a quadrupole-pairing force in the framework of the random phase approximation. If the quadrupole-pairing force were not taken into account, one can not reproduce the observed strong L = 2 transitions in the (p,t) reactions. The strengths of the quadrupole force and the quadrupole-pairing force are about $\chi_2 = 37.4A^{-5/3}$ MeV and $G_2 = 26.0A^{-5/3}$ MeV. These values give a good agreement of the excited energies of the first and the quadrupole-pairing 2^+ states and also of the large L = 2 transition strengths in the (p,t) reactions with the experimental data. This value for the quadrupole-pairing interaction strength is a little smaller than the

value $34.0A^{-5/3}$ MeV determined by analysing the cross sections of the two-neutron transfer reactions to the first 2^+ state in ^{140}Nd[6] and is larger by a factor of 2 than the value $17.4A^{-5/3}$ MeV determined by analysing the cross sections of the two-neutron transfer reactions to the 0^+ pairing vibrational states on Uranium isotopes[22]*. It should be noted, however, that the value of the interaction strength depends on the number of single-particle levels taken in the calculations.

The observed strong L = 2 transitions do not have a strong collectivity as seen in B(E2) value for the E2 transition between a first 2^+ state and a ground state. The quadrupole-pairing states have only transition strengths in the range of about 30% to 50% of the sum-rule values. In nuclei for N > 82, our theory predicts an existence of one more strong transition to a 2^+ state that lies higher in energy by about 1 MeV than the quadrupole-pairing state. The sum of the transition strengths for the first, quadrupole-pairing and the third 2^+ states add up to about 80 $\sim$90% of the sum-rule value.

The (p,t) reaction cross sections associated with the quadrupole-pairing and the third 2^+ states have a strong dependence on the incident proton energy and show a broad resonance-like peak with a maximum value around 30 MeV. This is due to the change in an overlap integral of the distorted waves and the form factor as the incident energy varies.

In nuclei for N < 82, a situation for an enhancement of the (p,t) transition to the first 2^+ state resembles that for the quadrupole-pairing and third 2^+ states in nuclei N > 82. Other strong L = 2 transitions in

---

*) Their definitions of the strength of the quadrupole-pairing force are related to ours as follows: G_2 (Udagawa et al.) = $5G_2$ (ours) and G_2 (Bés et al.) = $\frac{50}{16\pi}\left(\frac{m\omega_o}{\hbar}\right)^2 G_2$ (ours).

the (p,t) reactions on these nuclei are not seen in the range of the excitation energy below 10 MeV.

The formalism to describe the 2^+ states developed in this paper can not be applied to the closed shell nuclei since these are in the normal phase. However, the properties of a nucleus two neutrons removed or added from the closed shell nucleus are well described by the calculations for nucleus in the superconducting phase.

It is well known that in the case of only quadrupole force, the strength constant $V_2^c = V_2 A^{5/3}$ taken to fit the excitation energy of the first 2^+ state increases as the closed shell is approached. If an appropriate value of $G_2^c = G_2 A^{5/3}$ is used, however, one can well reproduce variations of the excitation energy of the first 2^+ state with the atomic mass number A with a constant value of the strength V_2^c. In our calculations, B(E2) values for the transition between the first 2^+ state and the ground state are found to be in good agreement with the experimental data by taking the effective charge $e_{eff} = 0.5e$.

References

1) K. Yagi, Y. Aoki, J. Kawa and K. Sato, Phys. Lett. 29B (1969) 647;
K. Yagi, K. Sato and Y. Aoki, J. Phys. Soc. Japan 31 (1971) 1838

2) Y. Ishizaki, Proc. Phys. Soc. Japan 26 (1971) 147

3) H. Taketani, M. Adachi, M. Ogawa, K. Ashibe and T. Hattori, Argonne National Laboratory Report PHY-1972H (1972) p.394

4) S. Yoshida, Nucl. Phys. 33 (1962) 685

5) T. Marumori, Prog. Theor. Phys. 24 (1960) 331;
R. Arvieu and M. Véneroni, Compt, rend. 250 (1960) 992;
M. Baranger, Phys. Rev. 120 (1960) 957;
T. Tamura and T. Udagawa, Prog. Theor. Phys. 26 (1961) 947;
S. Yoshida, Nucl. Phys. 38 (1962) 38

6) T. Udagawa, T. Tamura and T. Izumoto, Phys. Lett. 35B (1971) 129

7) A. Bohr, Proc. Intern. Symp. on Nuclear Structure (Dubna,1968) p.179

8) J. B. Ball, R. L. Auble, J. Rapaport and C. B. Fulmer, Phys. Lett. 30B (1969) 533

9) D. R. Bes, G. G. Dussel and J. Gratton, Proc. Intern. Nuclear Physics Conference, eds. R. L. Becker et al. (Gatlinburg, 1966) p.499

10) N. N. Bogoliubov, Nuovo Cim. 7 (1958) 794;
J. G. Valatin, Nuovo Cim. 7 (1958) 843

11) J. Bardeen, L. N. Cooper and J. R. Schrieffer, Phys. Rev. 108 (1957) 1175

12) N. K. Glendenning, Phys. Rev. 137 (1965) B102

13) C. L. Lin, Prog. Theor. Phys. 36 (1966) 251

14) R. A. Broglia, C. Riedel and T. Udagawa, Nucl. Phys. A135 (1969) 561

15) T. Takemasa, M. Sakagami and M. Sano, Phys. Rev. Lett. 29 (1972) 133

16) T. Takemasa, M. Sakagami and M. Sano, Phys. Lett. 37B (1971) 473

17) F. G. Perey, Phys. Rev. 131 (1963) 745;
J. B. Ball, R. L. Auble and R. M. Drisko, Phys. Rev. 177 (1969) 1699

18) R. Chapman, W. Mclatchie and J. E. Kitching, Nucl. Phys. A186 (1972) 603

19) R. J. Ascuitto and N. K. Glendenning, Phys. Rev. C2 (1970) 1260;
N. K. Glendenning, Proc. Intern. Conf. on Properties of Nuclear States, eds. M. Harvey et al. (Les Presses de L'Université de Montreal, Canada, 1969) p.245

20) T. Tamura, D. R. Bés, R. A. Broglia and S. Landowne, Phys. Rev. Lett 25 (1970) 1507;
R. J. Ascuitto, N. K. Glendenning and B. Sorensen, Phys. Lett. 34B (1971) 17;
C. H. King, R. J. Ascuitto, N. Stein and B. Sorensen, Phys. Rev. Lett. 29 (1972) 71

21) K. Yagi, K. Sato, Y. Aoki, T. Udagawa and T. Tamura, Phys. Rev. Lett. 29 (1972) 1334

22) D. R. Bés, R. A. Broglia and B. Nilsson, Phys. Lett. 40B (1972) 338

Table Captions

Table 1. Single particle energies (MeV).

Table 2. Optical potential parameters[17] for proton and triton.

Table 3. The (p,t) and (t,p) cross sections relative to the ground state transition for the 2^+ states of Nd isotopes. The cross section σ represents the sum of the differential cross sections taken for 5° intervals in the range of 5° to 40°. The 2^+_{qp} and 2^+_3 states are defined in the text and their excitation energies E_x are given in units of MeV. The results for case I and II were obtained by using the sets I and II of the single-particle levels listed in table 1. The strengths of the quadrupole-pairing interaction were taken as follows: $G_2 = 30.7A^{-5/3}$ MeV for case I and $G_2 = 26.0A^{-5/3}$ MeV for case II.

Table 4. Sum rule values for (p,t) and (t,p) reaction strengths. The sum-rule value S is given by the sum of the spectroscopic factor over various 2^+ state of residual nucleus. The spectroscopic factors S_n for the first 2^+ state, the quadrupole pairing state and the third 2^+ state were calculated for $G_2 = 0.0$, 0.006 and 0.007 MeV by using the single-particle levels for case II.

Table 5. The (p,t) cross sections for Ba isotopes. The cross section σ represents the sum of the differential cross sections taken for 5° steps in the range of 5° to 40°. The calculations were made with the pairing interaction strengths $G_0^p = 22.0A^{-1}$ MeV, $G_0^n = 17.0A^{-1}$ MeV and $G_2 = 20.7A^{-5/3}$ MeV by using the single-particle levels for case II.

Figure Captions

Fig. 1. The (p,t) cross sections of the ground-state transition as a function of neutron number.

Fig. 2. Angular distributions of the (p,t) reactions leading to the ground state and DWBA fits.

Fig. 3. The summed (p,t) cross sections relative to the ground-state transition cross section for 2^+ states of ^{146}Nd plotted as a function of G_2. The interaction strength G_2 = 0.0064 MeV can reproduce the experimental data for the quadrupole pairing state of ^{146}Nd.

Fig. 4. Angular distributions of the (p,t) reactions leading to the 2^+ states of Nd isotopes and DWBA fittings.

Fig. 5. Angular distributions of the (p,t) reactions leading to the first 2^+ states of Ba isotopes and DWBA fittings. The solid line denotes the calculated values with the quadrupole plus the quadrupole pairing forces and the dashed line denotes the results calculated with only the quadrupole force.

Fig. 6. Incident-proton energy dependence of the summed cross sections for the ground-state and the 2^+ state transitions.

Fig. 7. Form factors of the (p,t) reactions leading to the 2^+ states. The solid lines denote the results calculated with the quadrupole plus the quadrupole pairing forces and the dashed lines denote the results calculated with only the quadrupole force.

Fig. 8. Schematic representation of possible distributions of two-quasiparticle states coupled to 2^+ in ^{146}Nd. The 2^+ states shown in (a), (b), and (c) are composed of levels above the closed shell at N = 82, of levels above and below the closed shell, and of

levels below the closed shell, respectively. The lengths of the vertical bar give values of $(V_{j_1} V_{j_2})^2$, $V_{j_1} V_{j_2} U_{j_1} U_{j_2}$, and $V_{j_1} V_{j_2} (U_{j_1} V_{j_2} + U_{j_2} V_{j_1})$, which are factors in the spectroscopic amplitude related to the occupation of two-quasiparticle levels.

Neutron			Proton	
Nℓj	CASE I	CASE II	Nℓj	E_{sp}
$5p_{1/2}$	-2.761	-2.761	$5h_{11/2}$	-1.173
$5f_{5/2}$	-3.129	-3.129	$4d_{3/2}$	-0.117
$5p_{3/2}$	-4.169	-4.169	$4s_{1/2}$	0.0
$6i_{13/2}$	-2.018	-2.018	$4g_{7/2}$	-2.347
$5h_{9/2}$	-3.113	-3.113	$4d_{5/2}$	-2.151
$5f_{7/2}$	-4.991	-4.991	$4g_{9/2}$	-5.867
$5h_{11/2}$	-9.363	-8.182	$3p_{1/2}$	-6.672
$4d_{3/2}$	-8.659	-7.478	$3f_{5/2}$	-7.900
$4s_{1/2}$	-8.925	-7.744	$3p_{3/2}$	-7.705
$4g_{7/2}$	-9.919	-8.737		
$4d_{5/2}$	-10.935	-9.754		

Table 1.

	V (MeV)	r_R (F)	a (F)	W (MeV)	W_D (MeV)	r_I (F)	a_I (F)	r_C (F)
Proton	45.1	1.21	0.593	0.0	22.81	1.21	0.593	1.25
Triton	170.1	1.15	0.74	19.0	0.0	1.52	0.76	1.40

Table 2.

Final Nucleus	I^π	Exp.			CASE I			CASE II		
		E_x	σ(p,t)	σ(t,p)	E_x	σ(p,t)	σ(t,p)	E_x	σ(p,t)	σ(t,p)
^{144}Nd	0^+	0.0	100	100	0.0	100	100	0.0	100	100
	2^+_1	0.695	7	118	0.695	11	103	0.695	4	83
	2^+_{qp}	3.48	92		4.3	36		3.50	95	
	2^+_3				5.5	128		4.18	116	
^{146}Nd	0^+	0.0	100	100	0.0	100	100	0.0	100	100
	2^+_1	0.453	13	45	0.453	5	50	0.453	5	74
	2^+_{qp}	3.74	73		4.8	73		3.75	73	
	2^+_3				6.6	75		4.75	52	
^{148}Nd	0^+	0.0	100	100	0.0	100	100	0.0	100	100
	2^+_1	0.300	29	46	0.300	6	14	0.300	3	41
	2^+_{qp}	3.83	198		5.1	84		4.02	55	
	2^+_3				7.3	50		5.37	8	

Table 3

Final Nucleus	G_2	2_1^+		2_{qp}^+		2_3^+		Sum Rule	
		$S_1(p,t)$	$S_1(t,p)$	$S_{qp}(p,t)$	$S_{qp}(t,p)$	$S_3(p,t)$	$S_3(t,p)$	$S(p,t)$	$S(t,p)$
^{144}Nd	0.0	3.63	47.05	9.14	0.59	3.58	0.01	192.29	315.29
	0.006	0.43	187.09	54.07	0.36	78.52	0.00		
	0.007	15.86	278.56	74.03	0.02	64.00	0.00		
^{146}Nd	0.0	7.12	52.79	13.82	0.41	8.80	0.05	207.51	283.04
	0.006	0.43	153.76	75.93	5.23	65.77	0.07		
	0.007	23.32	225.60	107.45	5.80	75.74	0.08		
^{148}Nd	0.0	8.97	48.94	7.32	1.33	8.38	2.08	225.42	254.20
	0.006	0.27	122.54	79.69	2.49	3.42	0.96		
	0.007	28.10	185.78	105.27	2.42	59.29	0.78		

Table 4

Final Nucleus	I^π	Exp.		Theor.	Spectroscopic Factor	Sum Rule
		E_x	$\sigma(p,t)$	$\sigma(p,t)$	$S_1(p,t)$	$S(p,t)$
^{136}Ba	0^+	0.0	100	100	—	—
	2_1^+	0.818	182	185	110.3	153.4
^{134}Ba	0^+	0.0	100	100	—	—
	2_1^+	0.605	71	71	77.5	128.7
^{132}Ba	0^+	0.0	100	100	—	—
	2_1^+	0.464	41	28	50.4	107.9
^{130}Ba	0^+	0.0		100	—	—
	2_1^+	0.356		9	27.0	90.1

Table 5.

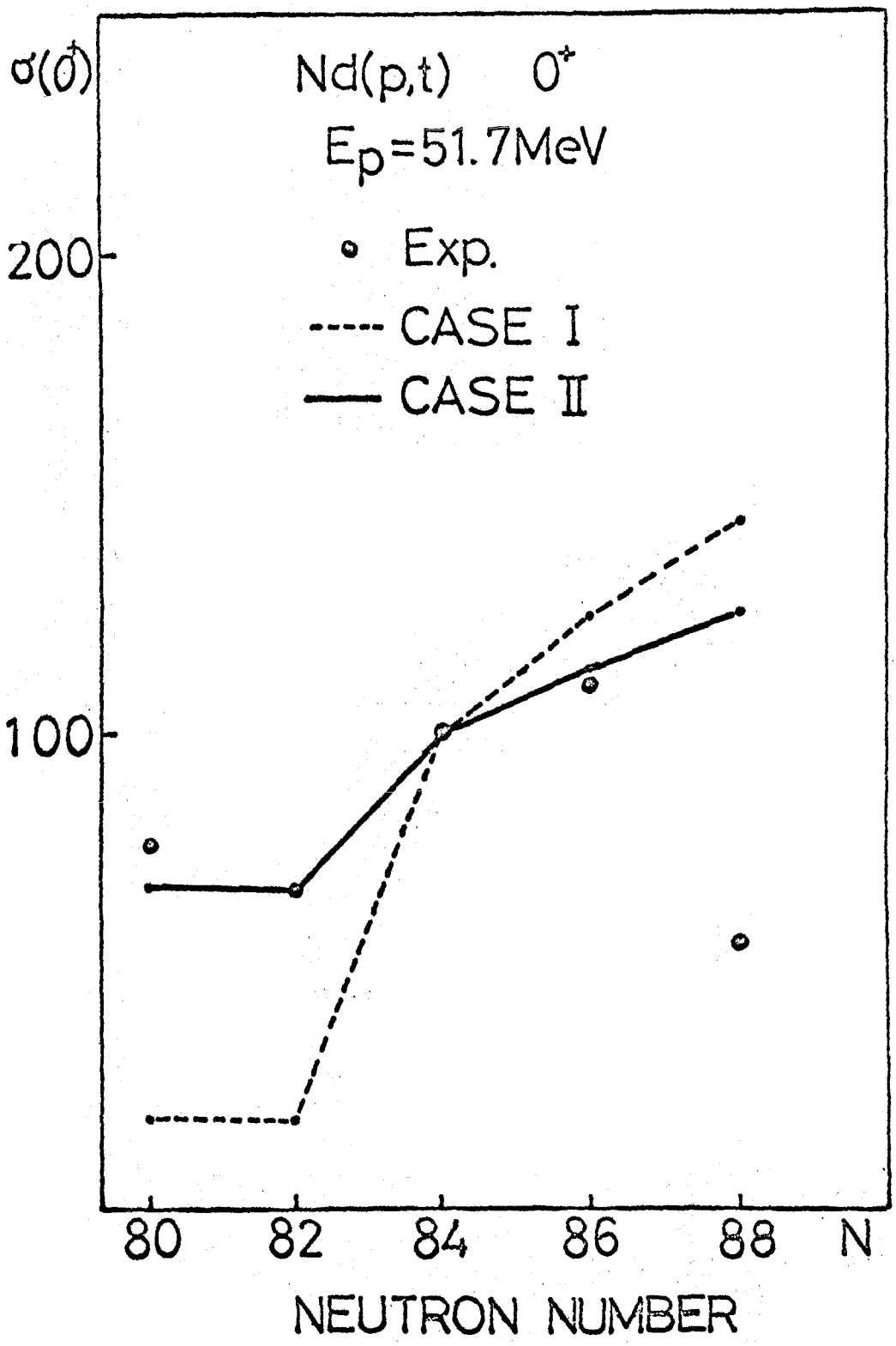
σ(0°)
Nd(p,t) 0+
Ep=51.7MeV
Exp.
CASE I
CASE II
200
100
80
82
84
86
88
N
NEUTRON NUMBER

Fig. 1

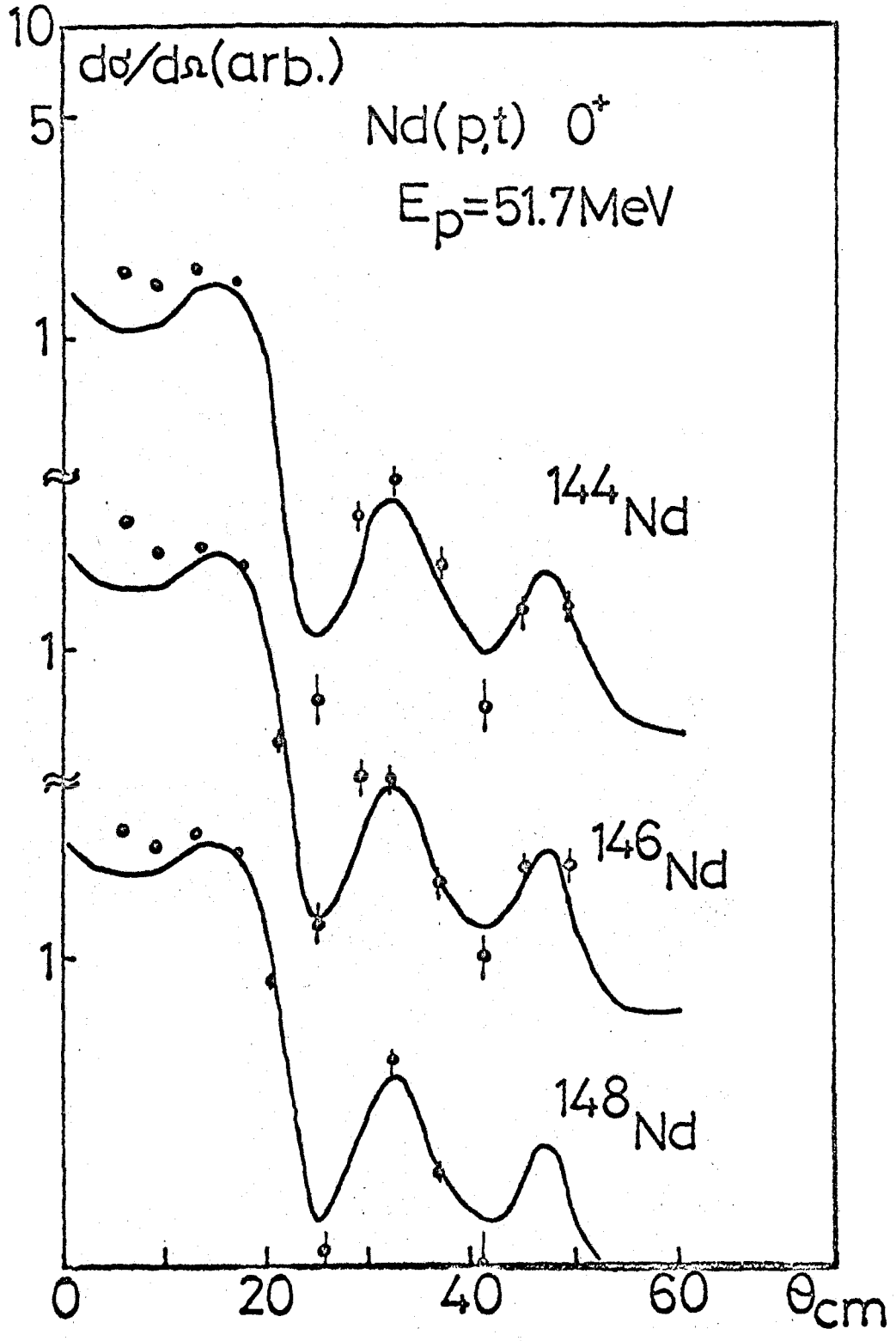
10
dσ/dΩ(arb.)
5
Nd(p,t) 0+
Ep=51.7MeV
1
144Nd
1
146Nd
1
148Nd
0
20
40
60
θcm

Fig. 2

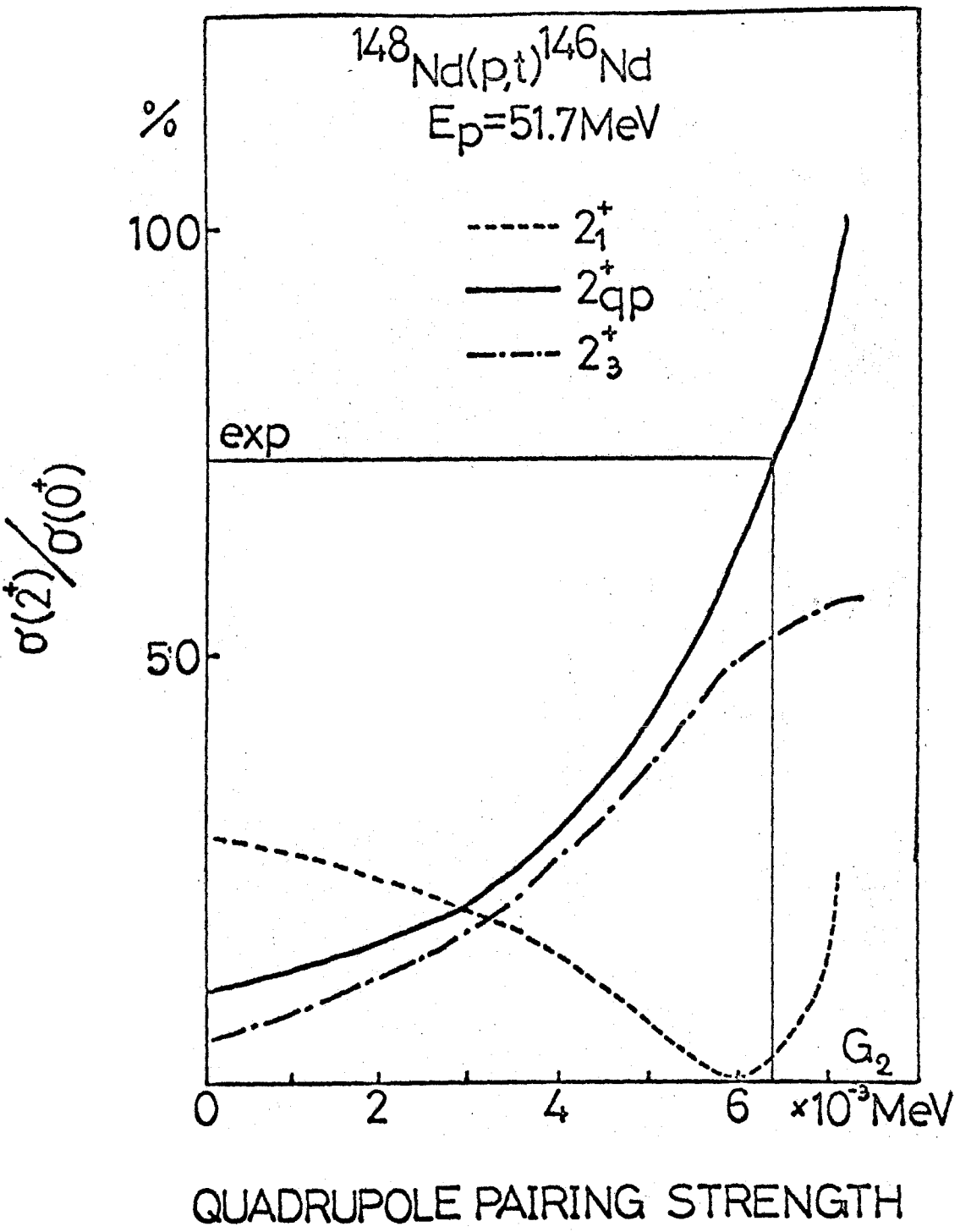
$^{148}Nd(p,t)^{146}Nd$
E_p=51.7MeV
%
100
50
$\sigma(2^+)/\sigma(0^+)$
2_1^+
2^+_{qp}
2_3^+
exp
G_2
0
2
4
6
$\times 10^{-3}$MeV
QUADRUPOLE PAIRING STRENGTH

Fig 3

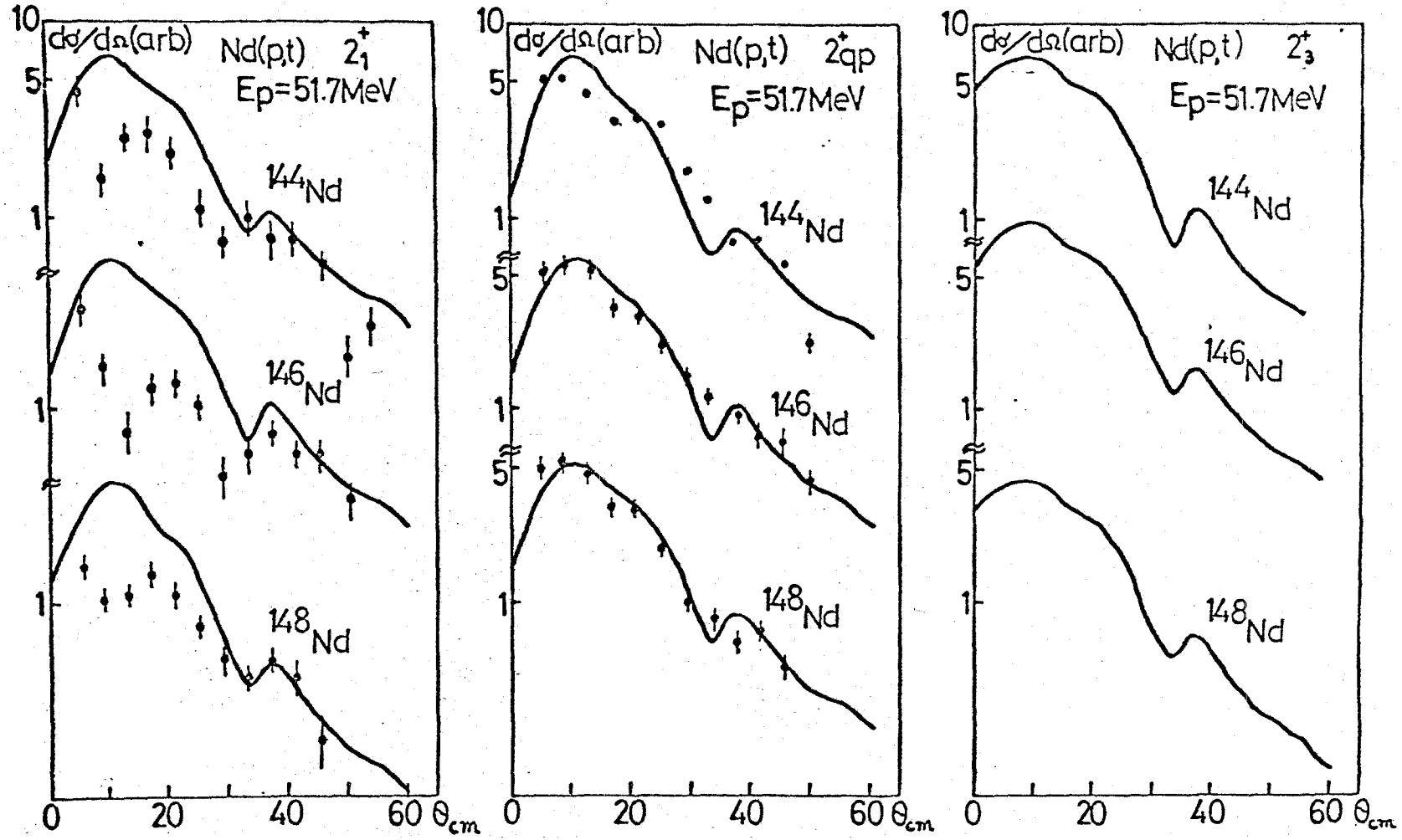
dσ/dΩ(arb)
Nd(p,t) 2₁⁺
Ep=51.7MeV
144Nd
146Nd
148Nd
dσ/dΩ(arb)
Nd(p,t) 2qp⁺
Ep=51.7MeV
144Nd
146Nd
148Nd
dσ/dΩ(arb)
Nd(p,t) 2₃⁺
Ep=51.7MeV
144Nd
146Nd
148Nd
10
5
1
5
1
5
1
0
20
40
60
θcm

Fig. 4

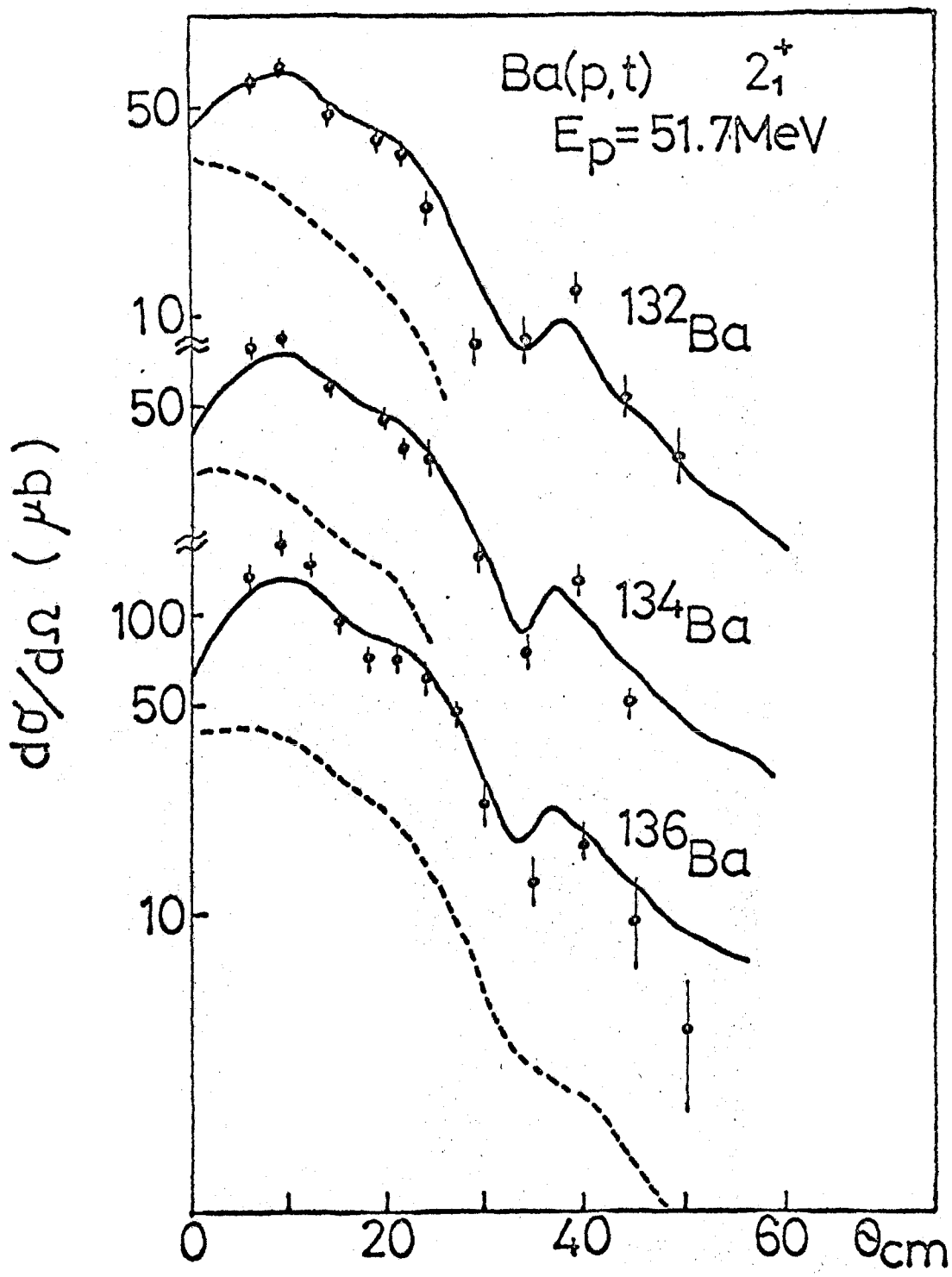
Ba(p,t) 2_1^+
E_p= 51.7MeV
^{132}Ba
^{134}Ba
^{136}Ba
50
10
50
100
50
10
0
20
40
60
θ_{cm}
$d\sigma/d\Omega$ (μb)

Fig. 5

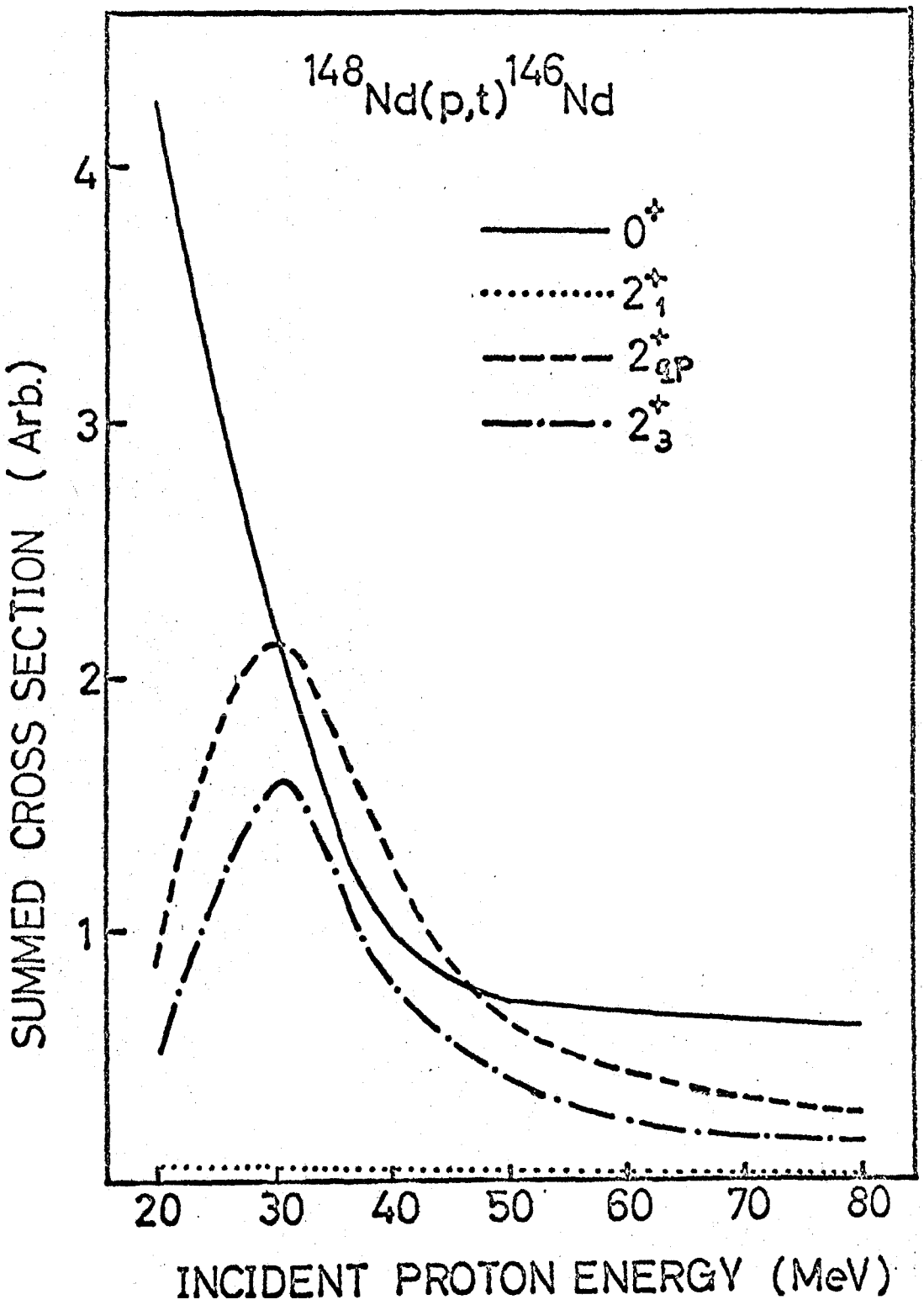
$^{148}Nd(p,t)^{146}Nd$
0^+
2^+_1
2^+_{gp}
2^+_3
SUMMED CROSS SECTION (Arb.)
1
2
3
4
20
30
40
50
60
70
80
INCIDENT PROTON ENERGY (MeV)

Fig. 6

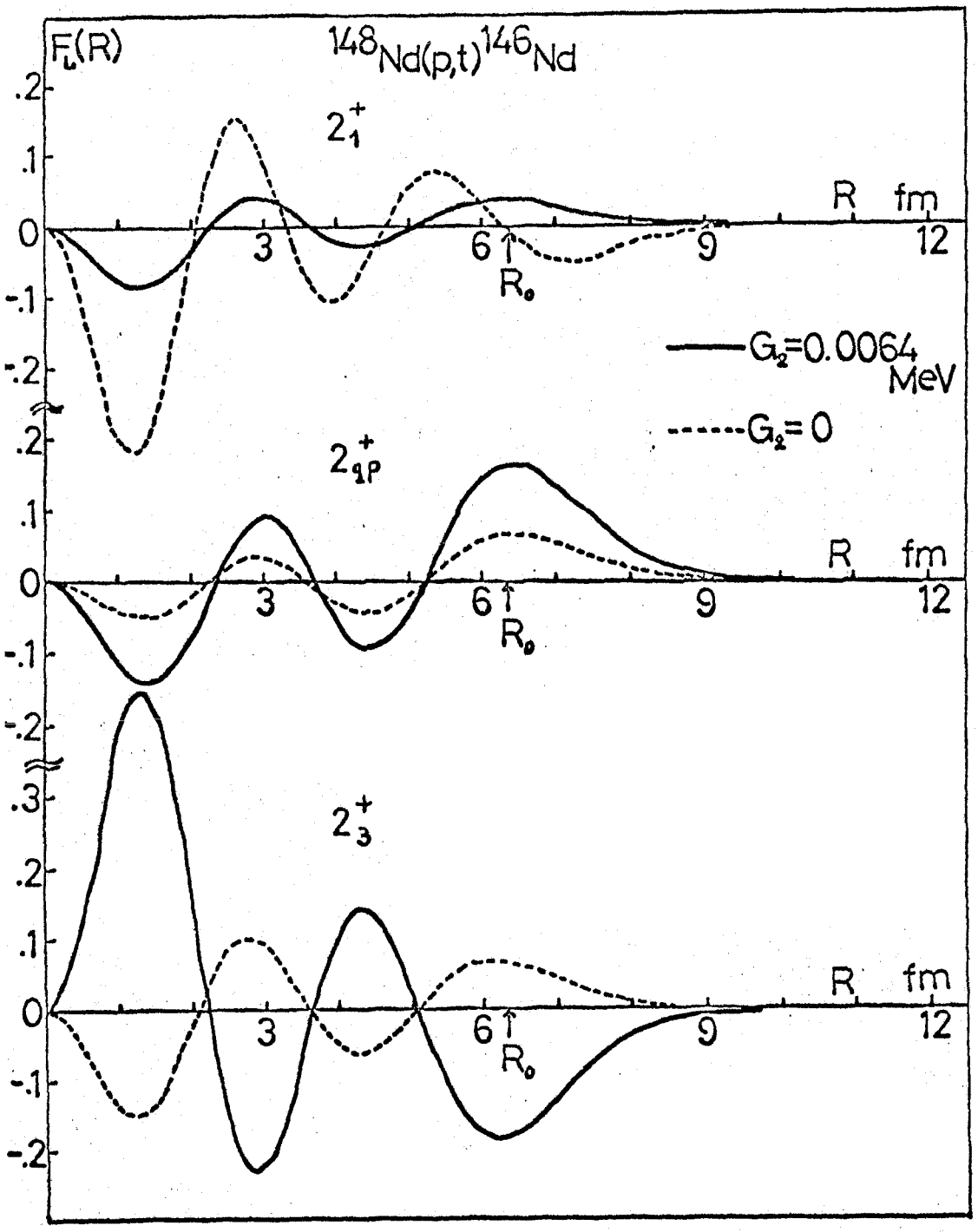
$F_L(R)$
$^{148}Nd(p,t)^{146}Nd$
2_1^+
2_{1P}^+
2_3^+
R fm
R_0
G_2=0.0064 MeV
G_2=0
.2
.1
0
-.1
-.2
.3
3
6
9
12

Fig. 7

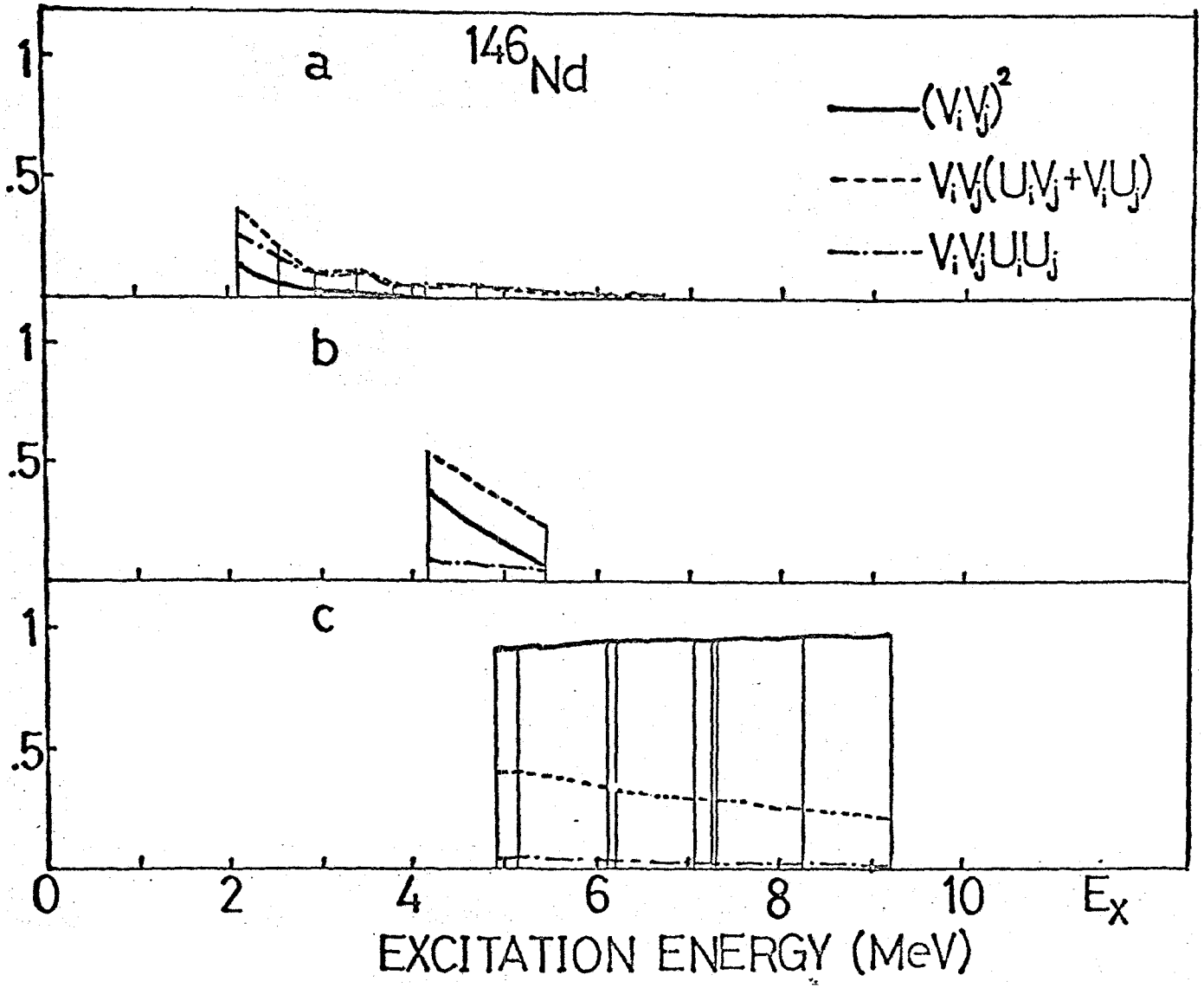
a
^{146}Nd
$(V_iV_j)^2$
$V_iV_j(U_iV_j+V_iU_j)$
$V_iV_jU_iU_j$
b
c
1
.5
0
2
4
6
8
10
E_x
EXCITATION ENERGY (MeV)

Fig. 8

CHAPTER 3 Unified Understanding of the (p,t) Reaction on Nd isotopes

1. Introduction

In the preceding chapter we discussed how the quadrupole-pairing states were reproduced by taking into account the quadrupole-pairing force.[1] The (p,t) intensities of the 2^+ states relative to that of the ground state were well reproduced in terms of the distorted-wave Born-approximation, but the angular distribution patterns of the first 2^+ states could not be reproduced. As discussed in the previous chapter, the angular distributions for the weak transitions were shown by Yagi et. al.[2] to be reasonably accounted for in terms of the coupled-channel Born-approximation calculations. The code of such a two-step process-calculation is now available by efforts of Toyama and Igarashi,[3] which is INS code TWOSTP.

The purpose of this chapter is to show the numerical results in terms of the two-step process-calculation for the first 2^+ states. For the nuclear-structure calculation, in the previous chapter, the parameers of the interaction strengths were decided so as to reproduce the (p,t) strength leading to the quadrupole pairing state. In this chapter these parameters are decided so as to reproduce the over all trend of the excitation energies of the first 2^+ states of the Nd isotopes. These parameters decided by the different methods are almost same. The excitation energies, B(E2) values and the (p,t) strengths of the 2^+ states of the Nd isotopes were calculated and shown in the next section.

2. Calculations

The details about the two-step process-calculation will be discussed

in chapter 6. In this chapter only the calculated results for the (p,t) reactions leading to the 2^+ states of the Nd isotopes are shown.

The parameter sets of G_2^c and V_2^c are shown in fig. 1, which are taken so as to reproduce the experimental-excitation energies of the first 2^+ states. As can be seen in fig. 1, there is a point into which the parameter sets concentrate. Thus, we can obtain the values G_2^c and V_2^c which reproduce the excitation energies of the first 2^+ states of the spherically stable nuclei. The values are G_2^c = 24.75MeV and V_2^c = 33.18MeV. These values are comparable with ones which were used in the previous chapter. The excitation energies and the B(E2) values of the first 2^+ states are shown in fig. 2, using these values. In order to compare the case of Q-Q force only, we also show the results using V_2^c = 34.76MeV, which are taken so as to fit the excitation energy of the first 2^+ state of ^{148}Nd.

The excitation energies and the B(E2) values for the case of P_2-P_2 plus Q-Q forces are fairly well reproduced, and at N = 92 the first 2^+ state does not have a positive energy. This situation will be discussed in chapter 4. The cross sections of the (p,t) reactions are calculated in terms of the distorted-wave Born-approximation. The calculated and the experimental results are listed in table 1. All the parameters except for the strengths of the forces are the same as (mentioned in) the previous chapter.

For the angular distribution patterns of the first 2^+ state we calculated the cross sections of the first 2^+ states in terms of the two-step process-calculation. As will be discussed in chapter 6, the cross section of the second order process is too large compared to the experimantal one, if the macroscopec form factor is used and the deformation parameter β, which is equal to the experimental value taken from the

B(E2) value, is used. Then we take the effective β value as $\beta_{eff} = \alpha\beta_{exp}$ ($\alpha \leq 1$) and asume α is a parameter. When $\alpha = \frac{1}{2}$ is used, the angular distribution pattern of the first 2^+ state becomes better than that of the distorted-wave Born-approximation calculation, which is shown in fig. 3. The relative ratios of the (p,t) intensities for the first 2^+ states to the ground states are also listed in table 1. The agreement with experiment is better than in the case of the distorted-wave Born-approximation. For other 2^+ states the second-order process does not contribute, because the cross section of the inelastic scattering is negligibly small.

The calculated and experimental angular distributions of the (p,t) reaction leading to the first 2^+ states are shown in fig. 3. In fig. 4 the components of each processes are shown. It can be seen that the direct process amplitude and the second-order processes amplitudes interfere destructively with each other and then the abnormal angular-distribution pattern is obtained. The detailed discussions of the two-step process and the relation between the random-phase approximation and the Hartree-Fock-Bogoliubov equation will be discussed in the following chapters.

References

1) H. Toki and M. Sano, OULNS 73-6 (1973) and to be published.

2) K. Yagi, K. Sato, Y. Aoki, T. Udagawa and T. Tamura, Phys. Rev. Lett. 29 (1972) 1334

3) M. Toyama and M. Igarashi, INS code TWOSTP (1972) and private communication

Table Caption

Table 1. The excitation energies, B(E2) values, (p,t) and (t,p) cross sections of the 2^+ states of Nd-isotopes. The cross section σ represents the sum of the differential cross sections taken for 5^c intervals in the range of 5° to 40°, and normalized to the cross section of the ground state. Effective charge is used as $e_{eff} = 0.7e$ for the B(E2) values. All the cross sections are calculated in terms of the distorted-wave Born-approximation. The cross sections for the first 2^+ state are also calculated in terms of the two-step process-calculation. σ(p,t) of the first 2^+ states is the TSP-cross section and the number in the parenthesis is the DWBA one.

Figure Captions

Fig. 1. Parameter sets of G_2^c and V_2^c , which reproduce the excitation energies of the first 2^+ states.

Fig. 2. Experimental and theoretical excitation energies and B(E2) values. Dots with bar are the experimental values. The solid lines denotes the calculated values , using the interaction composed of Q-Q and P_2-P_2 forces, and the dotted line denotes ones using Q-Q force only.

Fig. 3. Angular distribution of the (p,t) reaction leading to the first 2^+ state of ^{146}Nd. The TSP curve is denoted as the solid line and the DWBA curve as the dotted line, which are arbitrary normalized to the experimental data.

Fig. 4. The cross sections of each process. The solid line denotes the result obtained by mixing suitably these three processes.

		Experiment				Theory			
Nucl.	J^π	E_x	BE2	σ(p,t)	σ(t,p)	E_x	BE2	σ(p,t)	σ(t,p)
	0^+	0.0	-	100	100	0.0	-	100	100
^{144}Nd	2^+_1	0.695	4.0±1.5	7	118	0.750	4.15	7 (5)	93
	2^+_{qp}	3.48	-	92	-	3.38	0.16	84	4
	2^+_3	4.3	-	29	-	4.03	0.04	40	0
	0^+	0.0	-	100	100	0.0	-	100	100
^{146}Nd	2^+_1	0.453	8.5±2.5	13	45	0.456	6.79	10(1)	57
	2^+_{qp}	3.74	-	73	-	3.78	0.16	54	3
	2^+_3	4.4	-	47	-	4.75	0.01	32	0
	0^+	0.0	-	100	100	0.0	-	100	100
^{148}Nd	2^+_1	0.300	13.0±5.0	29	46	0.268	11.83	22(1)	43
	2^+_{qp}	3.83	-	198	-	4.08	0.11	46	1
	2^+_3	4.5	-	78	-	5.35	0.0	16	0

Table 1

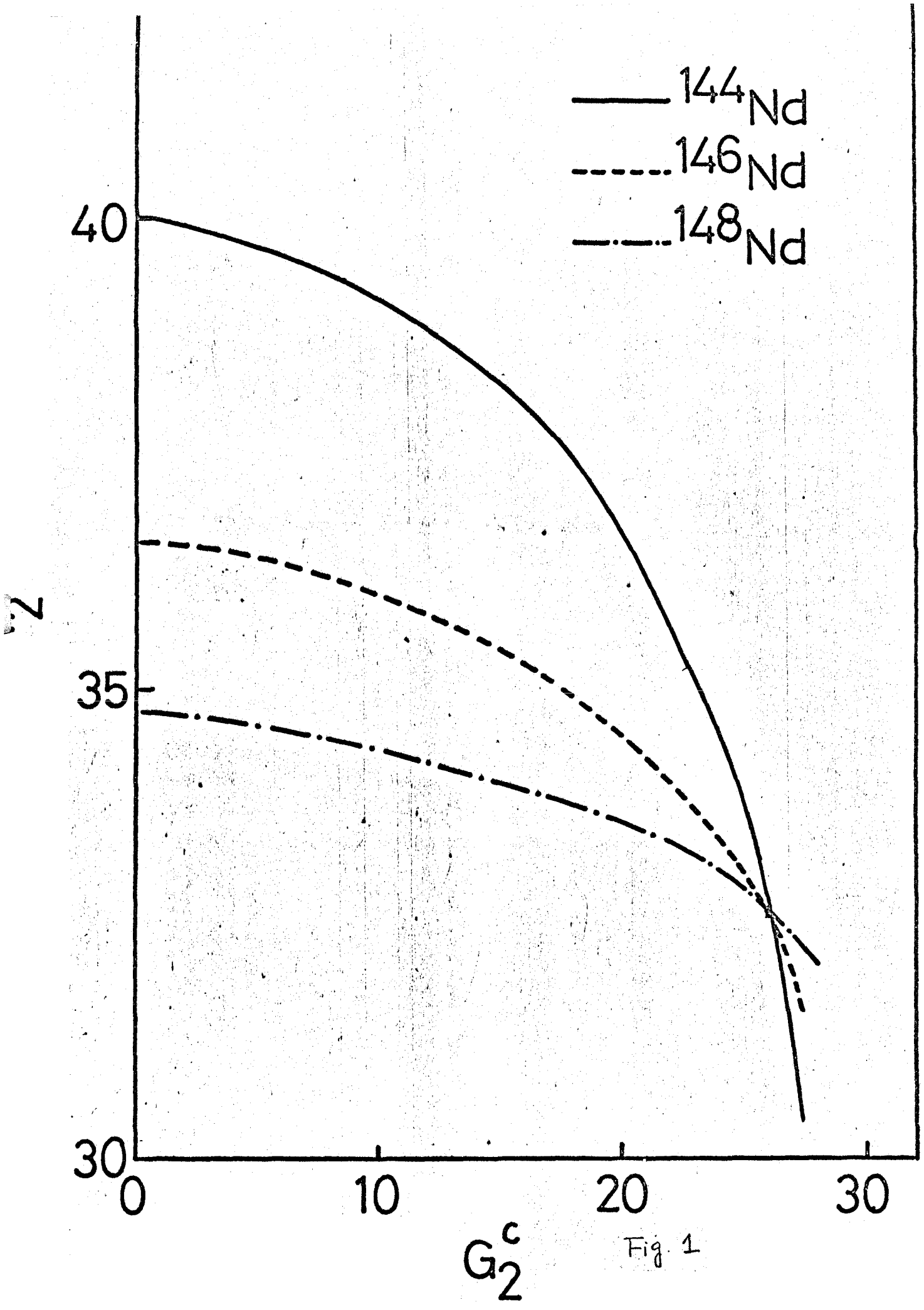

Fig. 1

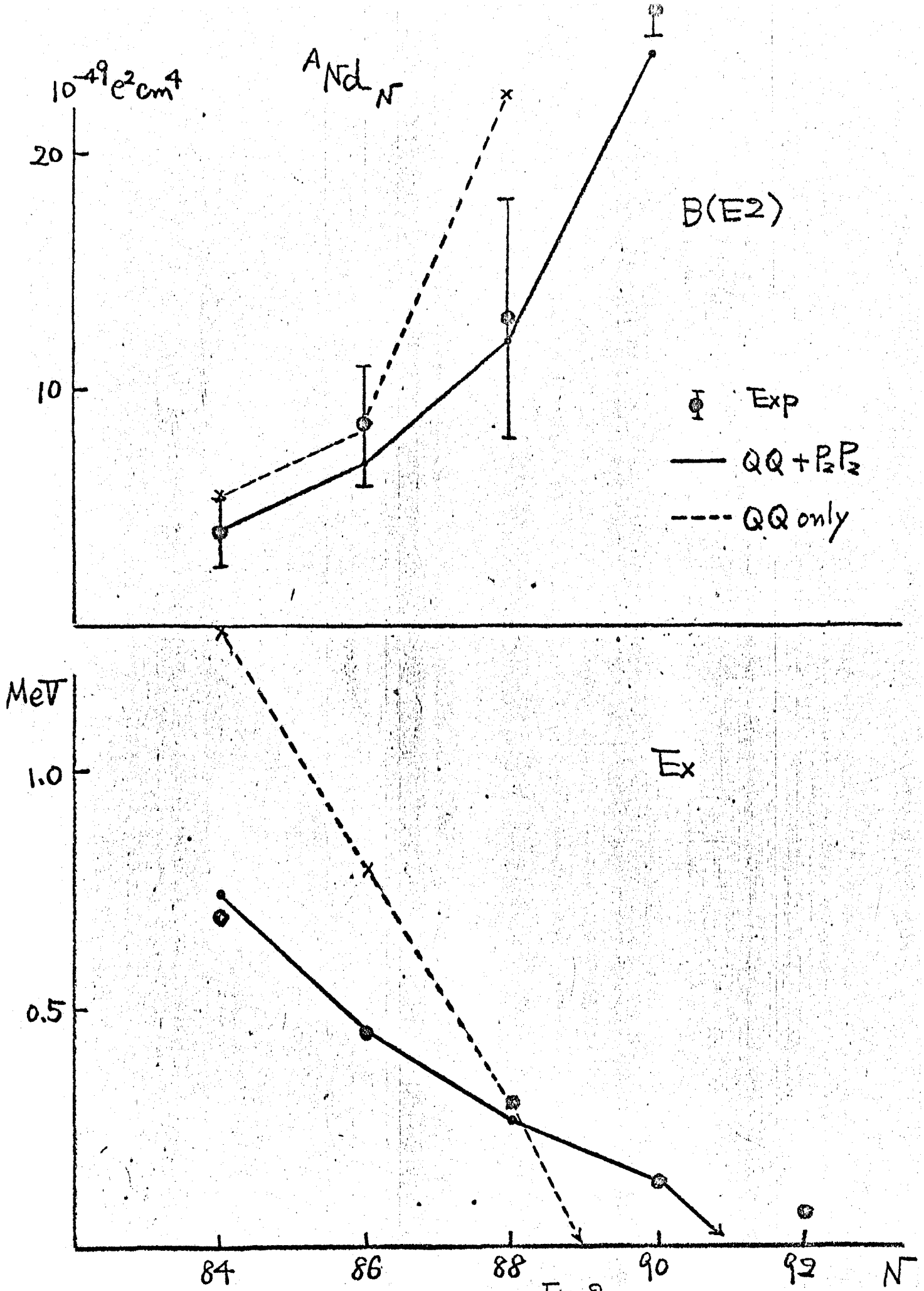
$10^{-49} e^2 cm^4$
A_{Nd_N}
20
10
B(E2)
Exp
QQ + P₂P₂
QQ only
MeV
1.0
0.5
Ex
84
86
88
90
92
N

Fig. 2

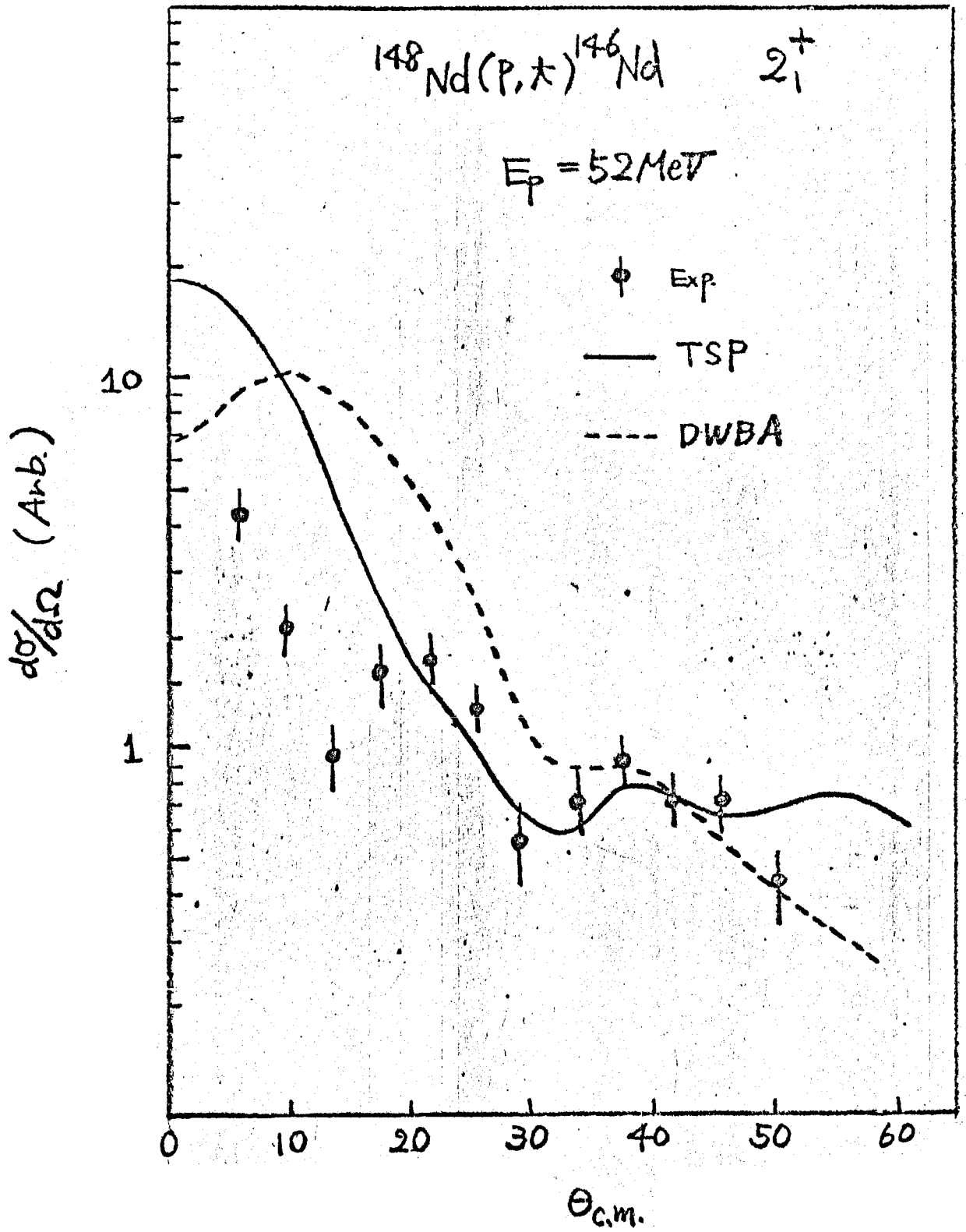
$^{148}Nd(p,t)^{146}Nd$ 2_1^+
$E_p = 52 MeV$
Exp.
TSP
DWBA
10
1
$d\sigma/d\Omega$ (Arb.)
0
10
20
30
40
50
60
$\theta_{c.m.}$

Fig.3

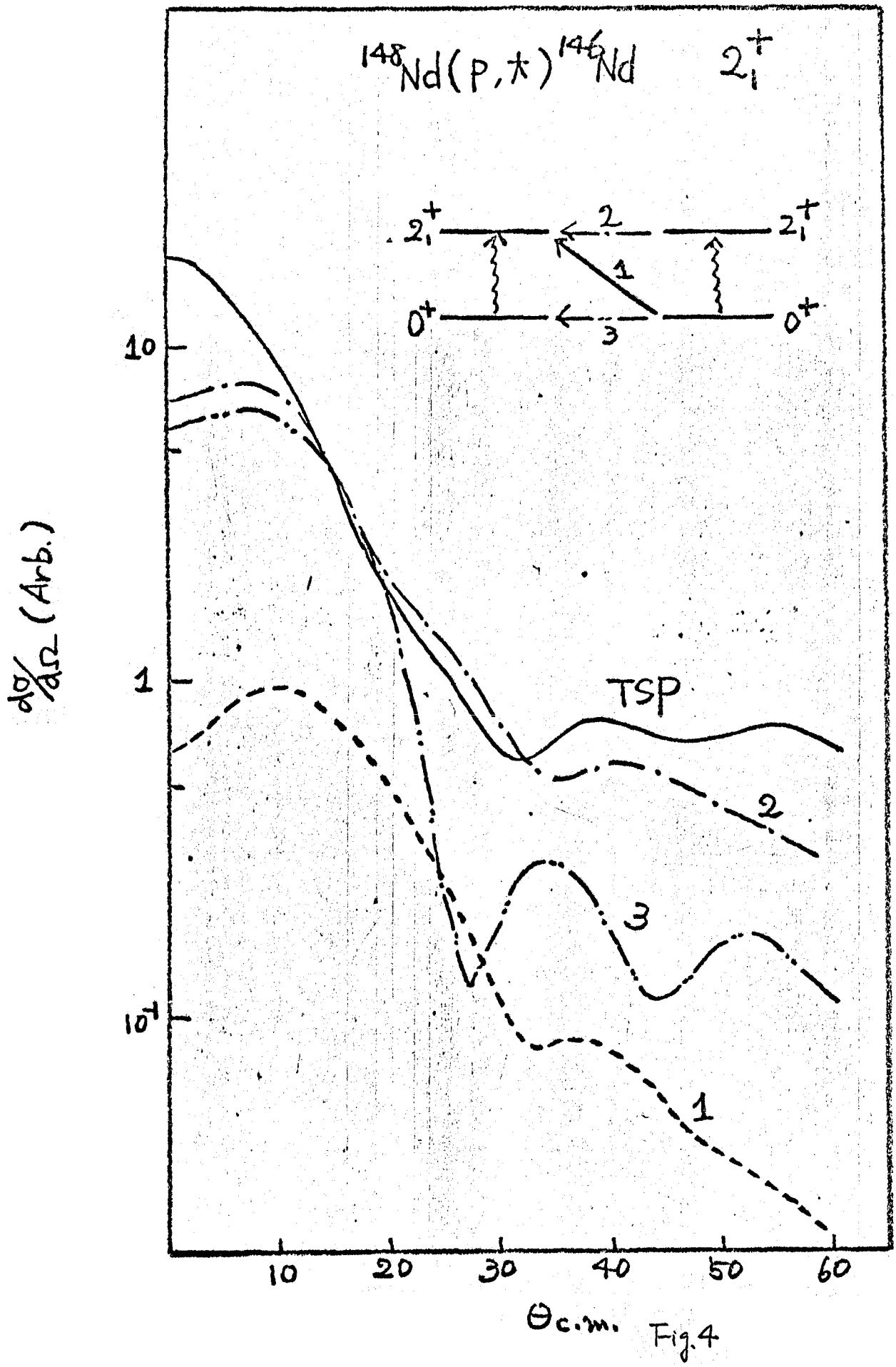
$^{148}Nd(P,t)^{146}Nd$ 2_1^+
2_1^+
2
2_1^+
1
0^+
3
0^+
10
1
10^{-1}
TSP
2
3
1
10
20
30
40
50
60
$\theta_{c.m.}$
$d\sigma/d\Omega$ (Arb.)

Fig.4

CHAPTER 4 Effects of $P_2 - P_2$ Force on 2_1^+ States in the Meadium and Heavy Nuclei

1. Introduction

So far 2^+ states in heavy spherical nuclei, especially first 2^+ states, have been discussed in the random-phase appromimation (RPA) by using a simple interaction composed of a monopole-pairing force and a quadrupole force (Q-Q).[1] Kisslinger and Sorensen have shown systematically the enhancement of B(E2) value for the transition between the first 2^+ state and the ground state using the simple model.[2] However, the strength constant $V_2^c = V_2 A^{5/3}$ of Q-Q force taken to fit the excitation energy of the first 2^+ state increases as the closed shell is approached. This is due to the fact that near the magic number the configuration of proton (or neutron) which is near the magic number can not contribute to the first 2^+ state, because of the large energy difference between the magic shells and the difference of the parity.

On the other hand, in order to explain the (p,t) strengths of the 2^+ states of Nd and Ba isotopes, the importance of the quadrupole-pairing force ($P_2 - P_2$) was pointed out by Toki and Sano[3] and discussed in the previous chapters. It was also indicated that if an appropriate value of $G_2^c = G_2 A^{5/3}$, the strength constant of $P_2 - P_2$ force, is used, we can well reproduce the variation of the excitation energy of the first 2^+ state with the atomic number A by using a constant value of the strength V_2^c.

As done in the previous chapter, we can obtain the strengths of these forces from nuclei which have spherical shape, and discuss the stability condition of spherical phase in terms of the spherical phase in

terms of the random-phase approximation.[4] Thus, the purpose of the present chapter is to show how well the exciation energy and B(E2) value of the first 2^+ state can be reproduced in terms of the random-phase approximation using an interaction composed of the quadrupole-pairing force and the quadrupole force and then where the instability of spherical phase happens. The calculation is especially focussed on the nuclei with the neutron number between 50 and 82: Cd, Te, Xe, Ba and Ce isotopes. There can be seen a rotational-like band in the nuclei below N = 70 of Xe, Ba and Ce isotopes, but it is not well studied. The energy ratio of the first 4^+ state to the first 2^+ state is not equal to 3.3, but is smaller than 3.0. This is in contrast with the rare-earth nucleus.

In sect.2 the relation between the stability condition of the Hartree-Fock Bogoliubov theory and the equation of the random-phase approximation are discussed. In sect.3 the numerical results are shown and comparison with experimental results are done. In sect.4 further posibilities are discussed.

2. Stability Condition of HFB Theory

In order to study nuclear structure we often have to use any model which starts from an independent particle model. Such independent particle states must be obtained by the Hartree-Fock Bogoliubov-method(HFB).[5] For actual convenience, however, we first assume independent particle states and calculate any excited state. We must investigate whether such independent particle states are stable or not. Such procedure is to investigate the stability condition of the Hartree-Fock Bogoliubov theory.[4),6)]

On the other hand, it is well known that the stability condition of the Hartree-Fock Bogoliubov theory has the contact relation with the equation of

the random-phase approximation. This was pointed out by Thoulless.[4] Following his prescription the point where the instability of the HFB-single particle states just happens coincides with the point where the solution of the random-phase approximation has zero energy. Thus, we can know the instability point of the phase by solving the equation of the random-phase approximation. The formal description is summarized in Appendix.

In nuclear physics, what phase a nucleus has will be of great importance. For example, it would not be possible to use ordinary perturbation theory to calculate the properties of a spheroidal nucleus starting from an independent particle model with spherical symmetry. It is one of the powerful points of the random-phase approximation (that it) does not have a positive solution when the instability of such a phase happens. For another model, such as Tam-Dancoff approximation or the diagonalization method of the shell model, we can not know the validity of the solutions of the models.

3. Calculations

In the previous chapter we discussed the case of Nd isotopes. The fit to the experimental excitation energies of the spherical nuclei is very good and the phase transition occurs at N = 92 in terms of the random-phase approximation. Our results support the shape-coexistence model around N = 90, which was done by Takemasa et al..[7]

In order to check the validity of our model, we took another experimental fact; that is the exitation energy of Cd and Te isotopes, proton number is 48 and 52 respectively. All the single-particle levels lying between 28 and 82 closed shells for protons and neutrons were taken. Single particle energies were listed in table 1. The strengths of the monopole-pairing force were set equal to $G_o = 23A^{-1}$MeV for protons and $G_o = 18A^{-1}$MeV for

neutrons. These values reproduce fairly well the experimental value of the gap energies.

The calculated and the experimental excitation energies are plotted against the neutron number in fig.1, using G_2^c = 26.0MeV and V_2^c = 29.3MeV. In order to compare the results with ones of the case of Q-Q force only, we also show them using V_2^c = 30.6MeV, which was taken so as to reproduce the excitation energy of ^{110}Cd. As can be seen in fig.1 the agreement with the experimental excitation energies is much better in the case of P_2- P_2 plus Q-Q force than in the case of Q-Q force only.

Further, we discuss the case of Xe, Ba and Ce isotopes, proton number is 54, 56 and 58 respectively, and neutron number is less than 80. In the calculations, all the single-particle levels lying between Z = 28 and 82 closed shells for protons and between N = 50 and 126 closed shells for neutrons were taken. Single particle energies were taken from the work of Toki et al., [3] which were denoted as case II in their paper. The strengths of the monopole-pairing force were set equal to $G_o = 23.2A^{-1}$MeV for protons and $G_o = 17.3A^{-1}$MeV for neutrons.

The parameter sets of V_2^c and G_2^c are shown in fig.2, which were decided so as to reproduce the experimental excitation energies of the first 2^+ states. As can be seen in fig.2, there is a point into which the parameter sets consentrate. Thus, we can obtain the values G_2^c and V_2^c which reproduce the excitation energies of the first 2^+ states of the spherical stable nuclei.

The excitation energies of the first 2^+ states are shown in fig.3 and listed in table 2., using G_2^c = 28.0MeV and V_2^c = 31.8MeV. This value of G_2^c is comparable with G_2^c = 26.0MeV, which has been decided from the (p,t) reaction on Nd isotopes. In order to compare the case of Q-Q force only,

we also show them using V_2^c = 34.2MeV, which was given from the experimental value of ^{130}Xe. The excitation energies for the case of P_2- P_2 plus Q-Q forces are fairly well reproduced, and the phase transition happens at N = 68 for Xe, N = 72 for Ba and N = 72 for Ce isotopes. This results is very interesting. The point at which the phase transition happens is different from an isotope to another.

From the G-matrix theory, which starts from the two-body interaction between nucleons, it is indicated that the strength of Q-Q force between unlike nucleons V_2(NP) must be larger than one between like nucleons V_2(NN) or V_2(PP). [8] However, the situations are not significantly changed, even if we take into account the difference between the strengths of Q-Q force; V_2(NP) ≒ V_2(PP) = V_2(NN).

In our calculation, B(E2) values for the transition between the first 2^+ states and the ground states are found to be in good agreement with the experimental values by taking the effective charge e_{eff} = 0.8e. The results are shown in table 2 with the experimental values and the results of Q-Q force only.

4. Conclusions

In this chapter the first 2^+ states in the medium-heavy nuclei have been studied in terms of the random-phase approximation with using the quadrupole-pairing force and the quadrupole force. The first 2^+ states are reproduced much better with P_2- P_2 plus Q-Q forces than with Q-Q force only. By using Q-Q force only, the phase transition happens rapidly, and this is contrary to the experimental facts. The quadrupole-pairing force may prevent a nucleus from having a deformed shape. Thus, 2^+ states in heavy spherical nuclei are well described in terms of the random-phase

approximation with using the quadrupole-pairing force and the quadrupole force.

It is very important to use the quadrupole-pairing force for the description of the 2^+ states, and then in all the calculations about the nuclear spectroscopy and the shape of nuclei [9], it is need to use the quadrupole-pairing force.

Appendix

1. Hartree-Fock-Bogoliubov equation

We consider a system of fermions with a spherically symmetric shell-model Hamiltonian

$$H = \sum_{\alpha} (\varepsilon_{\alpha} - \lambda) c_{\alpha}^{+} c_{\alpha} + \sum_{\alpha\beta\gamma\delta} V_{\alpha\beta\gamma\delta} c_{\alpha}^{+} c_{\beta}^{+} c_{\delta} c_{\gamma}, \tag{1}$$

where c_{α}^{+} and c_{α} are the creation and annihilation operators of a nucleon in the state α, ε_{α} the energy of this single particle state, and λ the chemical potential of the system. The interaction V has the following symmetry properties,

$$V_{\alpha\beta\gamma\delta} = -V_{\beta\alpha\gamma\delta} = -V_{\alpha\beta\delta\gamma} = V_{\gamma\delta\alpha\beta}^{*}. \tag{2}$$

We perform the generalized Bogoliubov transformation

$$a_{i}^{+} = \sum_{\alpha} (A_{\alpha}^{i} c_{\alpha}^{+} + B_{\alpha}^{i} c_{\alpha}). \tag{3}$$

The requirement that the a's also form a set of fermion operators entails the orthogonality relations

$$\begin{aligned}
&\sum_{\alpha} (A_{\alpha}^{i*} A_{\alpha}^{j} + B_{\alpha}^{i*} B_{\alpha}^{j}) = \delta_{ij}, \\
&\sum_{\alpha} (A_{\alpha}^{i} B_{\alpha}^{j} + B_{\alpha}^{i} A_{\alpha}^{j}) = 0, \\
&\sum_{i} (A_{\alpha}^{i} A_{\beta}^{i*} + B_{\alpha}^{i*} B_{\beta}^{i}) = \delta_{\alpha\beta}, \\
&\sum_{i} (A_{\alpha}^{i} B_{\beta}^{i*} + B_{\alpha}^{i*} A_{\beta}^{i}) = 0,
\end{aligned} \tag{4}$$

and the inverse relations

$$c_\alpha = \sum_i \left(A_\alpha^i a_i + B_\alpha^{i*} a_i^+ \right). \tag{5}$$

The new vacuum state $|0\rangle$ is defined by

$$a_i |0\rangle = 0 \tag{6}$$

We can obtain the Hartree-Fock-Bogoliubov equation from the requirement that the expectation value of the auxiliary Hamiltonian H in the new vacuum state must have a minimum value. Then A and B satisfy the following equations

$$\begin{aligned} &(\varepsilon_\alpha - \lambda) A_\alpha^i + \sum_\gamma \Gamma_{\alpha\gamma} A_\gamma^i + \sum_\beta \Delta_{\alpha\beta} B_\beta^i = E_i A_\alpha^i, \\ &-(\varepsilon_\alpha - \lambda) B_\alpha^i - \sum_\gamma \Gamma_{\alpha\gamma}^* B_\gamma^i - \sum_\beta \Delta_{\alpha\beta}^* A_\beta^i = E_i B_\alpha^i. \end{aligned} \tag{7}$$

The quantities Γ and Δ are defined by

$$\begin{aligned} \Delta_{\alpha\beta} &= -\Delta_{\beta\alpha} = 2 \sum_{\gamma\delta} V_{\alpha\beta\gamma\delta} \kappa_{\gamma\delta}, \\ \Gamma_{\alpha\gamma} &= \Gamma_{\gamma\alpha}^* = 4 \sum_{\beta\delta} V_{\alpha\beta\gamma\delta} \rho_{\beta\delta}, \\ \kappa_{\gamma\delta} &= -\kappa_{\delta\gamma} = \langle c_\delta c_\gamma \rangle = \sum_i A_\delta^i B_\gamma^{i*}, \\ \rho_{\beta\delta} &= \rho_{\delta\beta}^* = \langle c_\beta^+ c_\delta \rangle = \sum_i B_\beta^i B_\delta^{i*}, \end{aligned} \tag{8}$$

where the symbol $\langle \cdots \rangle$ denotes ground state expectation value. We see that $\Gamma_{\alpha\gamma}$ is the potential energy arising from the density δ of the particles and is the familiar Hartree-Fock self-consistent potential. On the other hand, $\Delta_{\alpha\beta}$ is the pairing potential arising from the pairing

density κ of the particles.

The expectation value of the Hamiltonian is given by

$$W = \langle H \rangle = \sum_{\alpha} (\varepsilon_{\alpha} - \lambda) \rho_{\alpha\alpha} + \frac{1}{2} \sum_{\alpha\beta} \Gamma_{\alpha\gamma} \rho_{\gamma\alpha} + \frac{1}{2} \sum_{\alpha\beta} \Delta_{\alpha\beta} \kappa_{\beta\alpha}^{*} . \qquad (9)$$

As usual, the chemical potential λ is determined by fixing the average number of particles

$$N = \langle \sum_{\alpha} c_{\alpha}^{+} c_{\alpha} \rangle = \sum_{\alpha} \rho_{\alpha\alpha} . \qquad (10)$$

The form of eq. (7) suggests the introduction of the Hermitian matrix

$$M = \begin{bmatrix} (\varepsilon - \lambda) + \Gamma & , & \Delta \\ -\Delta^{*} & , & -(\varepsilon - \lambda) - \Gamma^{*} \end{bmatrix} . \qquad (11)$$

The expectation value of H must be stationary against small change in ρ and κ. The variation of W with respect to ρ and κ can be written in terms of M as

$$\delta W = \frac{1}{2} \mathrm{Tr}\, M \cdot \delta K \qquad (12)$$

Here Tr means the trace and δK is the variation of the matrix K with the form

$$K = \begin{bmatrix} \rho & , & -\kappa \\ \kappa^{*} & , & 1 - \rho^{*} \end{bmatrix} \qquad (13)$$

The matrix K must follow the supplementary condition which deduces from the orthogonality relations of A and B in eq. (4).

$$K^2 = K. \tag{14}$$

Putting the result equal to zero for arbitary variation, we obtain the equation

$$[M, K] = 0, \tag{15}$$

where the bracket means the minus commutator. This is the matrix form of the Hartree-Fock-Bogoliubov equation which gives the stationary state.

2. Stability condition of the Hartree-Fock-Bogoliubov state

The condition that the first derivatives of the expectation value of the Hamiltonian with respect to ρ and κ should be zero gives the stationary state in the Hartree-Fock-Bogoliubov approximation. On the other hand, the condition that the second derivatives should be non-negative gives the absolute of the Hartree-Fock-Bogoliubov state. In this section we derive the stability condition in a general form.

We assume that $K^{(0)}$ is a solution of the stationary equation (15), and we wish to replace $\rho^{(0)}$ and $\kappa^{(0)}$ by ρ and κ containing arbitrary first- and second-order variations subject to the supplementary condition (14). Let μ be the parameter that defines the order of the variation. We write K and M as

$$K = K^{(0)} + \mu K^{(1)} + \mu^2 K^{(2)} + \cdots ,$$

$$M = M^{(0)} + \mu M^{(1)} + \cdots . \tag{16}$$

Then an expansion of the supplementary condition gives

$$K^{(0)} = K^{(0)2} , \tag{17a}$$

$$K^{(1)} = K^{(0)} K^{(1)} + K^{(1)} K^{(0)} , \tag{17b}$$

$$K^{(2)} = K^{(0)} K^{(2)} + K^{(2)} K^{(0)} + K^{(1)2} . \tag{17c}$$

We substitute ρ, κ given by eq. (16) into eq. (9) and expand W as a power series in μ. The requirement that W be stationary with respect to an arbitrary first-order variation of K is

$$W^{(1)} = \left(\partial W / \partial \mu \right)_{\mu=0} = 0 . \tag{18}$$

The requirement that W be an absolute minimum is equivalent to

$$W^{(2)} = \frac{1}{2} \left(\partial^2 W / \partial \mu^2 \right)_{\mu=0} > 0 . \tag{19}$$

We obtain from (18) and (19), taking account of eq. (16),

$$W^{(1)} = \frac{1}{2} \operatorname{Tr} M^{(0)} K^{(1)} , \tag{20}$$

$$W^{(2)} = \frac{1}{2}\,\mathrm{Tr}\left[M^{(0)}K^{(2)} + \frac{1}{2}M^{(1)}K^{(1)}\right]. \tag{21}$$

We already discussed $W^{(1)}$ in the last section, but let us now give the derivation of the stationary equation (15). Multipling eq. (17b) by $K^{(0)}$ it follows that

$$K^{(0)}K^{(1)}K^{(0)} = 0, \tag{22}$$

and there eq. (17b) can be written in the form

$$K^{(1)} = (1-K^{(0)})K^{(1)}K^{(0)} + K^{(0)}K^{(1)}(1-K^{(0)}). \tag{23}$$

If eq. (23) is substituted in eq. (20), it becomes

$$W^{(1)} = \frac{1}{2}\,\mathrm{Tr}\left[K^{(0)}M^{(0)}(1-K^{(0)}) + (1-K^{(0)})M^{(0)}K^{(0)}\right]K^{(1)} = 0. \tag{24}$$

For an arbitrary $K^{(1)}$, this implies that

$$K^{(0)}M^{(0)}(1-K^{(0)}) = 0. \tag{25}$$

This is equivalent to

$$\left[M^{(0)}, K^{(0)}\right] = 0. \tag{26}$$

In order to verify whether the solution of eq. (25) gives the minimum of the energy (9), we must examine the sign of the second variation of W. For this purpose we want to eliminate $K^{(2)}$ in $W^{(2)}$ by using the supple-

mentary condition (17). With the aid of eqs. (17a), (17b), (22) and (23) , eq. (17c) can be rewritten as follows:

$$K^{(2)} = VV^{+} - V^{+}V + V'^{+} + V' \,, \tag{26}$$

where

$$V = (1-K^{(0)})K^{(1)}K^{(0)} \quad , \quad V^{+} = K^{(0)}K^{(1)}(1-K^{(0)}), \tag{27a}$$

$$V' = (1-K^{(0)})K^{(2)}K^{(0)} \quad , \quad V'^{+} = K^{(0)}K^{(2)}(1-K^{(0)}). \tag{27b}$$

On substituting this result in (21), we obtain

$$W^{(2)} = \frac{1}{2}\mathrm{Tr}\left[M^{(0)}(VV^{+} - V^{+}V + V'^{+} + V') + \frac{1}{2}M^{(1)}(V+V^{+})\right]. \tag{28}$$

However, from the arbitrary part of the second-order variation the contribution to $W^{(2)}$ is equivalent to eq. (24) and hence must vanish if eq. (25) is satisfied. Thus the second-order variation of the energy can be written entirely in terms of V.

$$W^{(2)} = \frac{1}{2}\mathrm{Tr}\left[M^{(0)}(VV^{+} - V^{+}V) + \frac{1}{2}M^{(1)}(V+V^{+})\right]. \tag{29}$$

The necessary condition to minimize the expectation value of the Hamiltonian is that the quadratic form of the right of eq. (29) should be non-negative definite. We may find eigenvalues Λ by equating to $\mathrm{Tr}\ (VV^{+})$ the right hand side of eq. (29). The stability condition means that the eigenvalues must all be positive or zero. Applying the variational calculus with respect to V to above equation and using eqs. (17a), (22) and (25), we can

obtain the eigenvalue equations as

$$\begin{aligned} M^{(0)}V - VM^{(0)} + (1-K^{(0)})M^{(1)}K^{(0)} &= \Lambda V , \\ V^{+}M^{(0)} - M^{(0)}V^{+} + K^{(0)}M^{(1)}(1-K^{(0)}) &= \Lambda V^{+} . \end{aligned} \tag{30}$$

By substracting the two equations from eachother, we canwrite in more compact form as

$$[M^{(0)}, K^{(1)}] + [M^{(1)}, K^{(0)}] = \Lambda [K^{(1)}, K^{(0)}] \tag{31}$$

This is the eigenvalue equation which gives the stability condition of the Hartree-Fock-Bogoliubov states.

3. Relation between the stability condition of H-F-B state and the equation of RPA

The stability condition of the Hartree-Fock-Bogoliubov state has been discussed in the previous section, but the form is very complicated. In order to simplify the discussions we only take into account the density part: This is the Hartree-Fock situation. In this section we shall derive the stability condition of the Hartree-Fock equation, which is first studied by Thouless.[4)]

Ths stability condition of the Hartree-Fock equation is obtained by replacing M and K in eq.(32) with ν and ρ, that is

$$[\nu^{(0)}, \rho^{(1)}] + [\nu^{(1)}, \rho^{(0)}] = \Lambda [\rho^{(1)}, \rho^{(0)}] , \tag{32}$$

where $\nu^{(o)}$ is the Hartree-Fock one body Hamiltonian and $\nu^{(1)}$ is the residual Hamiltonian, and $\rho^{(o)}$ is the Hartree-Fock density matrix and $\rho^{(1)}$ is the matrix which is obtained by eq.(32). Λ is the eigenvalue, and the sign of Λ is very important which decides whether the Hartree-Fock state is stable or not.

In order to see the meaning of eq.(32), we take (mi) component of eq.(32), where m,n...means the state above the fermi surface and i,j... means the state below the fermi surface.

$$\nu_m^{(o)}\rho_{mi}^{(1)} - \rho_{mi}^{(1)}\nu_i^{(o)} + \nu_{mi}^{(1)}\rho_i^{(o)} - \rho_m^{(o)}\nu_{mi}^{(1)} = \Lambda\rho_{mi}^{(1)}\rho_i^{(o)} - \Lambda\rho_m^{(o)}\rho_{mi}^{(1)} \tag{33}$$

For the above definition of (m,n...) and (i,j...) $\rho_m^{(o)} = 0$ and $\rho_i^{(o)} = 1$. Then eq.(34) becomes.

$$(\nu_m^{(o)} - \nu_i^{(o)})\rho_{mi}^{(1)} + \nu_{mi}^{(1)} = \Lambda\rho_{mi}^{(1)} \tag{34}$$

$\nu_m^{(o)}$ and $\nu_i^{(o)}$ are E_m and E_i which are the Hartree-Fock energies, and

$$\begin{aligned}\nu_{mi}^{(1)} &= \sum_{\beta\delta}(V_{m\beta i\delta} - V_{m\beta\delta i})\rho_{\beta\delta}^{(1)} \\ &= \sum_{nj}(V_{mnij} - V_{mnji})\rho_{nj}^{(1)} + \sum_{nj}(V_{mjin} - V_{mjni})\rho_{jn}^{(1)} \\ &= \sum_{nj}(V_{mnij} - V_{mnji})\rho_{nj}^{(1)} + \sum_{nj}(V_{mjin} - V_{mjni})\rho_{nj}^{(1)*}.\end{aligned} \tag{35}$$

The (im) component of eq.(32) gives

$$(\nu_m^{(o)} - \nu_i^{(o)})\rho_{mi}^{(1)*} + \nu_{im}^{(1)} = \Lambda\rho_{mi}^{(1)*}. \tag{36}$$

Using eqs. (34), (35) and (36), we get the equations of the stability condition:

$$(E_m - E_i)\rho^{(1)}_{mi} + \sum_{nj}\left[(V_{mnij} - V_{mnji})\rho^{(1)}_{nj} + (V_{mjin} - V_{mjni})\rho^{(1)*}_{nj}\right] = \Lambda\rho^{(1)}_{mi},$$

$$(E_m - E_i)\rho^{(1)*}_{mi} + \sum_{nj}\left[(V_{ijmn} - V_{ijnm})\rho^{(1)*}_{nj} + (V_{inmj} - V_{injm})\rho^{(1)}_{nj}\right] = \Lambda\rho^{(1)*}_{mi}. \quad (37)$$

The form of eq. (37) is equal to the equations obtained by Thouless in another method.

The equation of the random-phase approximation can be obtained within the time-dependent Hartree-Fock formalism.[10] The equation of motion reads[11]

$$i\frac{\partial}{\partial t}\rho = [\nu, \rho], \quad (38)$$

where ρ is the density matrix, and ν the Hartree-Fock Hamiltonian. The density matrix ρ can be written as the time independent part and time dependent part:

$$\rho = \rho^{(0)} + \rho^{(1)}\exp(-i\omega t) \quad (39)$$

The Hamiltonian also can be written as the self-consistent Hamiltonian and the residual one.

$$\nu = \nu^{(0)} + \nu^{(1)} \quad (40)$$

Using the equation $[\nu^{(0)}, \rho^{(0)}] = 0$, eq. (38) becomes in the first order

$$[\nu^{(0)}, \rho^{(1)}] + [\nu^{(1)}, \rho^{(0)}] = \omega\rho^{(1)}. \quad (41)$$

It can be written in the familiar form as follows. As done in deducing the stability condition eq.(32), we take (m,i) and (i,m) components of eq.(41), and get

$$\begin{aligned}
&(E_m - E_i)\rho^{(1)}_{mi} + \sum_{nj}\left[(V_{mnij} - V_{mnji})\rho^{(1)}_{nj} + (V_{mjin} - V_{mjni})\rho^{(1)*}_{nj}\right] = \omega\rho^{(1)}_{mi}, \\
&(E_m - E_i)\rho^{(1)*}_{mi} + \sum_{nj}\left[(V_{ijmn} - V_{ijnm})\rho^{(1)*}_{nj} + (V_{inmj} - V_{injm})\rho^{(1)}_{nj}\right] = -\omega\rho^{(1)}_{mi}.
\end{aligned} \tag{42}$$

This is the equation of the random-phase approximation, which can be obtained in some methods.[12]

As can be seen from eqs. (38) and (42), one is the stability condition of the Hartree-Fock state and the other is the equation of the random-phase approximation, and there is a close relation between them. If eq.(38) has eigenvalue zero, so has eq. (42). If one eigenvalue of eq. (38) is negative, then eq. (42) has imaginary eigenvalues. If no eigenvalue of eq.(38) is negative, then all the eigenvalues of eq. (42) are real. Conversely, if the eigenvalue of eq. (42) is zero or imaginary, the eigenvalue of eq. (38) is zero or negative, so we can say that the Hartree-Fock state is unstable. For the case of the Hartree-Fock-Bogoliubov state the above situation can be shown generally.

References

1) J. P. Elliott, Proc. Roy. Soc. (London) A245 (1958) 128 and 562

2) L. S. Kisslinger and R. A. Sorensen, Rev. Mod. Phys. 35 (1963) 853

3) H. Toki and M. Sano, Osaka University, Laboratory of Nuclear Studies, OULNS 73-6 (1973), and to be published

4) D. J. Thouless, Nucl. Phys. 21 (1960) 225, and Nucl. Phys. 22 (1961) 78

5) N. N. Bogoliubov, Usp. Fiz. Nauk. 67 (1959) 549

6) M. Baranger, Phys. Rev. 122 (1960) 992;
M. Sano, T. Takemasa and M. Wakai, Nucl. Phys. A190 (1972) 471

7) T. Takemasa, M. Sakagami and M. Sano, Phys. Lett. 37B (1971) 473

8) K. Ando and H. Bando, private communication

9) M. Baranger and K. Kumar, Nucl. Phys. 62 (1965) 113

10) G. E. Brown, Unified Theory of Nuclear Models (North-Holland) (1964)

11) J. Goldstone and K. Gottfried, Nuovo Cim. 13 (1959) 849

12) K. Sawada, Phys. Rev. 106 (1957) 372

13) M. Sakai, INS- J - 140 (1973)

Table Captions

Table 1. Single particle energies. (MeV)

Table 2. Excitation energies and B(E2) values of the first 2^+ states of Xe, Ba and Ce isotopes. The letters "-" in the rows of experiment mean that there are not experimental data. The letters denoted by "unstable" mean that the enegy of the first 2^+ state is complex and the instability of the sherical phase happens. The strengths of the quadrupole-pairing force were taken as G_2^c = 28.0MeV and V_2^c = 31.8MeV for the case of P_2-P_2 plus Q-Q force, and as V_2^c = 34.2MeV for the case of Q-Q force only. The effective charge was used as e_{eff} = 0.8e for the first case and e_{eff} = 0.5e for the second case.

Figure Captions

Fig. 1. The excitation energies of the first 2^+ states of Cd and Te isotopes against the neutron number. The experimental values are denoted by the circles which are taken from the work of Sakai.[13] The solid line is the calculated one using the interaction composed of P_2-P_2 and Q-Q forces, and the dotted line and the dashed-dotted line are the calculated ones using Q-Q force only.

Fig. 2. Sets of G_2^c and V_2^c taken so as to fit the excitation energies of the first 2^+ states.

Fig. 3. Excitation energies of the first 2^+ states of the Xe, Ba and Ce isotopes. The black circles are the experimental ones, the solid lines are calculated one using an interaction composed of P_2-P_2 and Q-Q forces and the dotted lines are the ones of Q-Q force only.

Level	Proton	Neutoron
$5h_{11/2}$	-1.284	-0.573
$4d_{3/2}$	-0.128	0.120
$4s_{1/2}$	0.0	-0.137
$4g_{7/2}$	-2.567	-1.104
$4d_{5/2}$	-2.353	-2.114
$4g_{9/2}$	-6.418	-5.134
$3p_{1/2}$	-7.299	-6.871
$3f_{5/2}$	-8.643	-8.215
$3p_{3/2}$	-8.429	-8.001
$3f_{7/2}$	-11.637	-11.210

Table 1

Nucleus	Experiment		P_2-P_2 + Q-Q		Q-Q only	
	Ex	B(E2)	Ex	B(E2)	Ex	B(E2)
^{124}Xe	0.350	-	unstable	-		
^{126}Xe	0.386	7.81±0.50	0.256	7.594	unstable	-
^{128}Xe	0.455	6.5 ±2.5	0.405	4.761	0.475	10.3
^{130}Xe	0.538	-	0.539	3.415	0.928	5.0
^{132}Xe	0.670	3.1 ±1.0	0.677	2.450	1.307	3.3
^{134}Xe	0.850	-	0.847	1.576	1.679	2.1
^{128}Ba	0.279	-	unstable	-		
^{130}Ba	0.359	7.5 ±1.8	0.276	9.019	unstable	-
^{132}Ba	0.472	7.2 ±1.8	0.461	5.180	0.584	9.9
^{134}Ba	0.605	-	0.627	3.455	1.095	4.9
^{136}Ba	0.818	-	0.819	2.160	1.527	3.1
^{130}Ce	-	-	unstable	-		
^{132}Ce	-	-	0.136	22.075	unstable	-
^{134}Ce	0.410	-	0.401	7.155	0.095	70.3
^{136}Ce	-	-	0.591	4.413	0.930	3.3
^{138}Ce	0.790	-	0.799	2.681	1.415	2.1

Table 2

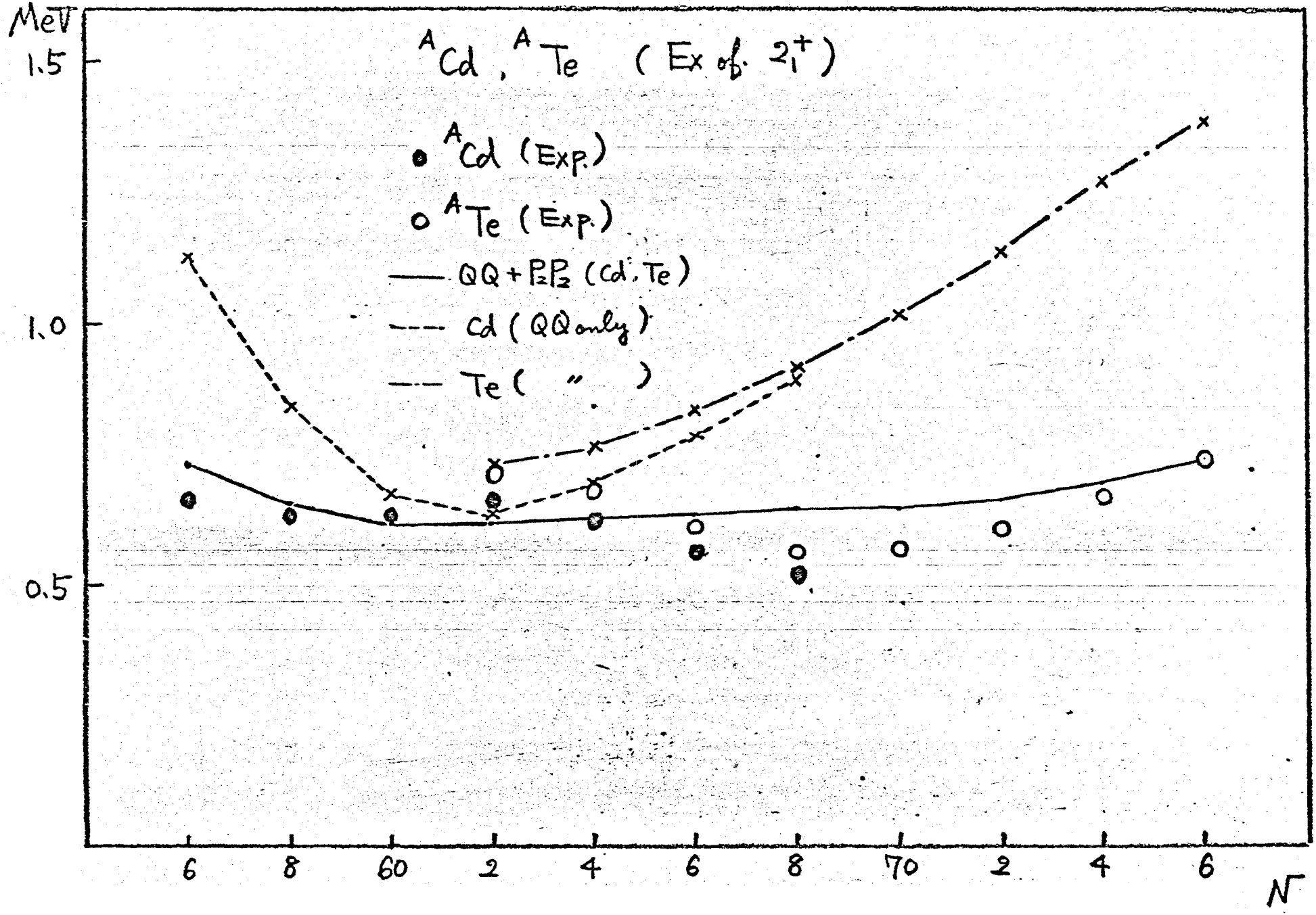
MeV
1.5
1.0
0.5
^{A}Cd , ^{A}Te (Ex of. 2_1^+)
^{A}Cd (Exp.)
^{A}Te (Exp.)
QQ + P₂P₂ (Cd, Te)
Cd (QQ only)
Te (")
6
8
60
2
4
6
8
70
2
4
6
N

Fig. 1

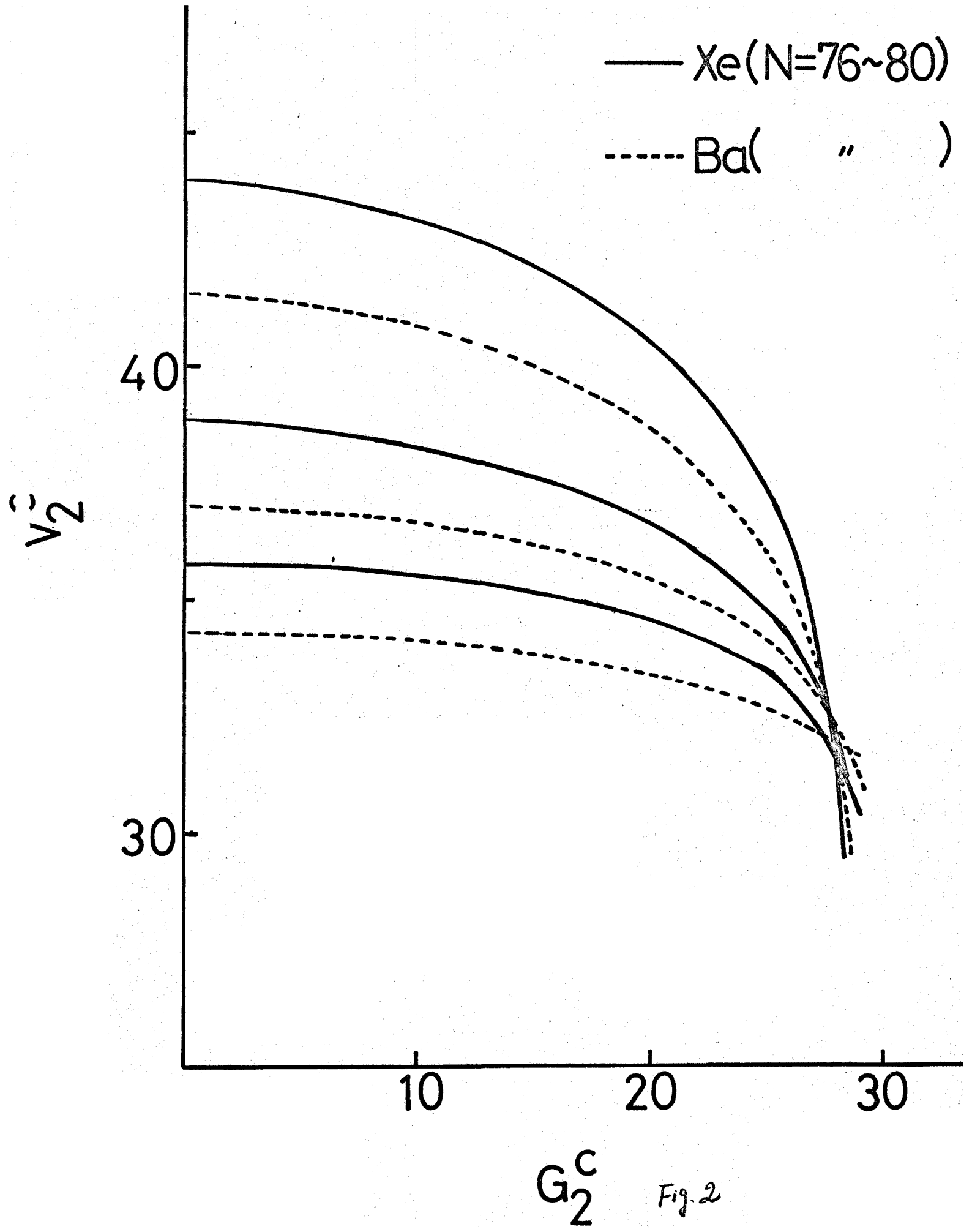

Fig. 2

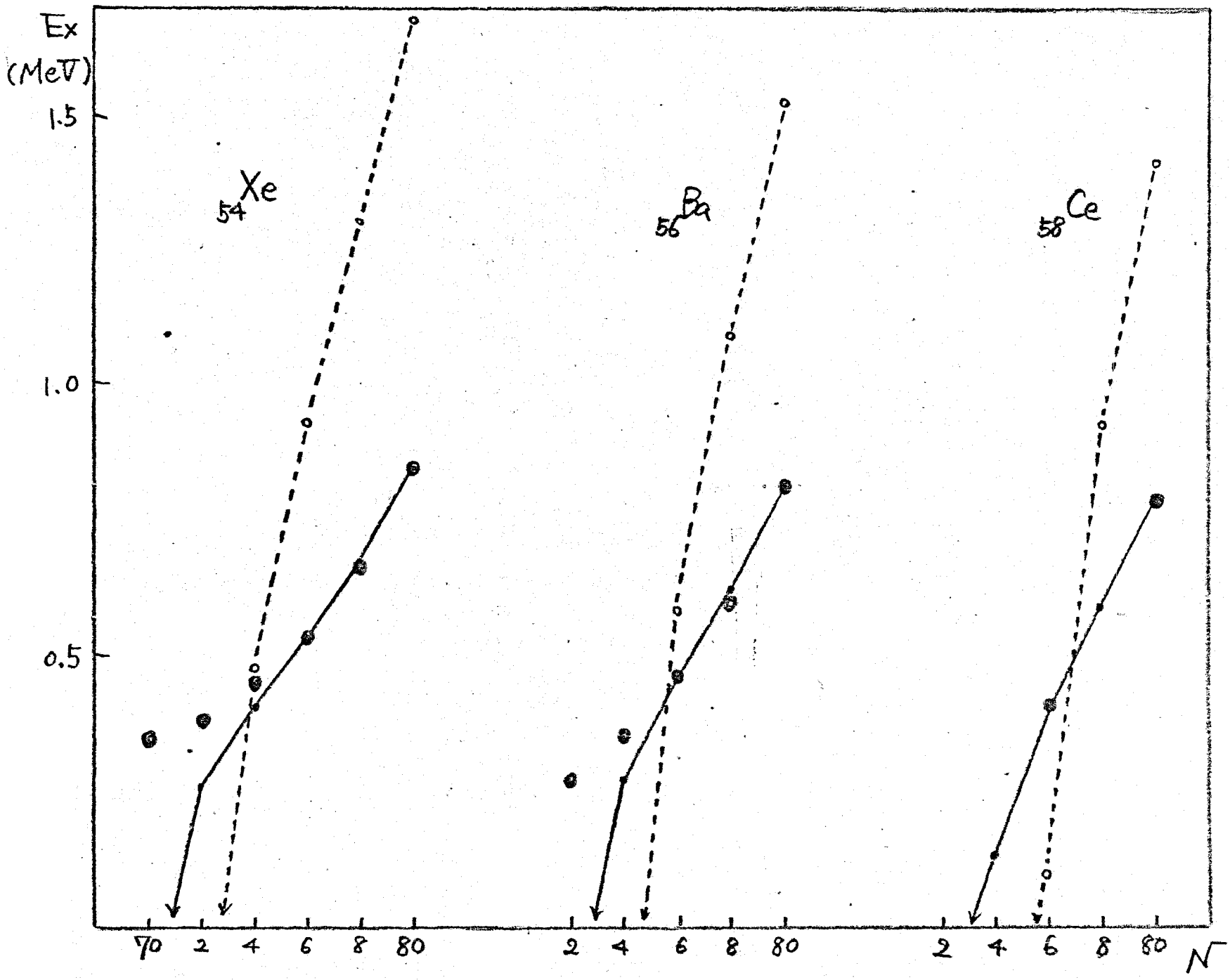

Fig. 3

CHAPTER 5 Incident Energy Dependence of (p,t) Reactions

1. Introduction

There have been done many experiments of (p,t) reactions on various nuclei by using various kinds of proton energy. In these experiments there are some nuclei on which (p,t) reaction have been done by using more than two incident energies of proton; as discussed in the previous chapter, Nd isotopes by E_p = 30MeV[1] and 52MeV,[2] and $^{208}Pb(p,t)^{206}Pb$ by E_p = 40MeV[3] and 50MeV[4] and so on.

Comparing these data, it can be seen that some level which is strongly excited at some incident energy is not excited so strongly at another incident energy. There might be large incident energy dependence on (p,t) reaction-cross sections. Thus the purpose of this chapter is to show how the cross section of (p,t) reaction changes with the incident energy in terms of the distorted-wave Born approximation.

2. $^{208}Pb(p,t)\ ^{206}Pb$

For the purpose, we took the data of the reaction $^{208}Pb(p,t)\ ^{206}Pb$ by E_p = 40MeV[1] and E_p = 52MeV[2]. The wave functions of ^{206}Pb have been well studied by many authors in terms of the shell model.[5),6)] The levels which have the angular momentum L = 0, 2, ... and 8 are excited by the (p,t) reaction with E_p = 52MeV. The interesting point in the experiments is that, as can be seen in figure 1, the cross sections to each angular-momentum states at E_p = 40MeV decrease as the transfered angular momentum increases, however, ones at E_p = 52MeV increase as the transfered angular

momentum increases.

The wave functions of ^{206}Pb were taken from the work of Kuo and Herling[5], which were indicated as set I in their paper. The form factors which were used in the DWBA calculation were made by using the formalism of Lin[7] and the tails of the form factors were modified by the prescription of Glendenning[8]. The optical potentials for proton and triton are listed in table 1, which are taken directly form the works of Fricke et al.[9] for proton and Glendenning [10] for triton.

The results of the DWBA calculation are shown in figure 2. The summed cross sections taken in steps of 5° from 5° to 40° leading to the first L^+ states are plotted as a function of the incident proton energy E_p. In order to avoid the ambiguity of wave functions the magnitude of the cross sections is normalized to the cross sections of E_p = 52MeV. As can be seen in figure 2, the peak position of the cross sections of each L^+ states moves to the higher incident-energy part as the transfered angular momentum increases. Thus at E_p = 52MeV, the summed cross secitons leading to the first 6^+ state is the largest of the cross sections. As an example, at E_p = 20MeV 0^+ and 2^+ states can be excited by the (p,t) reaction, but the higher L^+ states such as 4^+, 6^+ and so on can not be excited so strongly. On the other hand, at E_p = 70MeV the lower L^+ states such as 0^+ and 2^+ states can not be excited so strongly.

The experimental and the calculated differential cross sections are shown in figure 3. The angular distribution patterns at E_p = 40MeV and 52MeV are well reproduced by using the optical potentials listed in table 1. The energy dependence for the proton-optical potential was taken into account but for the triton-optical potential it was not taken into account. These arguments would be more clear, if the optical potential for triton was decided at the various triton energies.

In order to check the wave functions which were studied by many authors the ratios of the summed cross sections relative to one of the ground state are plotted in figure 4. The results of the work by Smith et al.[3] were used for the dotted line (denoted as the wave functions of True and Ford), and the energy dependence was made by using our results of the wave function of Kuo and Herling. The experimental results were not always reproduced by using the one wave functions.

3. Qualitative discussion

It was concluded in the previous section that the peak position of the cross sections moves to the higher incident-energy part as the transfered angular momentum increases. It may be understood by the following qualitative discussion.[11]

We consider the (t,p) reaction and then consider the (p,t) reaction and compare it with the DWBA results. The discussion is started from the following assumption; that is the reaction happens at the nuclear surface. This is a natural assumption for transfer reactions. At first we neglect the Coulomb effects and discuss the angular momentum conservation through the (t,p) reaction. The angular momentum just before transfer is

$$\ell_i = k_t \cdot R \ , \qquad (1)$$

where k_t is the wave number of the triton (neglecting the recoil effect.) and R is the nuclear radius. The angular momentum just after transfer is

$$\ell_f = \ell_0 + k_p \cdot R \ , \qquad (2)$$

where ℓ_0 is the angular momentum of the transfered di-neutron and k_p is the

wave number of the emitted proton. Assuming the emitted proton is scattered to the forward angle, the conservation 1 w of the angular momentum is $\ell_i = \ell_f$, then it becomes

$$k_t \cdot R = \ell_0 + k_p \cdot R \,, \tag{3}$$

Thus the transfered angular momentum must be

$$\ell_0 = (k_t - k_p) \cdot R = \frac{\sqrt{2m_p}}{\hbar} \cdot R \left(\sqrt{3E_t} - \sqrt{E_p} \right) , \tag{4}$$

where E_t and E_p are the energies of the triton and proton. Using the reaction Q value, the above equation becomes

$$\ell_0 = \frac{\sqrt{2m_p}}{\hbar} \cdot R \left(\sqrt{3(E_p+Q)} - \sqrt{E_p} \right) , \tag{5}$$

Next we consider the Coulomb effects. These effects can be taken into account by considering the energy conservation at the nuclear surface. At the nuclear surface the kinetic energies of the triton and the proton are

$$E_k(t) = E_t - E_c \,, \quad \text{and} \quad E_k(p) = E_p - E_c \,, \tag{6}$$

where E_c is the Coulomb energy (the positions) at where the reaction happens (i.e. nuclear surface). Thus the final result is

$$\ell_0 = \frac{\sqrt{2m_p}}{\hbar} \cdot R \left(\sqrt{3(E_p - E_c - Q)} - \sqrt{E_p - E_c} \right) , \tag{7}$$

For the (p,t) reaction, similar discussion can be done, and the condition can be written as the same form in eq.7.

For the analysis which uses the differential cross sections in the forward angles as we have done, the angular momentum of the emitted particle at the nuclear surface does not change drastically. If there is a change, this effect makes the transfered angular momentum through the (p,t) reaction smaller than the value of eq.7.

The peak positions of the first L^+ states by the DWBA analysis are plotted as islands in figure 5. The curve denoted by the dotted line is eq.5, which is neglecting the Coulomb effect. Using the Coulomb energy for ^{208}Pb at the nuclear surface as E_c = 15MeV, the curve of eq.7 becomes as the solid line. The value E_c = 15MeV becomes by assuming the nucleus is a point. The finiteness of the nucleus makes the solid line shift to the left hand side. The effect that the emitted particle scatters to a larger angle makes the solid line shift to the right hand side. These effects might be considered minor. The peak positions of each L^+ states calculated by DWBA were well reproduced by the simple qualitative discussion.

4. Conclusion

The incident energy dependence of (p,t) reaction has been discussed in this chapter. The conclusion is that the peak positions of the summed cross sections leading to each L^+ states move to the higher incident-energy part as the transfered angular momentum increases. In other words, the (p,t) reaction with higher incident energy can excite higher angular momentum states. In order to st dy the lower spin states you had better use the smaller energy proton, and in order to study the higher spin states

you had better to use the larger energy proton. High spin states in a deformed nucleus might be excited by the (p,t) reaction with using high energy proton. To study the high spin states is very interesting to know the point of the phase transition of rotational states.

The calculation in this chapter was done by using the constant optical potential for triton. To make the above discussions more strict we must study the optical potential for triton at high energy.

References

1) J. B. Ball, R. L. Auble, J. Rapaport and C. B. Fulmer, Phys. Lett. 30B (1969) 533

2) K. Yagi, Y. Aoki, J. Kawa and K. Sato, Phys. Lett. 29B (1969) 647; K. Yagi, K. Sato and Y. Aoki, J. Phys. Soc. Japan 31 (1971) 1838

3) S. M. Smith, P. G. Roos, A. M. Bernstein and C. Moazed, Nucl. Phys. A158 (1970) 497

4) Y. Ishizaki, private communication

5) G. Herling and T. T. S. Kuo, private communication

6) W. W. True and W. K. Ford, Phys. Rev. 109 (1958) 1675; W. W. True, Phys. Rev. 168 (1968) 1388

7) C. L. Lin, Prog. Theor. Phys. 36 (1966) 251

8) N. K. Glendenning, Phys. Rev. 137 (1965) B102

9) M. P. Fricke, E. E. Gross, B. J. Morton and A. Zucker, Phys. Rev. 156 (1967) 1207

10) N. K. Glendenning, Phys. Rev. 156 (1967) 1344

11) D. M. Brink, Phys. Lett. 40B (1972) 37

Figure Captions

Fig. 1 The excitation energies of the first L^+ states of ^{206}Pb, and the (p,t) strengths. The left hand side is the result of the (p,t) reaction with E_p = 40MeV, and the right hand side is with E_p = 52MeV. The strengths are the summed cross section taken in steps of 5° from 5° to 40°.

Fig. 2 The incident-energy dependence of the cross sections for each L^+ states.

Fig. 3 (a) The experimental and theoretical angular distributions for 0^+ and 2^+ states populated by $^{208}Pb(p,t)$ with E_p = 40MeV.
(b) The experimental and theoretical angular distributions for 4^+, 6^+ and 8^+ states populated by $^{208}Pb(p,t)$ with E_p = 40MeV. The cross section for the 8^+ state is not measured at this incident energy.
(c) The experimental and theoretical angular distributions for 0^+ and 2^+ states populated by $^{208}Pb(p,t)$ with E_p = 52MeV.
(d) The experimental and theoretical angular distributions for 4^+, 6^+ and 8^+ states populated by $^{208}Pb(p,t)$ with E_p = 52MeV.

Fig. 4 Relative ratios of the (p,t) strengths for each L^+ states to the ground state. The solid lines are the experimental ones. The dotted lines are the theoretical results with using the wave functions calculated by Kuo and Herling. The dashed- dot lines are the ones with using the wave functions calculated by True and Ford.

Fig. 5 The peak positions of the (p,t) strengths for each L^+ states The vertical axis is the transfered angular momentum, and the horizontal axis is the incident proton energy. The islands are the peak positions calculated in terms of DWBA. The solid line is the curve of eq. (7) and the dotted line is the one of eq.(5).

	Proton	Triton
V (MeV)	54.62	160.0
W_v(MeV)	5.31	20.0
W_s(MeV)	5.60	0.0
$V_{s.o.}$(MeV)	5.84	0.0
r_R(F)	1.125	1.1
a_R(F)	0.873	0.75
r_I(F)	1.386	1.6
a_I(F)	0.624	0.75
$r_{s.o.}$(F)	1.026	-
$a_{s.o.}$(F)	0.794	-
r_c(F)	1.25	1.4

Table 1

Table 1. The optical potential parameters for proton and triton.

$^{208}Pb(p,t)^{206}Pb\ (L_1^+)$ $\sum_{\theta=5^\circ}^{40^\circ(5^\circ)} \sigma(\theta)$

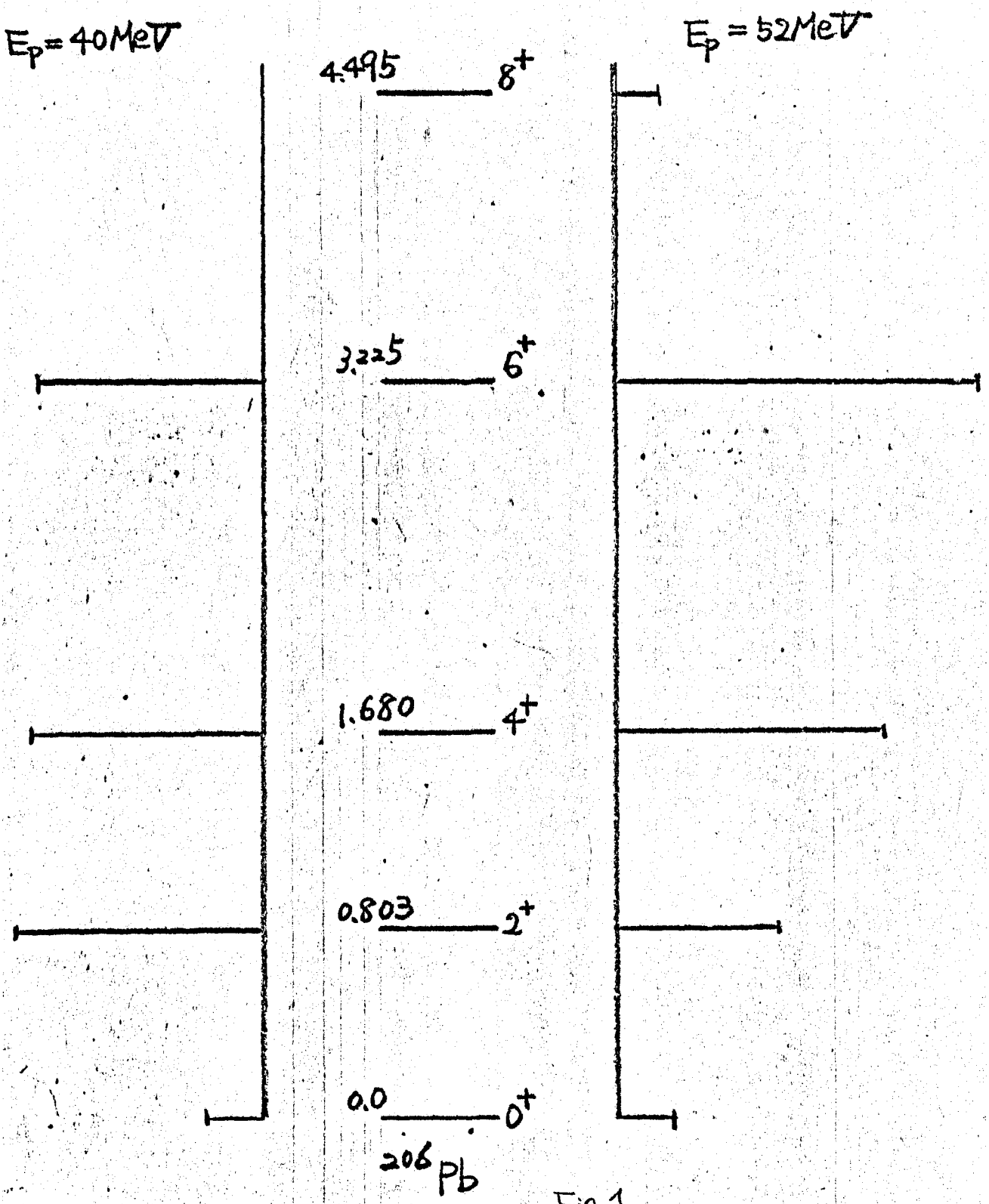

Fig. 1

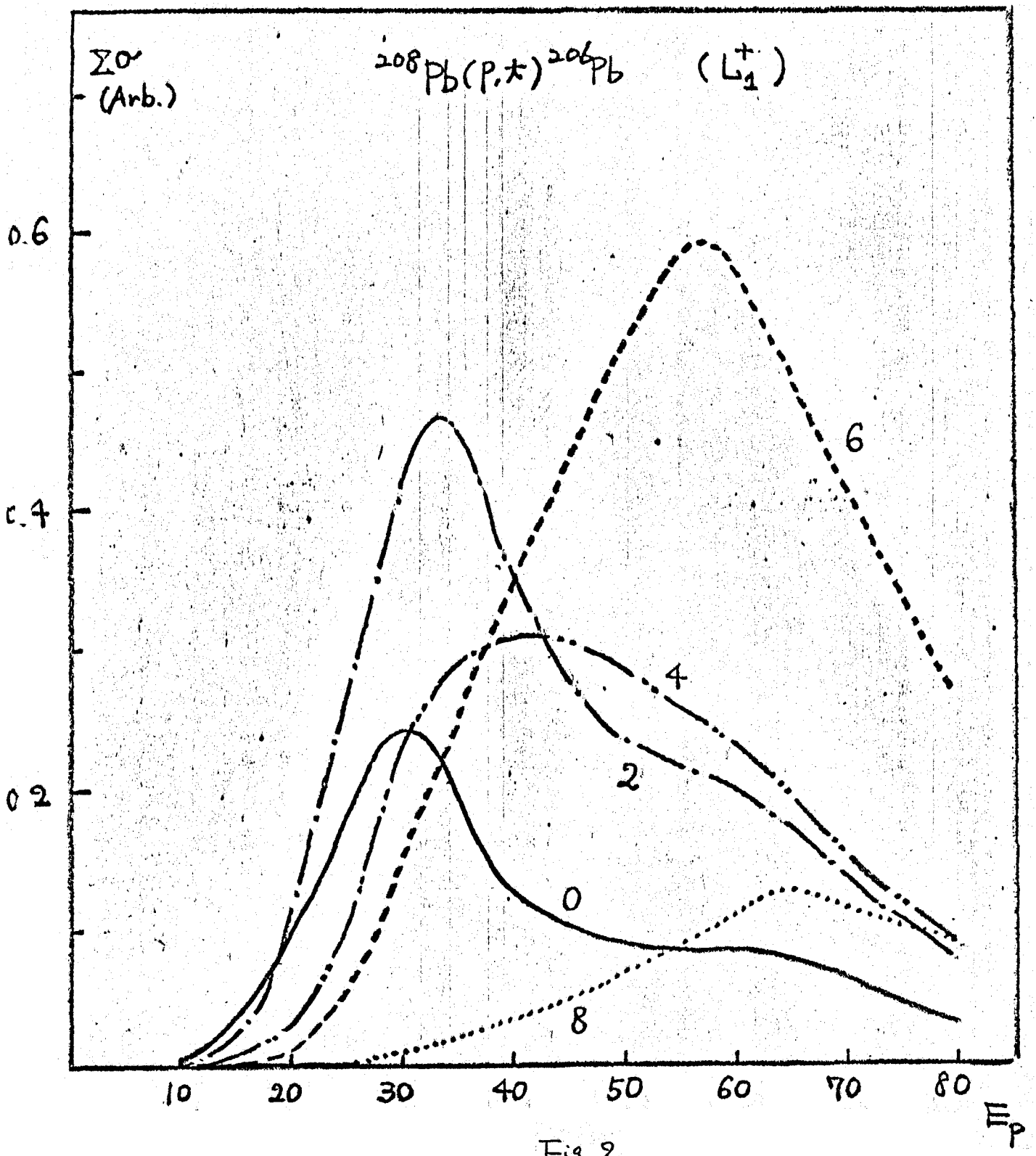

Fig. 2

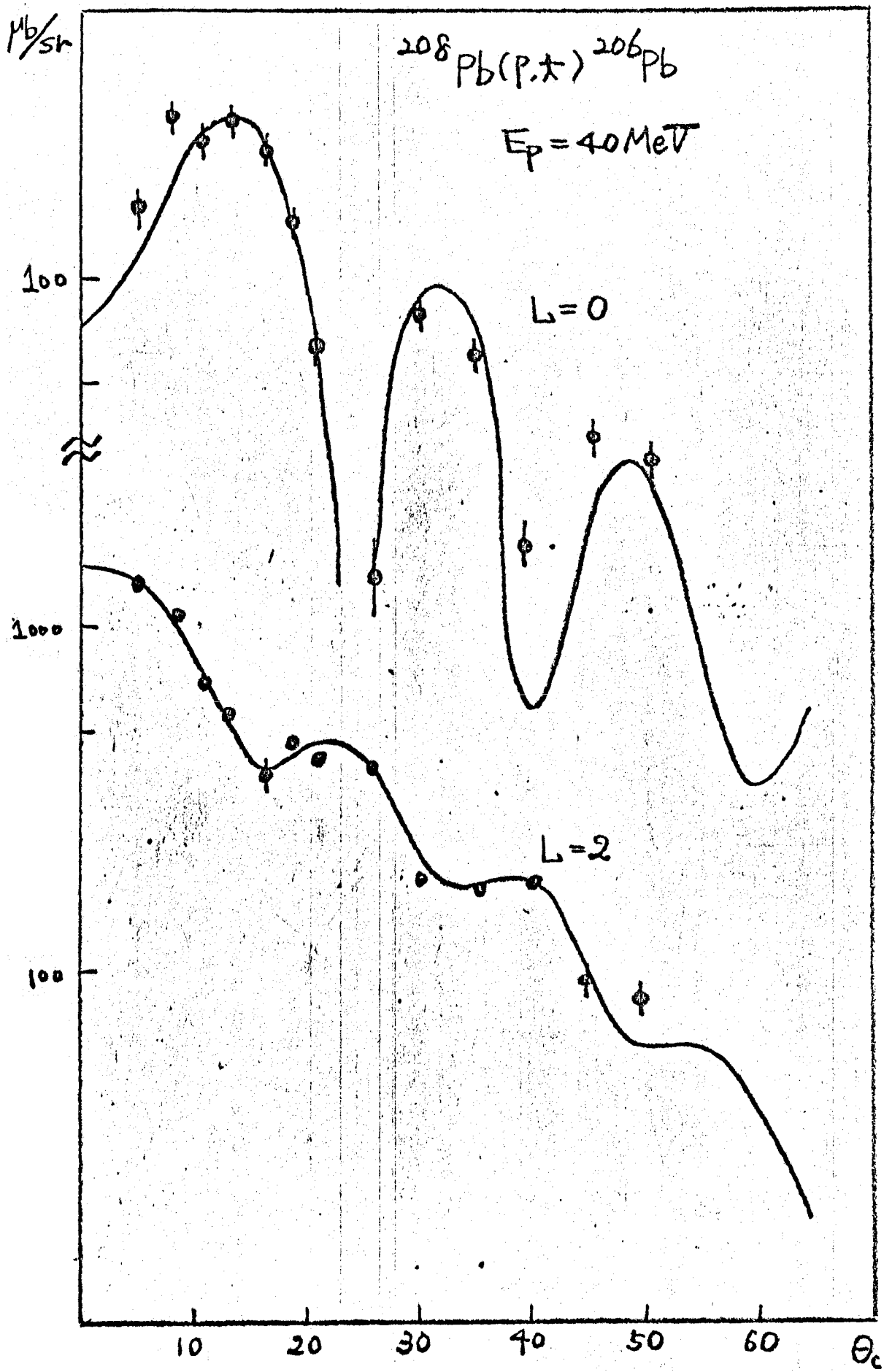
mb/sr
$^{208}Pb(p,t)^{206}Pb$
$E_p = 40 MeV$
100
1000
100
L=0
L=2
10
20
30
40
50
60
$\theta_{c.m.}$

Fig. 3(a)

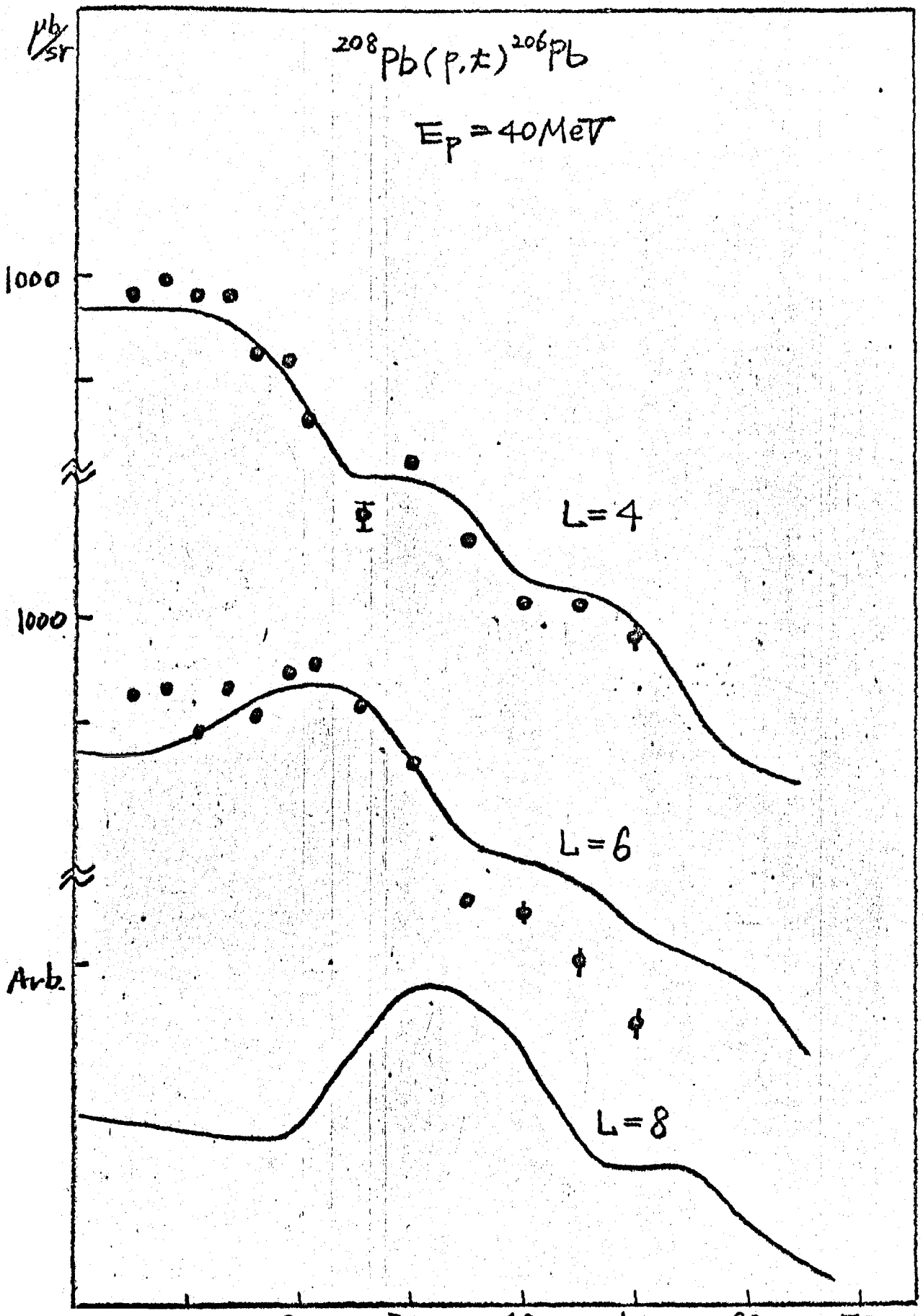
μb/sr
$^{208}Pb(p,t)^{206}Pb$
$E_p = 40 MeV$
1000
1000
Arb.
L=4
L=6
L=8
10
20
30
40
50
60
70
$\theta_{c.m.}$

Fig. 3(b)

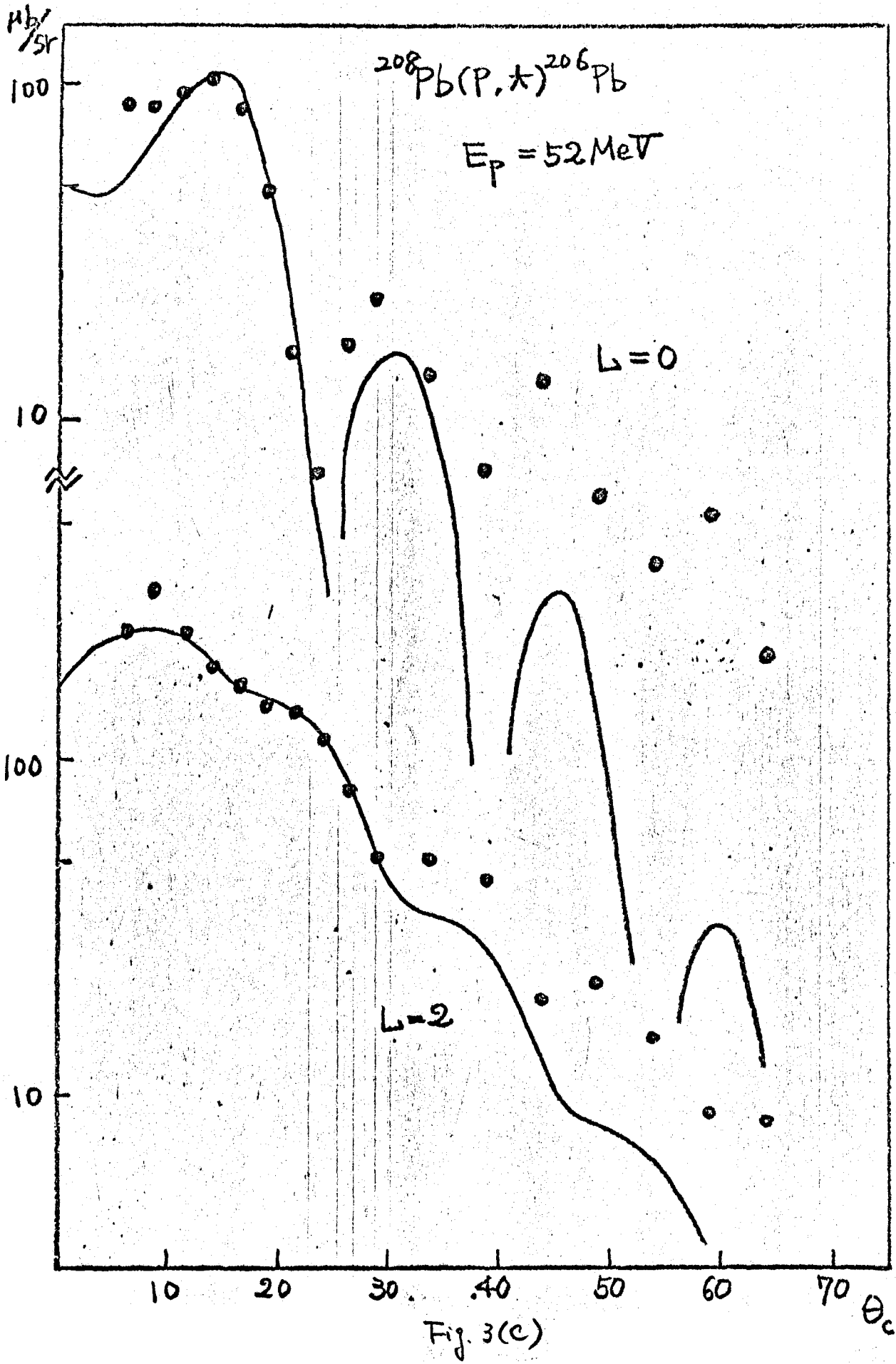
μb/sr
100
10
100
10
$^{208}Pb(p,t)^{206}Pb$
$E_p = 52$ MeV
L=0
L=2
10
20
30
40
50
60
70
$\theta_{c.m.}$

Fig. 3(c)

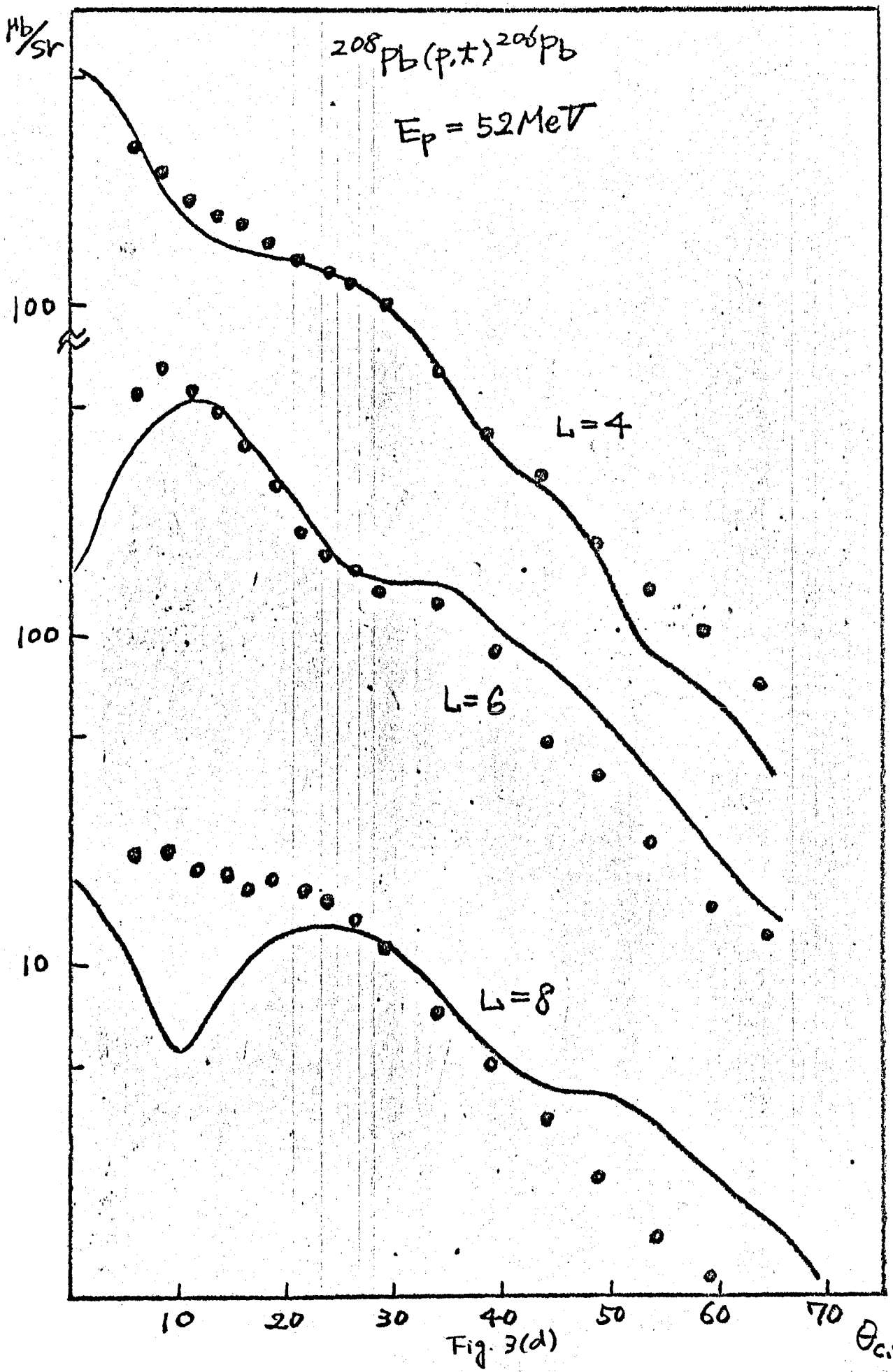
mb/sr
$^{208}Pb(p,t)^{206}Pb$
$E_p = 52 MeV$
100
100
10
L=4
L=6
L=8
10
20
30
40
50
60
70
$\theta_{c.m.}$

Fig. 3(d)

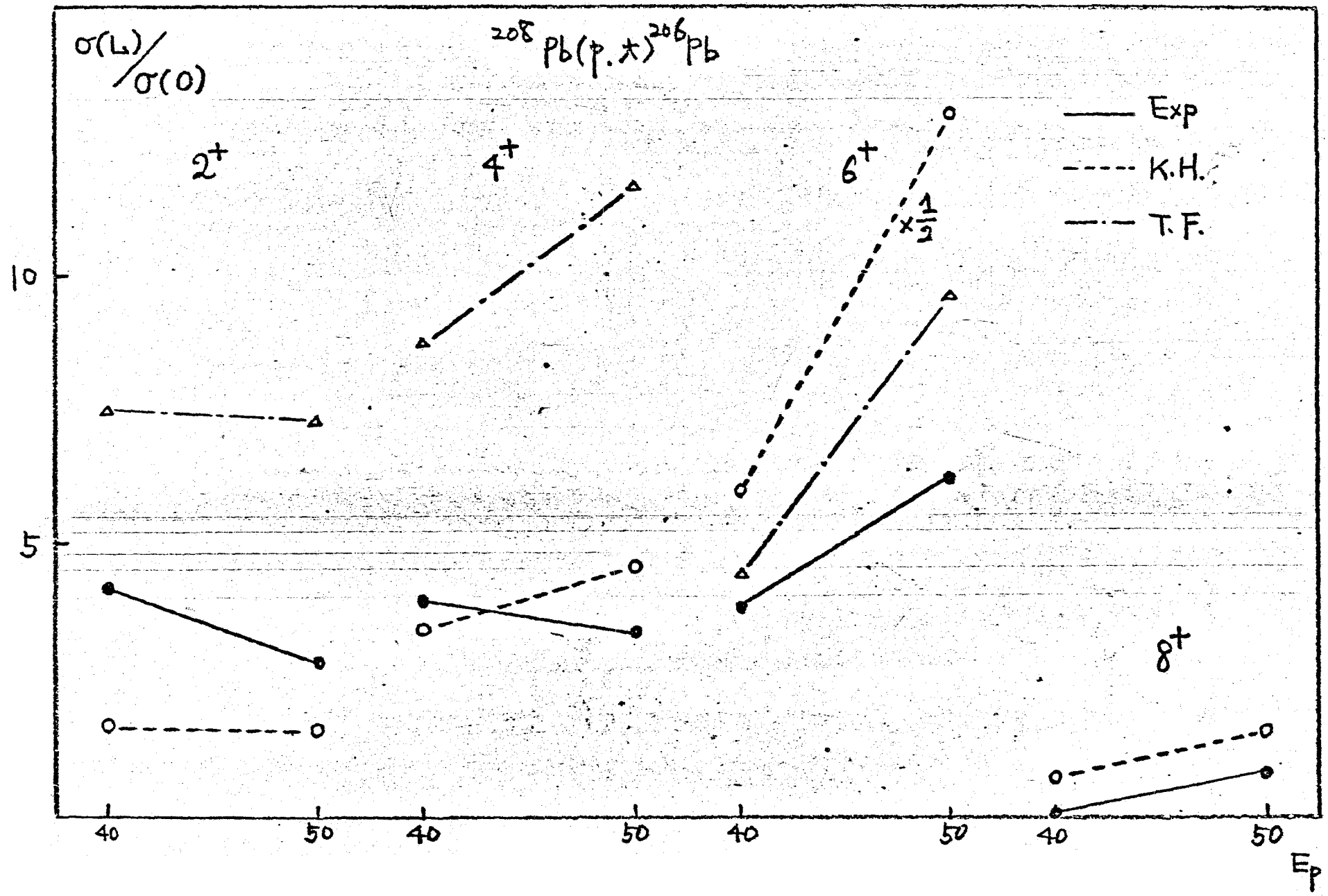
σ(L)/σ(0)
208Pb(p.x)206Pb
2+
4+
6+
8+
Exp
K.H.
T.F.
×1/2
10
5
40
50
40
50
40
50
40
50
Ep

Fig. 4

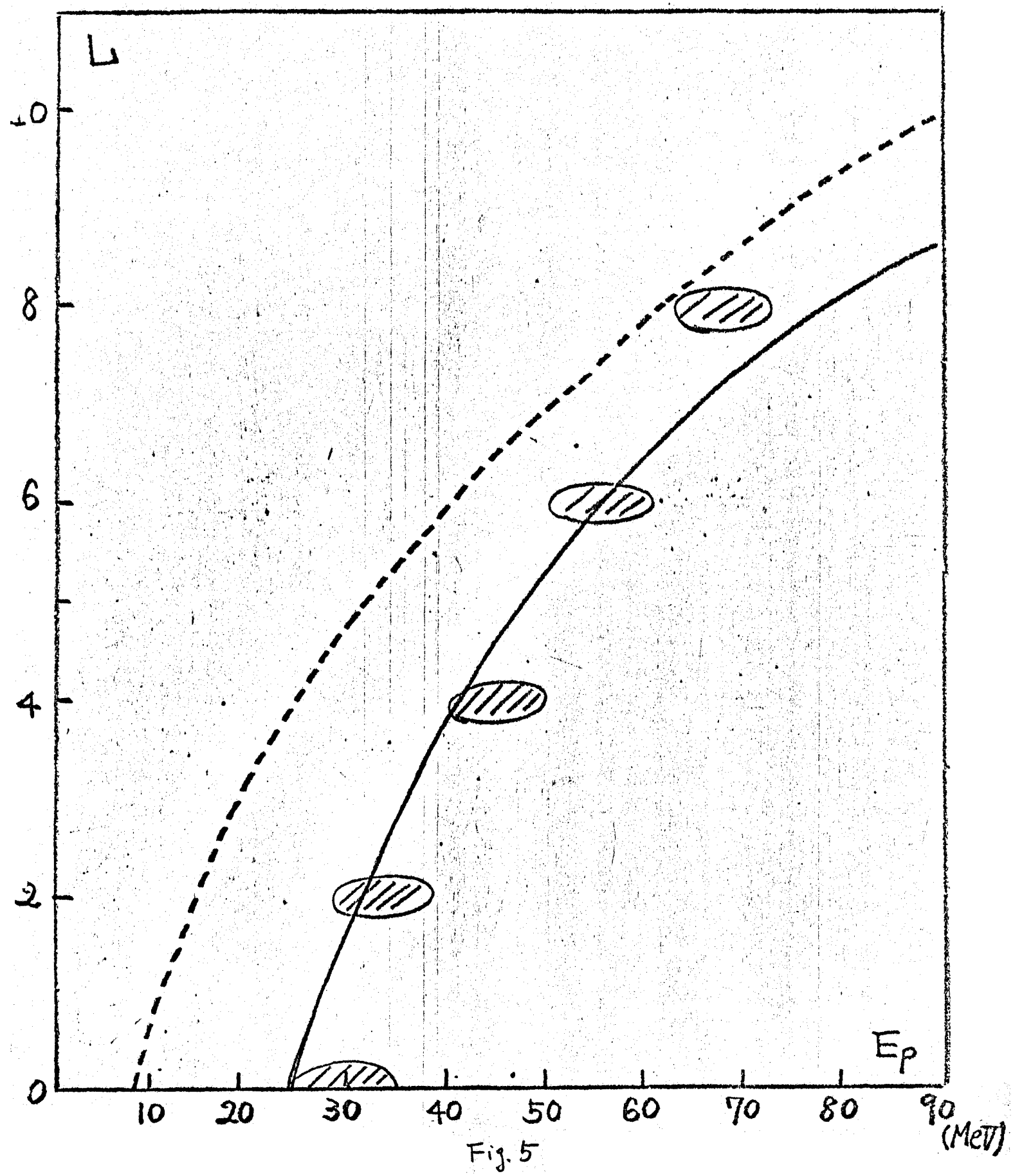

Fig. 5

CHAPTER 6 Effect of Two-Step Process on (p,t) Cross Sections

1. Introduction

Two types of angular distribution patterns for (p,t) reactions leading to the first 2^+ states are reported in many cases.[1] One type of distribution exhibits a peak around $\theta = 10^\circ$-15°, which can be well reproduced by conventional DWBA calculations. The other type does not show any peak in that range of angles and is accounted for by including higher order processes[2].

Experiment of the (p,t) reaction on Te isotopes with $E_p = 52$MeV was done by Yagi et al.[3]. The shape of the angular distribution changes gradually from the one type to the second one as mass number decreases. The experimental data are useful to check effects of higher order processes in the (p,t) reaction. The purpose of the present chapter is to report results of the two-step process calculation (TSP) and to point out the inadequacy of the usual approaches.

2. Two-step process-calculations

The T-matrix consisting of one-step and two-step processes is written by[4]

$$T_{p,t} = \langle \phi_t^{(-)} | V_* | \phi_p^{(+)} \rangle + \langle \phi_t^{(-)} | V_* \frac{1}{E - H_0 + i\varepsilon} V_p | \phi_p^{(+)} \rangle , \qquad (1)$$

where $\phi_p^{(+)}$ ($\phi_t^{(-)}$) is the distorted wave times the intrinsic wave function, v_p (v_t) is the residual interaciton and the propagator $1/(E-H_o + i\varepsilon)$ describes the propagation of waves in the intermediate states. The first

term on the right hand side of Eq. 1 is the DWBA-matrix element and the second term corresponds to the second order processes, involving inelastic scattering in the entrance and exit channels.

The ground states of Te isotopes are described by the BCS-wave function and the first 2^+ states are described in terms of RPA with both the quadrupole pairing force (P_2-P_2) and the quadrupole force (Q-Q)[5]. The (p,t) form factors which were necessary in the calculation of TSP were prepared following the formalism of Lin et al.[6], and the tails of the form factors were modified according to the prescription of Glendenning.[7] The form factors of the inelastic processes are the macroscopic ones which are the derivative of the optical potentials. In the usual calculation the values of deformation parameter β of Te isotopes were taken from Stelson et al..[8]

The optical parameters for the proton were taken from the work of Fulmer et al.,[9] which reproduce the angular distributions of (P, P_o) reaction of Te isotopes with E_p = 52MeV.[10] The optical parameters for triton were adjusted so as to fit the angular distribution of the (p,t) reaction leading to the ground state, since they are not well known at this energy. They are listed in Table 1. The calculations of TSP were done by using the program of TWOSTP coded by Toyama and Igarashi.[11]

Figure 1 shows the calculated (DWBA and TSP) and the experimental angular distributions for (p,t) reactions leading to the first 2^+ state of Te isotopes. The variation of angular distribution from nucleus to nucleus can not be reproduced over all of Te isotopes even if the TSP calculation was done, and also the magnitude of the cross section is too large in comparison with the experimental cross section.

The summed cross sections taken in steps of 2.5° from 5° to 55° are plotted as a function of mass number A in figure 2. The interaction

strength of the (p,t) reaction is normalized to the reaction ^{130}Te (p,t) ^{128}Te (gnd.). As can be seen from figure 2, the experimental cross sections gradually increase as the mass number increases, but the trend can not be reproduced by TSP calculation with $\beta = \beta_{exp}$. Further the magnitude of the cross sections calculated by TSP is too large compared with the experimental ones. This is due to the fact that the cross sections of the second order process are too large and the second order process mainly contribute to the cross section. The magnitude of the second step process is proportional to the β^2 value, so the intensity of TSP is completely opposite to the experimental trend.

On the other hand, the trend of the cross section calculated by DWBA is the same with the experimental one. In order to reproduce both the variation of angular distribution patterns and the trend of the cross section we might use the deformation parameter smaller than β_{exp} taken from Stelson et al.. When $\beta_{eff} = \frac{1}{3}\beta_{exp}$ was used, the trend of the cross sections was well reproduced and the variation of angular distribution patterns were fairly well reproduced. The calculated and the experimental angular distributions were shown in figure 3.

3. Experimental evidence

In the previous section, it was concluded that the deformation parameter $\beta_{eff} = \frac{1}{3}\beta_{exp}$ must be used to explain the variation of the angular distribution patterns and the trend of the magnitude of the cross section. There are other evidences to have to use such a smaller β value. There are systematic data about the (p,t) reaction on the spherical vibrational nuclei: $_{44}$Ru[12], $_{46}$Pd[13], $_{48}$Cd[13], $_{50}$Sn[13], and $_{52}$Te[13] isotopes. (Nd and

Ba isotopes ha already been studied in the previous chapter.) The neutron number of these nuclei is between 50 and 82. The magnitude of the summed cross sections leading to the 2_1^+ states and 0^+ states is plotted against to the neutron number in figure 4(a) and (b). The deformation parameters β are also plotted in figure 4(c).

The neutron number dependence of the summed cross sections leading to the ground states will be reproduced by using the BCS wave functions as the ground states. (The (p,t) strength of the ground state can be written as $(\frac{\Delta}{G_o})^2$; Δ is the gap energy and G_o is the strength of the monopole pairing interaction.[14]) The interesting point in these figures is to compare the result of the Sn isotopes with one of the Cd isotopes. For example we compare the nuclei with N = 66. The summed cross section of $^{116}_{50}Sn_{66}$ is about 1070 and the deformation parameter β is about 0.116. On the other hand the summed cross section of $^{114}_{48}Cd_{66}$ is about 420 and the deformation parameter β is about 0.193. The angular distribution pattern of ^{116}Sn is the first type and one of ^{114}Cd is the second type. If the second order process mainly contributes to the cross section for ^{114}Cd as Te isotopes, and we assume the amplitude of the direct process is same between Cd and Sn with same neutron number, then the direct processes are small and the magnitude of the cross section of ^{114}Cd must be larger than that of ^{116}Sn by about 4. Thus the second order process must be smaller than the direct process.

These data might be explained by taking into account the effective β value, that is $\beta_{eff} = \alpha\beta_{exp}$ and $\alpha(\leq 1)$ is a constant. This situation was used for the discussion about the first 2^+ states of Nd isotopes.

4. Microscopic description for the inelastic processes

In the above calculations the form factors of the inelastic process are

the macroscopic one. On the other hand the form factors of the (p,t) reaction process are the microscopic one. The interference of the direct process and the second order process is very important in such a calculation. We have to start on the same basis and discuss the interference between the different processes. In this section the spectroscopic amplitude and the form factors by the microscopic description will be given.

The spectroscopic amplitude and the form factor are defined by

$$\langle I_B M_B S_b m_b | V | I_A M_A S_a m_a \rangle = \sum_{\ell s j} i^{-\ell} (-)^{S_b - m_b} (I_A M_A j M_B - M_A | I_B M_B)$$

$$\times (S_a m_a S_b - m_b | s\, m_a - m_b)(\ell m s m_a - m_b | j M_B - M_A) A_{\ell s j} F_{\ell s j}(r) Y^*_{\ell m}(\hat{r}) \delta(r_b - \frac{M_A}{M_B} r_a), \quad (2)$$

where ℓ, s and j are transfered angular momentum, spin and total spin respectively. $I_B M_B$ and $I_A M_A$ are magnitude and Z component of the spins of target and residual nuclei and $S_b m_b$ and $S_a m_a$ are the ones of the emited and the incident particles. V is the interaction by which the reaction is induced.

(1) (P, P') reaction ($0^+ \rightarrow 2_1^+$)

The form factor and the spectroscopic amplitude of (P, P') reaction leading to the first 2^+ state are given by

$$A_{\ell s j} = \frac{V_s}{\sqrt{2j+1}\sqrt{2}}, \quad (3)$$

$$F_{\ell s j}(r) = \sum_{j_1 j_2} \langle j_1 \| i^{\ell} T^{(\ell s; j)}(\hat{\xi}) \| j_2 \rangle U^{(s)}_{j_1 j_2} (\psi_{j_1 j_2} + (-)^S \phi_{j_1 j_2}) \langle n_1 \ell_1 | \psi_{\ell}(r, \xi) | n_2 \ell_2 \rangle, \quad (4)$$

where V_s is the interaction strength between nucleons, and s = 0 is the spin independent part and s = 1 is the spin dependent part. $T^{(s1:j)}(\xi)$ is given by

$$T^{(s\ell;j)}_m(\hat{\xi}) = \sum_{m_s m_\ell} (s m_s \ell m_\ell | j m) Y_{\ell m_\ell}(\hat{\xi}) \chi_{s m_s}. \quad (5)$$

The factors $u^{(s)}_{j_1 j_2}$, $\psi_{j_1 j_2}$ and $\phi_{j_1 j_2}$ were given in chapter 2. $v_\ell(r,\xi)$ is the multipole expansion function of the radial part of the interaction:

$$v(|\vec{r}-\vec{\xi}|) = \sum_{\ell m} v_\ell(r,\xi) Y_{\ell m}(\hat{\xi}) Y^*_{\ell m}(\hat{r}). \tag{6}$$

In the radial part of the interaction is the gauss type, the expansion function can be written by

$$v_\ell(r,\xi) = 4\pi i^\ell j_\ell(-2ia^2 r\xi)\, e^{-a^2(r^2+\xi^2)}, \tag{7}$$

where $j_1(x)$ is the bessel function and a^2 is the range parameter of the interaction.

The sign of the form factor around the nuclear radius is very important in the calculation of TSP. It is useful to know the sign of the form factor. If we use the δ interaction for the (P,P') reaction and the Q-Q force as the residual interaction in the nucleus, the form factor is written by

$$F_{\ell s j}(r) = \delta_{s0}\delta_{\ell j} \sum_{j_1 j_2} \langle j_1 \| i^\ell Y_\ell(\hat{\xi}) \| j_2 \rangle^2 \left(y^{(\omega)}_{j_1 j_2}\right)^2 \left(\frac{1}{E_{j_1 j_2} - \hbar\omega} + \frac{1}{E_{j_1 j_2} + \hbar\omega}\right) N$$

$$\times \frac{1}{4\pi} R^*_{n_1\ell_1}(r)\, R_{n_2\ell_2}(r) \times \frac{m\omega_0}{\hbar} \times \langle n_1\ell_1 | r^2 | n_2\ell_2 \rangle, \tag{8}$$

where the marix element $\langle n_1 1_1 |\, r^2 \,| n_2 1_2 \rangle$ has the same sign with the value of $R_{n_1 1_1}(r)\, R_{n_2 1_2}(r)$ around the nuclear radius $r = R_0$. Thus the sign of the form factor around the nuclear radius is always positive.

(2) (t,t') Reaction

For the (t,t') reaction, only the magnitude of the interaction is different from the (P, P') reaction: That is

$$V(r,r') = \sum_{i} 2\left(V_0 + V_1(\sigma_i \cdot \sigma_n)\right) C_n \exp\left[-\beta_n |\vec{r}_i - \vec{r}|^2\right]$$

$$+ \sum_{i} \left(V_0 + V_1(\sigma_i \cdot \sigma_p)\right) C_p \exp\left[-\beta_p |\vec{r}_i - \vec{r}|^2\right], \qquad (9)$$

where

$$C_n = \left[\frac{12\delta^4}{12\delta^4 - a^4/36}\right]^{3/2}, \quad C_p = 1 \qquad (10)$$

and

$$\beta_n = a^2\left[1 - \frac{a^2}{12\delta^2} - \frac{a^2(12\delta^2 - a^2)^2}{3\cdot 12^2\delta^2(12\delta^4 - a^4/36)}\right],$$

$$\beta_p = a^2\left[1 - \frac{a^2}{9\delta^2}\right] \qquad (11)$$

These coeficients come from the integration over triton intrinsic coordinates,

$$V(r,r') = \int d\vec{r}\, d\vec{\xi}\, \psi_T^*(\vec{r},\vec{\xi}) \sum_{k,i}^{A,A} \left[V_0 + V_1(\sigma_k \cdot \sigma_i)\right] \exp\left[-a^2|\vec{r}_k - \vec{r}_i|^2\right] \psi_T(\vec{r},\vec{\xi}) \qquad (12)$$

Thus the spectroscopic factor and the form factor of (t, t') reaction leading to the first 2^+ state are given by

$$A_{lsj} = \frac{V_s}{\sqrt{2j+1}\sqrt{2}},$$

$$F_{lsj}(r) = \sum_{j_1 j_2} \langle j_1 \| i^l T^{(sl;j)}(\hat{r}) \| j_2 \rangle u_{j_1 j_2}^{(s)} \left(\psi_{j_1 j_2} + (-)^s \psi_{j_1 j_2}\right)$$

$$\times \left[2C_n \langle n_1 l_1 | v_l^n(r;\xi) | n_2 l_2 \rangle + C_p \langle n_1 l_1 | v_l^p(r;\xi) | n_2 l_2 \rangle\right], \qquad (13)$$

where $v_{\ell}^{n}(v, \xi)$ and $v_{\ell}^{p}(v, \xi)$ is the expansion functions with the range parameters S_n and S_p.

The calculations with using the microscopic form factors are now in progress.

References

1) K. Yagi, Y. Aoki, J. Kawa and K. Sato, Phys. Lett. 29B (1969) 647;
K. Yagi, K. Sato and Y. Aoki, J. Phys. Soc. Japan 31 (1971) 1838

2) R. J. Ascuitto, N. K. Glendenning and B. Sorensen, Phys. Lett. 34B (1971) 17;
T. Tamura, D. R. Bes, R. A. Broglia and S. Landowne, Phys. Rev. Lett.
25 (1970) 1507

3) K. Yagi, Y. Aoki, C. Rangacharyulu, M. Matoba, M. Hyakutake and J. Nidome,
Phys. Lett. 44B (1973) 447

4) M. Toyama, Phys. Lett. 38B (1972) 147;
M. Toyama, Nucl. Phys. A211 (1973) 254

5) H. Toki and M. Sano, OULNS 73-6 (1973) and to be published.

6) C. L. Lin, Prog. Theor. Phys. 36 (1966) 251

7) N. K. Glendenning, Phys. Rev. 137 (1965) B102

8) P. H. Stelson and L. Grodzins, Nucl. Data. 1 (1965) 1

9) C. B. Fulmer, J. B. Ball, A. Scott and L. Whiten, Phys. Rev. 181 (1969) 1565

10) M. Matoba, M. Hyakutake, S. Nakamura, T. Katayama, T. Tonai, K. Yagi,
K. Sato and Y. Aoki, Phys. Lett. 44B (1973) 159

11) M. Toyama and M. Igarashi, INS code TWOSTP (1972) and private communication

12) H. Taketani, private communication

13) K. Yagi, Y. Aoki and C. Rangacharyulu, private communication

14) S. Yoshida, Nucl. Phys. 33 (1962) 685

Figure Captions

Fig. 1 (a) Angular distributions for the first 2^+ states of Te isotopes populated by (p,t) reactions. Lines are drawn to guide the eye.

(b) Angular distributions for the first 2^+ states of Te isotopes calculated in terms of the distorted-wave Born-approximation. The strength of the P_2-P_2 force is taken as G_2^c = 20MeV.

(c) Angular distributions for the first 2^+ states of Te isotopes calculated in terms of the two-step process-calculation. There is an ambiguity in the sign of the β value, and $\beta = \beta_{exp}$ is used.

(d) $\beta = -\beta_{exp}$ is used. See caption to fig. 1(c).

Fig. 2 The summed cross sections for the first 2^+ states of Te isotopes taken in steps of 2.5° from 5° to 55° as a function of mass number.

Fig. 3 Angular distribution for the first 2^+ states of Te isotopes calculated in terms of the two-step process-calculation. $\alpha = \frac{1}{3}$ is used.

Fig. 4 (a) The summed cross sections for the ground states of the indicated isotopes taken in steps of 2.5° from 5° to 55°. The horizontal axis is neutron number.

(b) The summed cross sections for the first 2^+ states of the indicated isotopes taken in steps of 2.5° from 5° to 55°. The horizontal axis is neutron number.

(c) The deformation parameter β obtained from the B(E2) value. The horizontal axis is neutron number.

	Proton	Triton
V (MeV)	V(A)[a]	185.1
W_v(MeV)	6.0	20.0
W_s(MeV)	W(A)[b]	0.0
$V_{s.o.}$(MeV)	6.04	0.0
r_R(F)	1.16	1.23
a_R(F)	0.75	0.7
r_I(F)	1.37	1.52
a_I(F)	0.63	0.7
$r_{s.o.}$(F)	1.064	-
$a_{s.o.}$(F)	0.74	-
r_c(F)	1.25	1.25

	A	122	124	126	128	130
a)	V(A)	46.7	47.1	47.5	47.7	48.0
b)	W(A)	2.85	2.89	2.91	2.95	3.00

Table 1.

Table 1. Optical potential parameters for proton and triton.

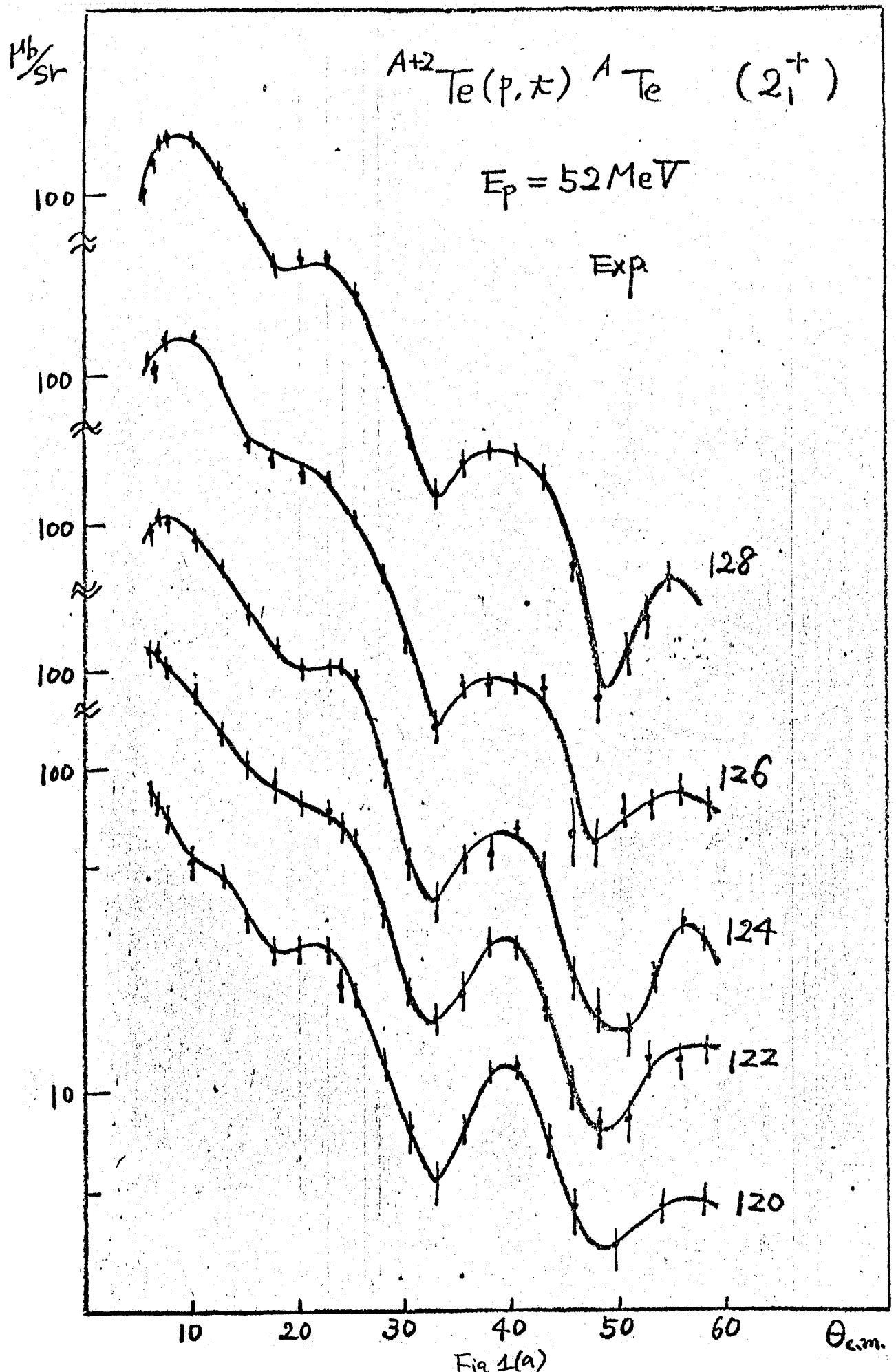
μb/Sr
$^{A+2}$Te(p,t)^{A}Te (2$_1^+$)
E_p = 52 MeV
Exp
100
100
100
100
100
10
128
126
124
122
120
10
20
30
40
50
60
θc.m.

Fig 1(a)

1(a)

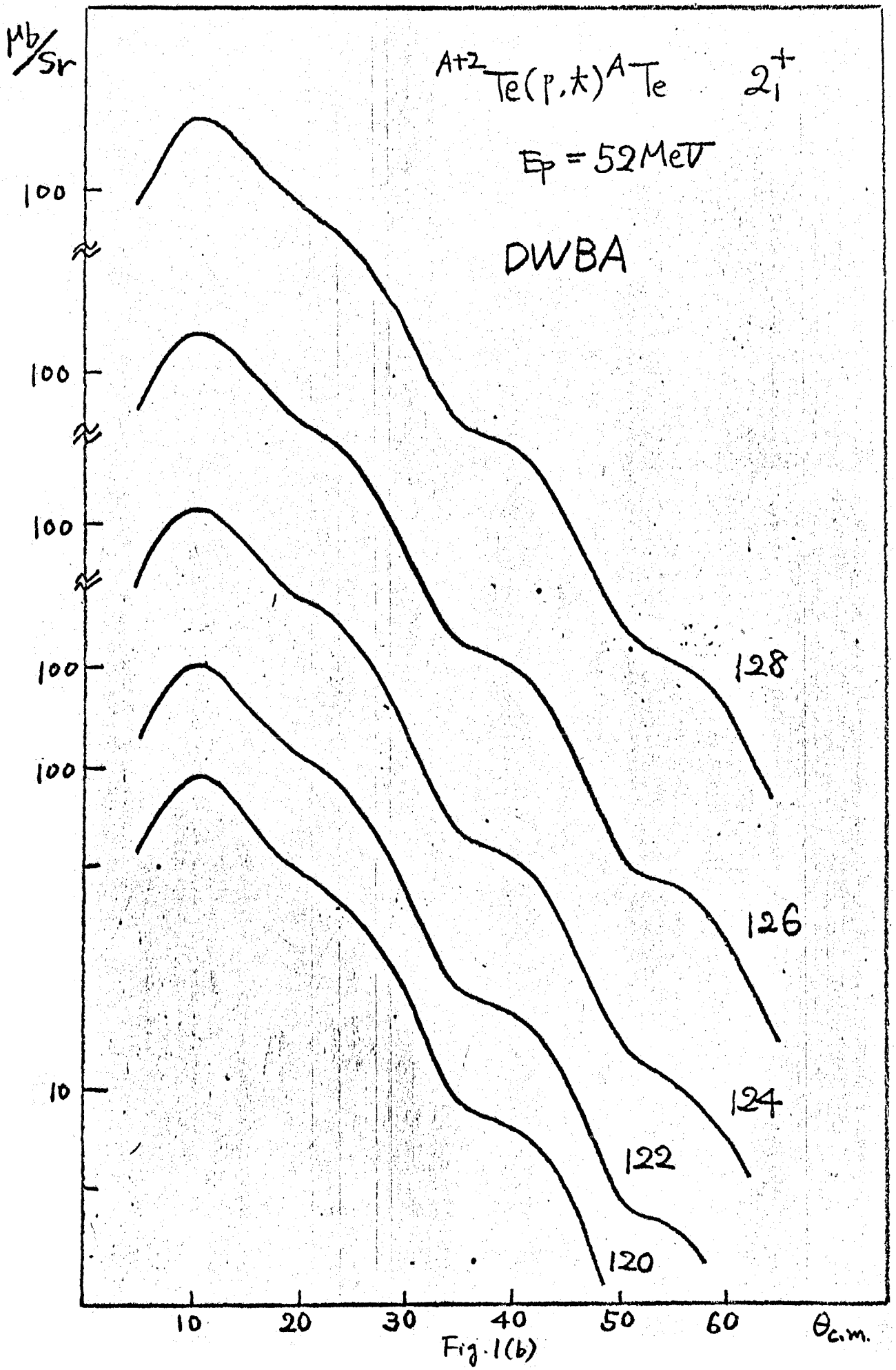
μb/Sr
$^{A+2}$Te(p,t)^{A}Te 2_1^+
Ep = 52 MeV
DWBA
100
100
100
100
100
10
128
126
124
122
120
10
20
30
40
50
60
θc.m.

Fig. 1(b)

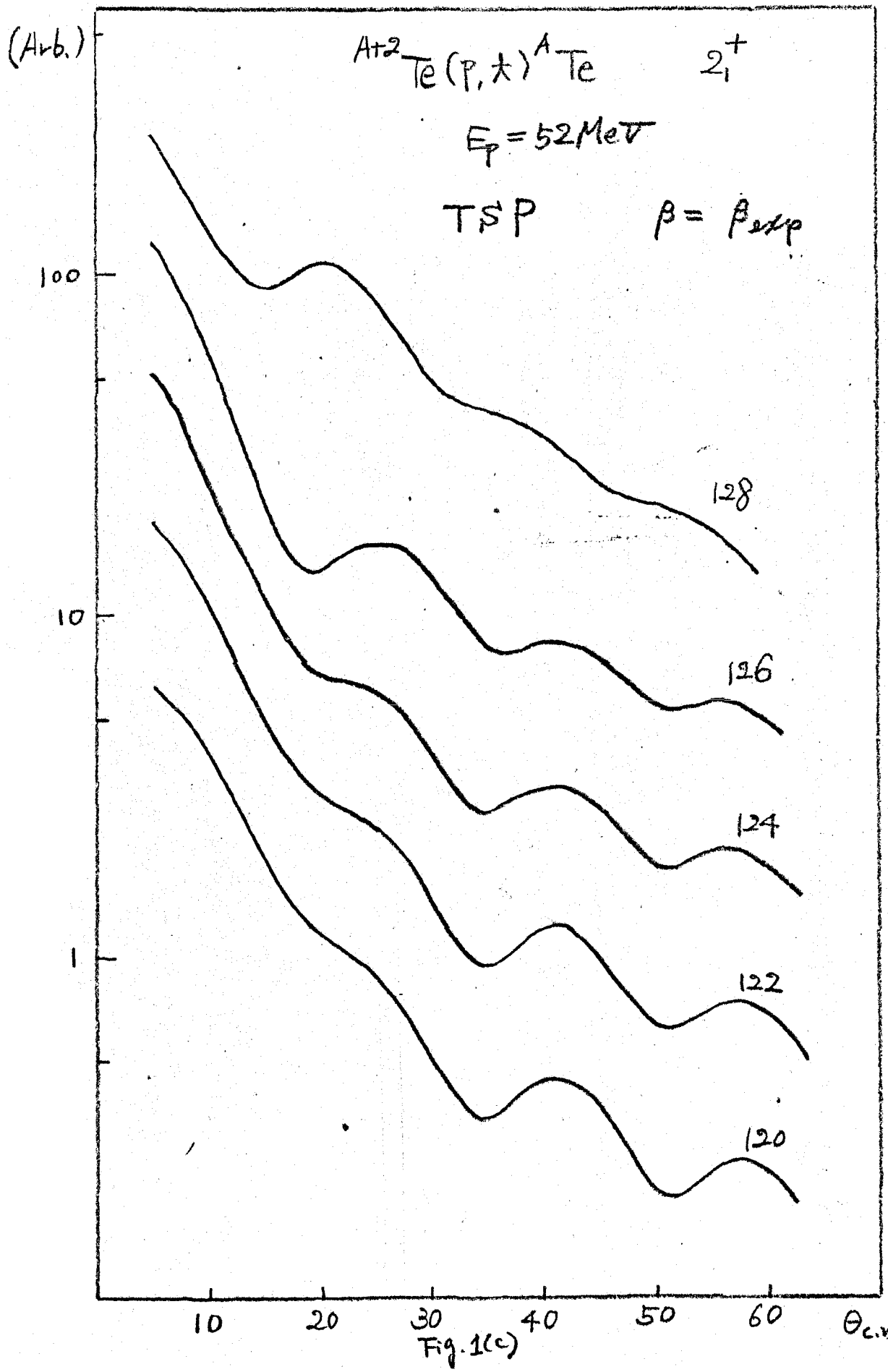
(Arb.)
$^{A+2}$Te (p, t) ^{A}Te
2_1^+
$E_p = 52$ MeV
TSP
$\beta = \beta_{exp}$
100
10
1
128
126
124
122
120
10
20
30
40
50
60
$\theta_{c.m.}$

Fig. 1(c)

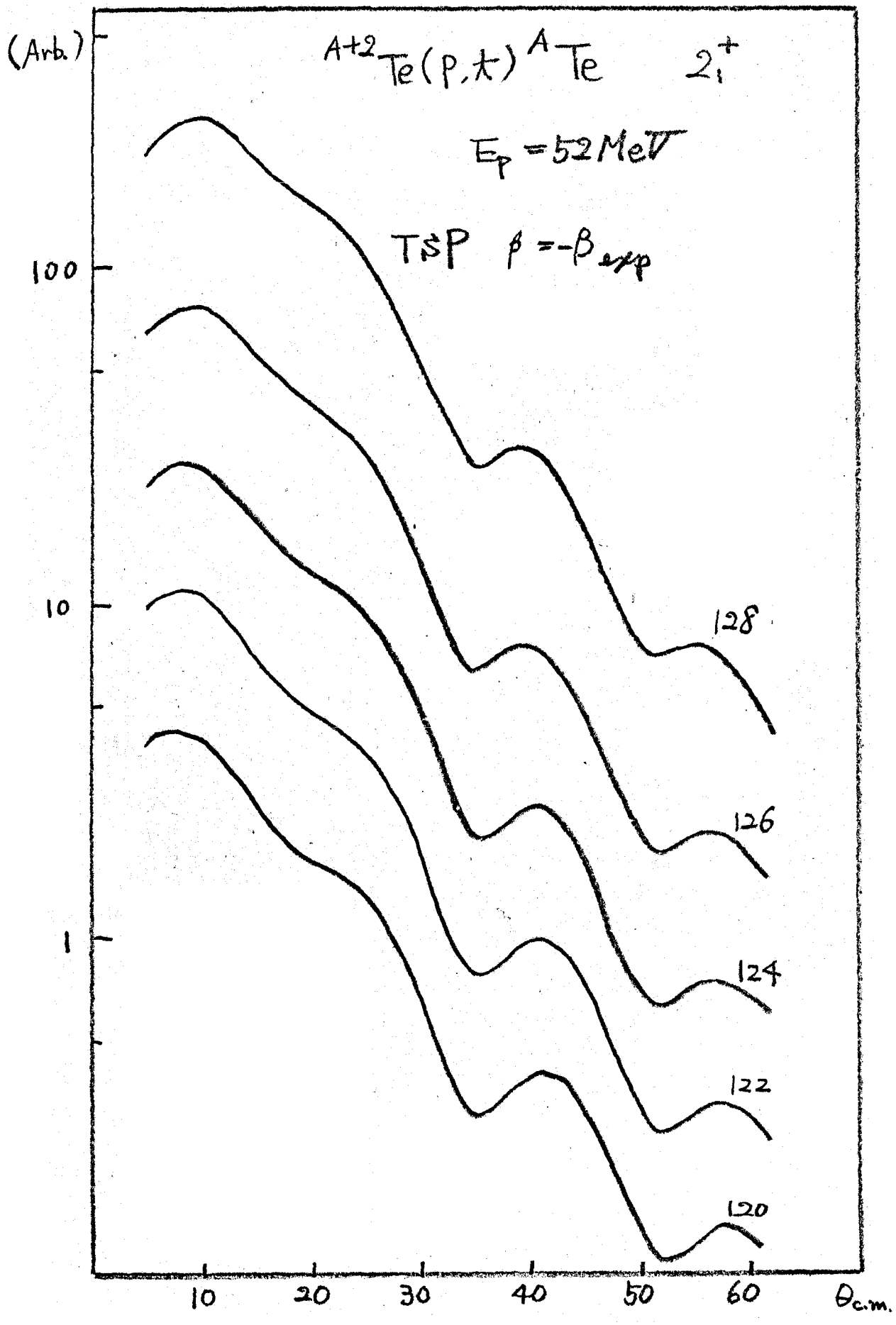
(Arb.)
$^{A+2}Te(p,t)^{A}Te$ 2_1^+
$E_p = 52 MeV$
TSP $\beta = -\beta_{exp}$
100
10
1
128
126
124
122
120
10
20
30
40
50
60
$\theta_{c.m.}$

Fig. 1(d)

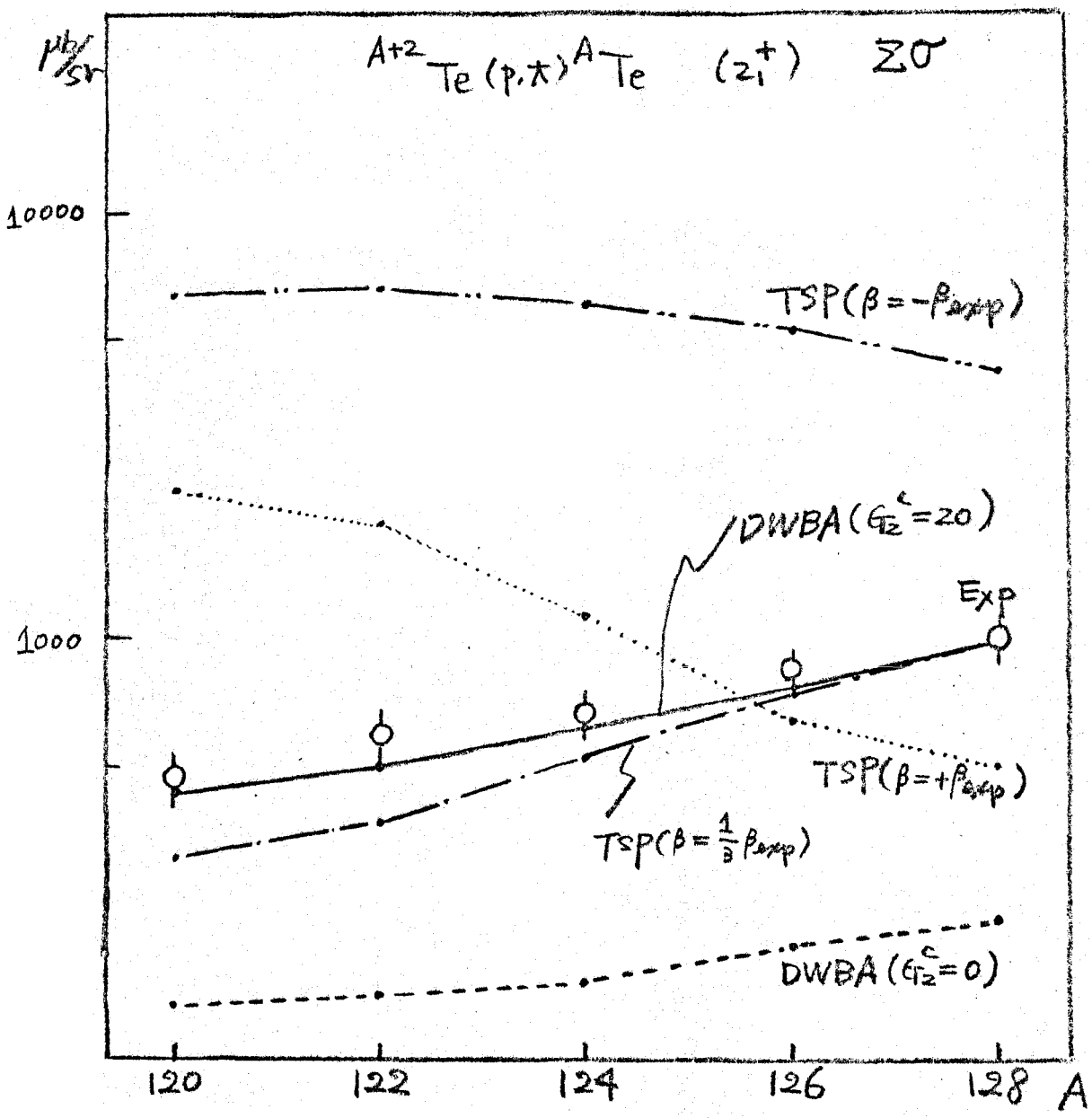
μb/sr
$^{A+2}Te(p,t)^{A}Te$ (2_1^+) $\Sigma\sigma$
10000
1000
TSP($\beta=-\beta_{exp}$)
DWBA($G_{12}^c=20$)
Exp
TSP($\beta=+\beta_{exp}$)
TSP($\beta=\frac{1}{3}\beta_{exp}$)
DWBA($G_{12}^c=0$)
120
122
124
126
128
A

Fig. 2.

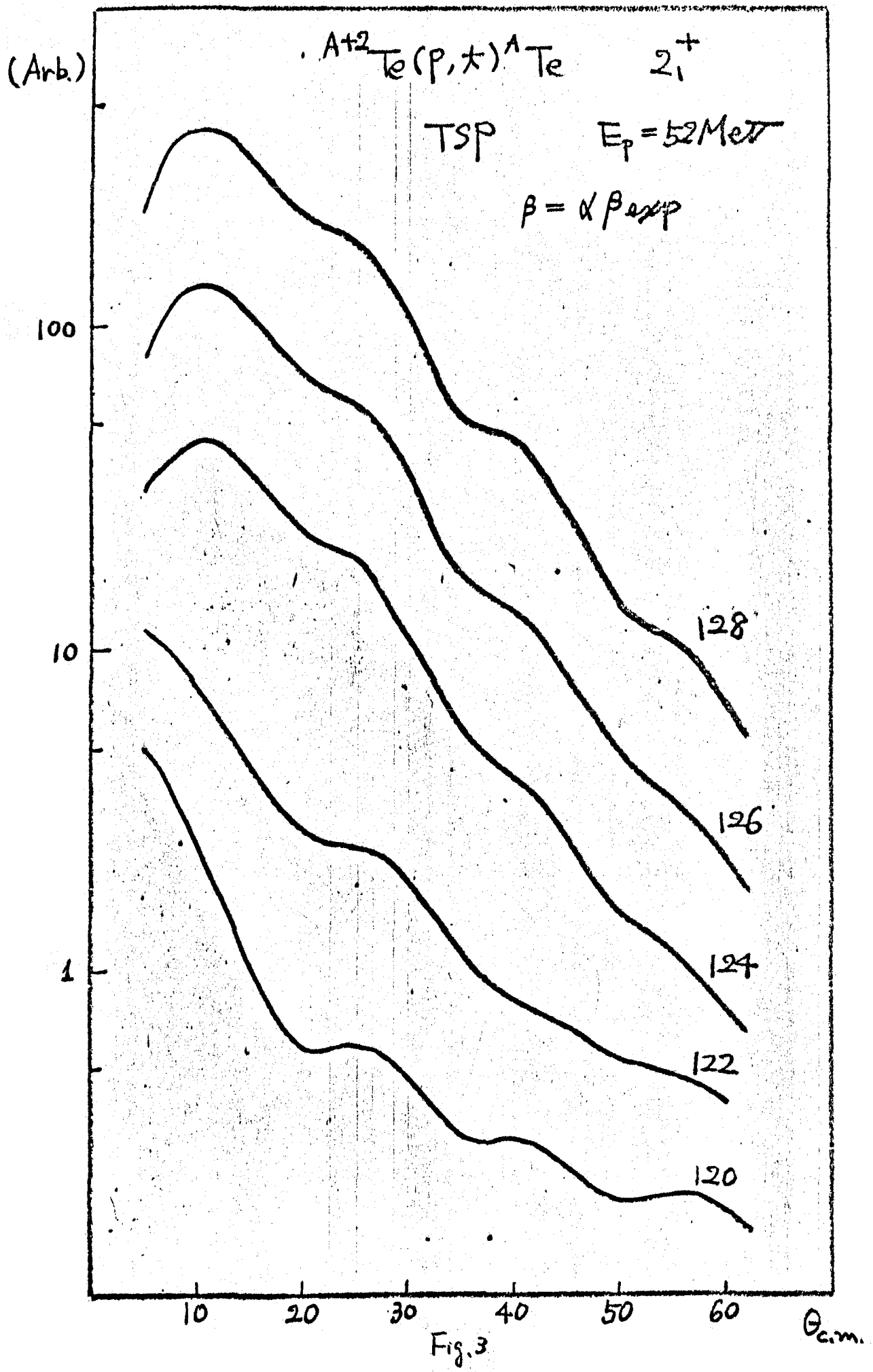
(Arb.)
$^{A+2}$Te(p,t)^{A}Te 2_1^+
TSP
E_p = 52 MeV
$\beta = \alpha \beta_{exp}$
100
10
1
128
126
124
122
120
10
20
30
40
50
60
$\theta_{c.m.}$

Fig. 3

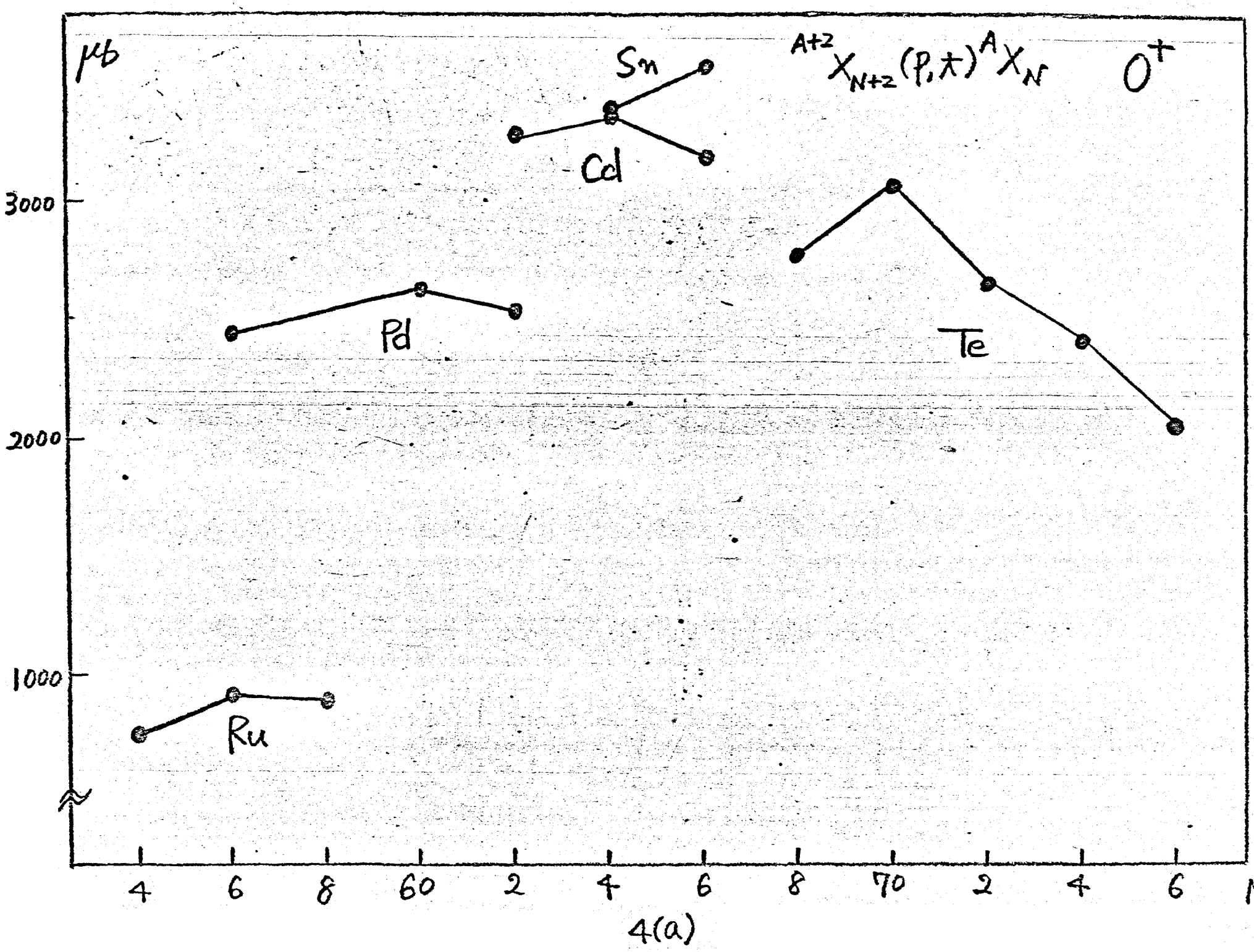
μb
Sn
Cd
$^{A+2}X_{N+2}(p,t)^{A}X_{N}$
0^{+}
3000
2000
1000
Pd
Te
Ru
4
6
8
60
2
4
6
8
70
2
4
6
N

4(a)

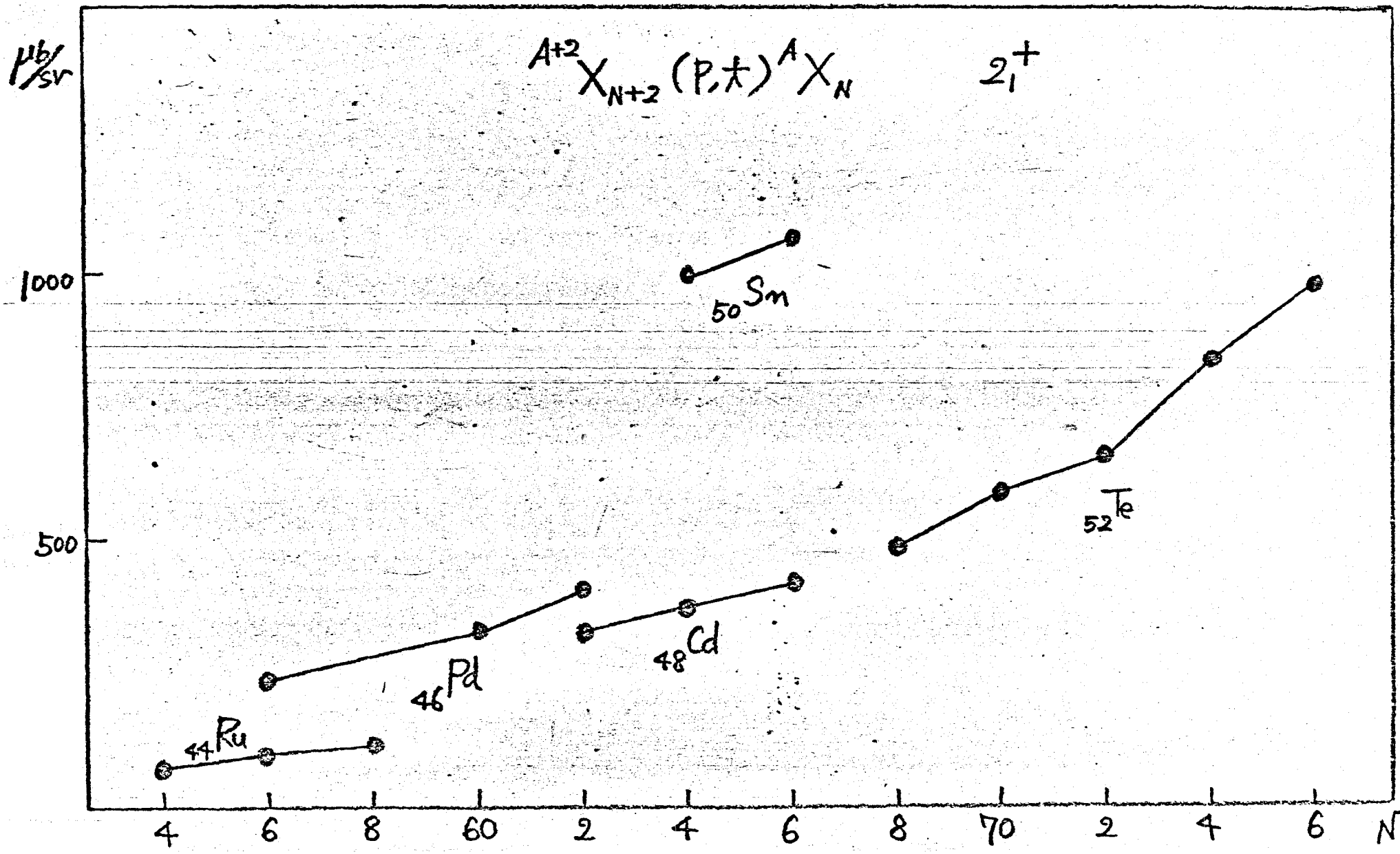
μb/sr
$^{A+2}X_{N+2}(P,t)^{A}X_{N}$
2_1^+
1000
500
$_{50}Sn$
$_{52}Te$
$_{48}Cd$
$_{46}Pd$
$_{44}Ru$
4
6
8
60
2
4
6
8
70
2
4
6
N

4(b)

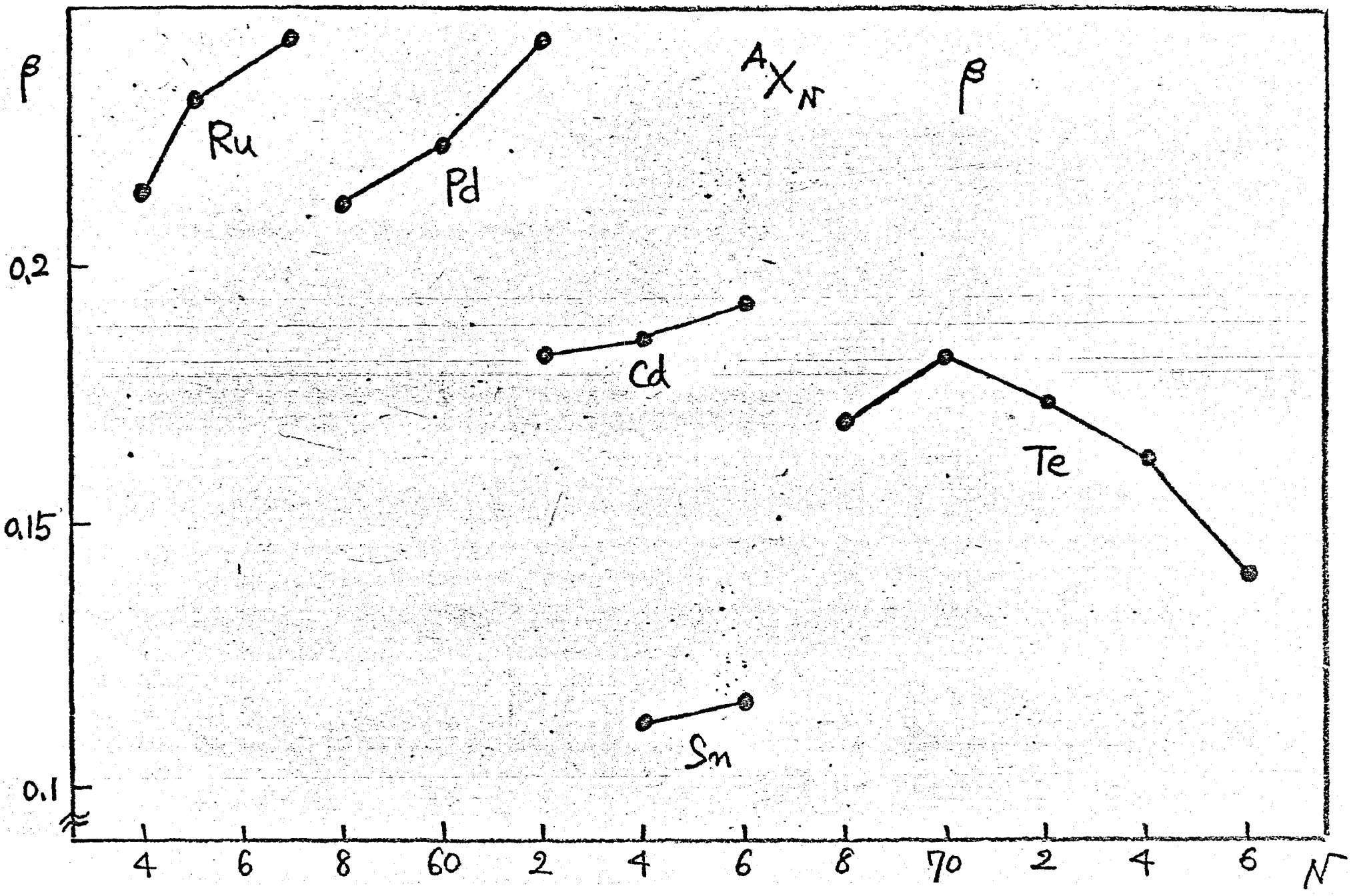

4(c)

CHAPTER 7 Concluding Remarks

In concluding the present paper we should like to stress the importance of the quadrupole-pairing force.[9] The quadrupole-pairing force was introduced so as to explain the strongly excited 2^+ states by the (p,t) reaction on the Nd isotopes. The 2^+ states were described by adding the quadrupole-pairing force to the quadrupole force in the framework of the random-phase approximation. The quadrupole-type density-vibrational mode couples to the quadrupole-type pairing-vibrational mode.

The two-body interaction V can be expanded in two ways, one being in terms of a rotationally invariant particle-particle matrix element G, the other in terms of an invariant particle-hole matrix element F.[1] There is a relation between G and F which is expressed using a Racah coefficient. In our calculation for G type matrix the monopole-and the quadrupole-pairing forces were taken and for F type matrix the quadrupole force was taken. Thus there might be a possibility of double-counting for the two-body interaction, but the recoupling spreads the strength of one type over many angular momenta and it can therefore be neglected. For quadrupole parts of these two type matrices F and G, the quadrupole force and the quadrupole-pairing force have quite different effects with each other as can be seen in this paper.

The systematics of the results of the (p,t) reaction on the Nd and Ba isotopes were well explained by the vibrational model described by a simple interaction composed of a quadrupole force and a quadrupole-pairing force in the framework of the random-phase approximation. For the change of the angular distribution pattern of the (p,t) reaction leading to the first 2^+ states of the medium-heavy nuclei with the neutron

number between 50 and 82, the quadrupole pairing force has an important effect to make the magnitude of the cross section larger and the two-step process calculation well described the systematics of the (p,t) reaction.

In the calculations there were many sets of G_2^c and V_2^c which were used so as to explain different kinds of experiments. These are listed in table 1. As can be seen from table 1, the value of G_2^c spreads over 20 to 30 MeV, and the value of V_2^c over 30 to 35 MeV. The values of the interaction strengths are strongly effected by how many single-particle levels are taken in the calculations. To compare these values which were decided by various experiments we must take same number of single-particle levels. Further the calculations considering the situation should be done in the medium-heavy nuclei.

The B(E2) value of the transition between first 2^+ state and ground state calculated by taking three major shells into consideration exceeds the experimental value. The collectivity for the B(E2) value is too strong if only the quadrupole force is taken in terms of the random-phase approximation. The correlations never turn out to be so large as estimated from the quadrupole force when we calculate the correlations with more realistic forces.[2] The quadrupole-pairing force interferes with the quadrupole force and reduces the quantities with particle hole nature; B(E2) value and cross section of inelastic scattering and so on. Thus the effective charge of a proton and a neutron must be larger than old one.[3] Although we must use a rather large effective charge e_{eff} for protons and neutrons, the trend of the experimental values was well reproduced as can be seen in this paper.

All the calculations on the (p,t) reactions were done with the zero-range assumption. For the transfer reactions such as (p,t) reaction we

must calculate the six dimensional integral, but the zero-range assumption allows for reduction of the six-dimensional integral to a three-dimensional one. The physical justification about the zero-range assumption in need. In terms of the plane-wave Born approximation we can see the effect of the zero-range assumption, and when the relative energy of the system is high, the finite-range effect can not be neglected. Finite range DWBA calculation was done for the (p,t) reaction by Bayman et al.[4] and Takemasa et al..[5] From their calculations the relative magnitude of the cross section for excited states to the ground-state transition is not effected so largely by such a finite calculation. But the magnitude of the cross section is largely affected and to discuss the magnitude we must do the finite range calculation.

It was shown that there are strong incident-energy dependence on the (p,t) reactions. In order to study a high spin state we would rather use a high-energy proton beam. It is necessary to study the optical potential for tritons at a high energy to make clear the energy dependence.

There is a problem in the mechanism of (p,t) reaction. It was shown that the angular distribution patterns of the first 2^+ states was reproduced when the two-step processes including the inelastic scattering in the entrance and the exit channels were taken into account. It was also pointed out that the succesive process, one nucleon is transfered after another, was important for the two nucleon transfer reaction.[6] How much does the successive process effect to (p,t) reaction is an open problem.

The so called two phonon states have been discussed by many authors.[7] It can not be said, however, that these problems are over. Odd nuclei have been also studied by Matsuyanagi et al..[8] For these problems the quadrupole pairing force might affect successfuly.

References

1) M. Baranger, Phys. Rev. 120 (1960) 957;
M. Baranger, Phys. Rev. 122 (1961) 992

2) G. E. Broun, Unified Theory of Nuclear Models (North-Holland) (1964)

3) L. S. Kisslinger and R. A. Sorensen, Rev. Mod. Phys. 35 (1963) 853

4) B. F. Bayman, Nucl. Phys. A168 (1971) 1

5) T. Takemasa and H. Yoshida, Phys. Lett. 46B (1973) 313

6) R. A. Broglia, U. Götz, M. Ichimura, T. Kammuri and A. Winther,
Phys. Lett. 45B (1973) 23

7) T. Tamura and T. Kishimoto, J. Phys. Soc. Japan 34 Suppl. (1973) 393;
B. Sorensen, J. Phys. Soc. Japan 34. Suppl. (1973) 399

8) A. Kuriyama, T. Marumori and K. Matsuyanagi, Prog. Theor. Phys. 47 (1972) 498;
K. Matsuyanagi, private communication

9) H. Toki and M. Sano, OUNLS 73-6 (1973), and to be published

Nucleus	Nd	Ba	Nd	Cd,Te	Xe,Ba,Ce	Te
Chapter	2	2	3	4	4	6
G_2^c	26.0	20.7	24.75	26.0	28.0	20.0
V_2^c	-	-	33.18	29.3	31.8	-

Table 1. Sets of G_2^c and V_2^c used in the various chapters. Second row denotes the chapter in which the parameter sets indicated in third and fourth rows were used. The letter "-" in the fourth row means that the parameter V_2^c is nuclear dependent which was decided so as to reproduce the excitation energy of the first 2^+ state with using the value G_2^c in the third row.

Acknowledgment

The author would like to express his sincerest thanks to Professor M. Muraoka for his guidance, warm encouragement and valuable discussions. Thanks are also due to Professor S. Takagi for helpful discussions, and to Professors K. Yagi, Y. Ishizaki and H. Taketani for a number of discussions and makig him available the experimental data of (p,t) reactions, which made him introduce the idea of P_2- P_2 force. Appreciation ismentioned to Dr. C. Rangacharyulu and Dr. Y. Aoki for their collaboration in the calculation of the two-step process on $^{A+2}$Te (p,t) ^{A}Te reaction, and many discussions.

The author indebted to Dr. H. Yoshida for letting him use the OULNS-DWBA4 code,and to Dr. I. Isomoto for letting him use his DWBA code. He also wishes to thank Dr. M. Sakagami for help in the calculation of ^{150}Nd (p,t) ^{148}Nd cross section, in which the difference between the nuclear deformations of the targer and residual nucleus is taken into account. In addition, with regard to the (p,t) reaction mechnism, He is indebted to Dr. C. L. Lin and Dr. T. Takemasa for the formalism of the (p,t) reaction in terms of the distorted-wave Born-approximation, and to Dr. M. Toyama and Dr. M. Igarashi for the formalism of the two-step process-calculation and letting him use thir code INS-TWOSTP.

Thanks are also due to Dr. C. Rangacharyulu for reading the paper, and to Miss A. Iijima for help in typing this manuscript.